Title
The Role of HIF-1α and iNOS in IFN-γ Mediated Control of Mycobacterium tuberculosis Infection

Author
Braverman, Jonathan

Publication Date
2017

Peer reviewed|Thesis/dissertation

The Role of HIF-1α and iNOS in IFN-γ Mediated Control of *Mycobacterium tuberculosis* Infection

By

Jonathan Braverman

A dissertation submitted in partial satisfaction of the

requirements for the degree of

Doctor of Philosophy

in

Molecular and Cell Biology

in the

Graduate Division

of the

University of California, Berkeley

Committee in charge:

Professor Sarah Stanley, Chair
Professor Daniel Portnoy
Professor Russell Vance
Professor James Olzmann

Spring 2017

Abstract

The Role of HIF-1α and iNOS in IFN-γ Mediated Control of *Mycobacterium tuberculosis* Infection

by

Jonathan Braverman

Doctor of Philosophy in Molecular and Cell Biology

University of California, Berkeley

Professor Sarah Stanley, Chair

Mycobacterium tuberculosis, the causative agent of tuberculosis, is responsible for an enormous burden of morbidity and mortality worldwide, and is responsible for nearly 2 million deaths annually. As a pathogen, *M. tuberculosis* is extraordinarily successful, infecting an estimated 2 billion people worldwide. *M. tuberculosis* is able to thrive in macrophages, an immune cell type that specializes in eating and killing bacteria. Despite the remarkable capabilities of *M. tuberculosis* to infect and persist in humans, the large majority of immunocompetent people are able to successfully control infection, and there is great interest in understanding what characterizes a successful immune response to *M. tuberculosis* infection. One of the key molecules in the immune response to *M. tuberculosis* is the cytokine Interferon gamma (IFN-γ), which is primarily produced by CD4+ T Cells during the adaptive response to infection. IFN-γ is thought to activate macrophages, allowing them to kill *M. tuberculosis*. Within this dissertation, I describe novel insights into the effects IFN-γ has on macrophages during *M. tuberculosis* infection.

My dissertation work has focused primarily on two proteins, Hypoxia Inducible Factor 1 alpha (HIF-1α) and Inducible Nitric Oxide Synthase (iNOS), which are both activated by IFN-γ in macrophages during *M. tuberculosis* infection. First I demonstrate that HIF-1α activation during *M. tuberculosis* infection is IFN-γ dependent, and that this activation of HIF-1α is required for successful control of infection both in macrophages and in mice, and that HIF-1α regulates a variety of immune responses including aerobic glycolysis, eicosanoid production, inflammatory cytokine production, and nitric oxide production. Next, I explore the signaling roles of nitric oxide during *M. tuberculosis* infection. In the context of *M. tuberculosis* infection, nitric oxide has been assumed to primarily be a direct bactericidal effector. However, nitric oxide has well documented signaling roles in a variety of other contexts. Here, I show that nitric oxide plays key signaling roles during IFN-γ activation of *M. tuberculosis* infected macrophages. I find that nitric oxide is strongly anti-inflammatory via inhibition of NF-kB signaling, while at the same time nitric oxide activates antimicrobial responses via stabilization of HIF-1α.

This dissertation is dedicated to my grandmother, Gloria Braverman
And in memory of my grandfather, Leopold Braverman

Acknowledgements:

It has been my great fortune to have had three exceptional mentors as I have trained to be a scientist: Tom Schultheiss who first introduced me to science and the mysteries of development, Justin Cassidy who mentored me as an undergraduate and taught me the power of looking at things slowly and carefully, and most importantly Sarah Stanley who has prepared me to work independently as a scientist and have the confidence to pursue new ideas and challenge existing models.

I would also like to thank all the members of the Stanley lab for making my time at Berkeley delightful. It has been a true privilege to work with such clever and intensely focused scientists, and people I could rely on to work side by side with in a BSL3 facility.

Finally, I would like to thank my thesis committee for their advice and support during my time at Berkeley. In particular, I would like to thank Dan Portnoy for his valuable guidance in finding the right lab to join.

Table of Contents

Chapter One: HIF-1a Is an Essential Mediator of IFN-γ–Dependent Immunity to *Mycobacterium tuberculosis*

This work has been published in the Journal of Immunology
J Immunol. 2016 Aug 15;197(4):1287-97
Jonathan Braverman, Kimberly M. Sogi, Daniel Benjamin, Daniel K. Nomura and Sarah A. Stanley
PMID: 27430718

Abstract:
The cytokine IFN-γ coordinates macrophage activation and is essential for control of pathogens including *Mycobacterium tuberculosis*. However, the mechanisms by which IFN-γ controls *M. tuberculosis* infection are only partially understood. Here, we show that the transcription factor HIF-1α is an essential mediator of IFN-γ dependent control of *M. tuberculosis* infection both *in vitro* and *in vivo*. *M. tuberculosis* infection of IFN-γ activated macrophages results in a synergistic increase in HIF-1α protein levels. This increase in HIF-1α levels is functionally important, as macrophages lacking HIF-1α are defective for IFN-γ dependent control of infection. RNA-seq profiling demonstrates that HIF-1α regulates nearly half of all IFN-γ inducible genes during infection of macrophages. In particular, HIF-1α regulates production of important immune effectors including inflammatory cytokines and chemokines, eicosanoids, and nitric oxide (NO). In addition, we find that during infection HIF-1α coordinates a metabolic shift to aerobic glycolysis in IFN-γ activated macrophages. We find that this enhanced glycolytic flux is crucial for IFN-γ dependent control of infection in macrophages. Furthermore, we identify a positive feedback loop between HIF-1α and aerobic glycolysis that amplifies macrophage activation. Finally, we demonstrate that HIF-1α is crucial for control of infection *in vivo* as mice lacking HIF-1α in the myeloid lineage are strikingly susceptible to infection, and exhibit defective production of inflammatory cytokines and microbicidal effectors. In conclusion, we have identified HIF-1α as a novel regulator of IFN-γ dependent immunity that coordinates an immunometabolic program essential for control of *M. tuberculosis* infection *in vitro* and *in vivo*.

Introduction:

Mycobacterium tuberculosis, the causative agent of tuberculosis, infects 2 billion people worldwide and is responsible for more deaths annually than any other single bacterial pathogen (1). Interferon-γ (IFN-γ) activation of macrophages leads to restriction of *M. tuberculosis* growth and is crucial for successful immunity. Patients lacking components of the IFN-γ signaling pathway are highly susceptible to mycobacterial infection (2). Similarly, mice lacking IFN-γ rapidly succumb to infection with *M. tuberculosis* (3, 4). Some of the proposed anti-bacterial responses induced by IFN-γ include nutrient restriction (5), enhanced production of antimicrobial peptides (6, 7), autophagy (8), expression of cell intrinsic restriction factors including interferon inducible GTPases (9, 10), and production of nitric oxide (NO) by inducible nitric oxide synthase (iNOS). NO has bactericidal activity against *M. tuberculosis* (11) and is essential for host defense against *M. tuberculosis* infection in mice (12), accounting for a substantial portion of the susceptibility of IFN-γ deficient mice.

The transcription factor hypoxia inducible factor-1α (HIF-1α) canonically functions to induce glycolytic gene expression under conditions of hypoxia. More recently, HIF-1α has been implicated in macrophage function. HIF-1α contributes to the transition to aerobic glycolysis and expression of genes associated with M1 polarization in response to LPS stimulation (13). In the context of sepsis, HIF-1α was demonstrated to mediate a transition from a pro-inflammatory to an immunosuppressive phenotype while maintaining antimicrobial and protective functions (14). Further, HIF-1α has been identified as important for control of Group A *Streptococcus* (GAS), *Pseudomonas aeruginosa,* and uropathogenic *E. coli* (15-17). The susceptibility of HIF-1α deficient mice to infection has been attributed to an inability to produce the ATP required for migration to sites of inflammation (15, 18) and to decreased production of iNOS and antimicrobial peptides (15-17). Intriguingly, recent studies suggest that HIF-1α may play a role in host defense against mycobacteria. Exogenously increasing the levels of active HIF-1α using pharmacological or genetic tools in zebrafish embryos enhances bactericidal activity against *Mycobacterium marinum* (19). Mice lacking HIF-1α in the myeloid lineage exhibit more rapid progression of hypoxic granulomatous lesions in the liver following intravenous infection with *Mycobacterium avium* (20). These data suggest the intriguing possibility that HIF-1α may be an important mediator of resistance to *M. tuberculosis* infection. Importantly, HIF-1α is thought to be important in the context of hypoxia or during innate immune responses to infection, and has not previously been shown to be involved in IFN-γ dependent immunity.

In this study, we demonstrate that HIF-1α is required for host defense against infection with virulent *M. tuberculosis.* Mice lacking HIF-1α in the myeloid lineage are strikingly susceptible to infection. Surprisingly, we do not find evidence that HIF-1α is important for innate defense of macrophages against *M. tuberculosis*. In contrast, we find that HIF-1α is critical for IFN-γ dependent control of *M. tuberculosis* infection. RNA-seq reveals that approximately half of the transcriptional response to IFN-γ during *M. tuberculosis* infection requires HIF-1α. Further, HIF-1α deficient macrophages are impaired for important effector functions including production of NO, PGE2, as well as inflammatory cytokines and chemokines. In addition to regulating these key immune effector functions, we find that HIF-1α regulates a metabolic transition to aerobic

glycolysis in IFN-γ activated macrophages during *M. tuberculosis* infection. We show that this transition to aerobic glycolysis is required for IFN-γ dependent control of *M. tuberculosis* infection of macrophages. In addition, we identify a positive feedback loop between HIF-1α and glycolytic flux that reinforces IFN-γ mediated activation of macrophages and control of *M. tuberculosis* infection.

Materials and Methods:

Ethics Statement

All procedures involving the use of mice were approved by the University of California, Berkeley IACUC, the Animal Care and Use Committee (protocol number R353-1113B). All protocols conform to federal regulations, the National Research Council's *Guide for the Care and Use of Laboratory Animals* and the Public Health Service's (PHS's) *Policy on Humane Care and Use of Laboratory Animals*.

Reagents

Recombinant mouse IFN-γ (485 MI/CF) was obtained from R&D systems, Minneapolis, MN, and was used at indicated concentrations. 2-deoxyglucose (2-DG) and D-glucose were obtained from Sigma Aldrich, St Louis, MO and were used at indicated concentrations. U-^{13}C-glucose was obtained from Cambridge Isotope Laboratories, Andover, MA. Dimethyloxalylglycine (DMOG) was obtained from Cayman Chemical, Ann Arbor, MI and was used at indicated concentrations.

Mice and cell culture

WT mice were C57BL/6 and were obtained from the Jackson Laboratory, Bar Harbor, ME. All knockout mice were backcrossed to C57BL/6. B6.129-*Hif1a*^{tm3Rsjo}*/J* mice were obtained from the Jackson Laboratory and were crossed with B6.129P2-*Lyz2*$^{tm1(cre)Ifo}$*/J* to generate mice that had *Hif1a* deletion targeted to the myeloid lineage. B6.129P2-*Nos2*^{tm1Lau}*/J* mice were obtained from the Jackson Laboratory and were bred in house. Bone marrow derived macrophages (BMDM) were obtained by flushing cells from the femurs and tibias of mice and culturing in DMEM with 10% FBS and 10% supernatant from 3T3-M-CSF cells (BMDM media) for 6 days with feeding on day 3. After differentiation, BMDM continued to be cultured in BMDM media containing M-CSF.

Bacterial culture

The *M. tuberculosis* strain Erdman was used for all experiments. *M. tuberculosis* was grown in Middlebrook 7H9 liquid media supplemented with 10% ADS (albumin-dextrose-saline), 0.4% glycerol, and 0.05% Tween-80 or on solid 7H10 agar plates supplemented with 10% Middlebrook OADC (BD) and 0.4% glycerol. The TB-lux strain used for measuring bacterial growth was derived from an Erdman strain, and was cultured as described above.

In vitro infections

BMDM were plated into 96-well or 24-well plates with $5x10^4$ and $3x10^5$ macrophages per well respectively, and were allowed to adhere and rest for 24 hours. BMDM were then treated with vehicle or IFN-γ (1.25 ng/mL) overnight and then infected in DMEM supplemented with 5% horse serum and 5% FBS at an MOI of 5 unless otherwise noted. After a 4 hour phagocytosis period, infected BMDM were washed with PBS before replacing with BMDM media. For experiments with DMOG, 2-DG or galactose, these reagents were added to the BMDM media after the 4 hour phagocytosis. For 2-DG and galactose treatment, this was done to minimize the amount of time that the BMDM experienced glycolytic inhibition. For IFN-γ pretreated wells, IFN-γ was also added after

infection at the same concentration. To measure intracellular growth of *M. tuberculosis*, cells were infected with TB-lux (Erdman) and luminescence was measured at 32°C immediately following the 4 hour phagocytosis, PBS wash, and media replacement. Luminescence was then read again at the noted time points. All growth was normalized to day 0 luminescence readings for each infected well, and is presented as fold change in luminescence compared to day 0. For enumeration of CFU, *M. tuberculosis* Erdman strain was used, and infected BMDM were washed with PBS, lysed in water with 0.1% Triton-X 100 for ten minutes, and serial dilutions were prepared in PBS with 0.05% Tween-80 and were plated onto 7H10 plates.

***In vivo* infections**

Cohorts of age and sex matched wild-type, *Nos2*$^{-/-}$, and *Hif1a*$^{fl/fl}$*LysMcre*$^{+/+}$ mice were infected by aerosol route with *M. tuberculosis* strain Erdman. All mice were on the C57BL/6 background, and were 7-10 weeks of age when infected, with cohorts of 10-12 mice for each genotype for time to death experiments. Aerosol infection was done using a Nebulizer and Full Body Inhalation Exposure System (Glas-Col, Terre Haute, IN). 9mL of an OD_{600}=.01 culture was loaded into the nebulizer. This resulted in ~400 CFU per mouse 1 day after infection. Mice were weighed the day of infection, and weights were followed until a humane 15% weight loss cutoff was reached at which point the mice were euthanized. For CFU, one lung lobe (the largest) was homogenized in PBS+.05%Tween-80, and serial dilutions were plated on 7H10 plates. For CFU experiments, cohorts of 4-5 mice were used for each genotype at each timepoint. For qRT-PCR experiments, lung lobes from 3-5 mice per genotype were pooled, and a cell suspension was obtained by pressing the lungs through a 40um filter. The cells were then washed and CD11b+ cells were purified by MACS magnetic bead separation using CD11b MicroBeads (130-049-601, Miltenyi Biotec, San Diego, CA) as described in the manufacturer's protocol. Cells were purified to ~95% CD11b+. For qPCR, purified CD11b+ cells were lysed in TRIzol and qRT-PCR was performed as described below. For NO measurements from CD11b+ cells *ex vivo*, the same procedure described above was performed, and CD11b+ cells were re-plated in 96-well plates with $3x10^5$ cells per well, and griess assays were performed on the supernatants at the indicated timepoints.

Griess Assays

The griess reaction was used to detect nitrite in the supernatants of BMDM or *ex vivo* CD11b+ cells as a proxy for NO production. Briefly, a solution of .2% napthylethylenediamine dihydrochloride was mixed 1:1 with a 2% sulfanilamide, 4% phosphoric acid solution. 50uL of supernatant from cultured cells was added to 50uL of this mixture, and absorbance was measured at 546nm. Concentrations were determined by comparing to a standard curve of nitrite in BMDM media.

Western blots

Infected BMDM were washed with PBS, lysed in 1x SDS-PAGE buffer on ice, and heat sterilized for 30 min at 100°C. Total protein lysates were analyzed by SDS-PAGE using pre-cast Tris-HCl criterion gels (Bio-Rad, Hercules, CA). The following primary antibodies were used: rabbit antibody against HIF-1α (NB100-479, Novus Biologicals, Littleton, CO and also D2U3T, Cell Signaling Technology, Danvers, MA), goat antibody

against mouse IL-1b (AF-401-NA, R&D systems, Minneapolis, MN). HRP conjugated secondary antibodies were used. Western Lightning Plus-ECL chemiluminescence substrate (PerkinElmer, Waltham, MA) was used and blots were developed on film or using a ChemiDoc MP System (Bio-Rad, Hercules, CA). Blots were stripped using 0.2 M NaOH then washed in ddH_2O and TBST before blocking and reprobing for actin as a loading control, using an HRP conjugated rabbit antibody against β-actin (13E5, Cell Signaling Technology, Danvers, MA).

qRT-PCR and RNA-seq

For q-RT-PCR, $3x10^5$ BMDM were seeded in 24-well dishes and infected as described. At 24h post-infection, cells were washed with room temperature PBS and lysed in 500uL TRIzol (Invitrogen Life Technologies, Carlsbad, CA). Total RNA was extracted using chloroform (100 μL) and the aqueous layer was further purified using RNeasy spin columns (Qiagen, Limburg, Germany). For qPCR, cDNA was generated from 1 μg of RNA using Superscript III (Invitrogen Life Technologies, Carlsbad, CA) and Oligo-dT primers. Select genes were analyzed using Maxima SYBR green qPCR master mix (Thermo Scientific, Waltham, MA). Each sample was analyzed in triplicate on a CFX96 Real-time PCR detection system (Bio-Rad, Hercules, CA). C_Q values were normalized to values obtained for actin and relative changes in gene expression were calculated using the $\Delta\Delta C_Q$ method.

For RNA-seq, three independent experiments were performed. For each experiment, BMDM were seeded in 24-well dishes and infection and RNA preparation were performed as described. For each sample in each experiment two duplicate wells were pooled. RNA-seq was performed at the Genome Center and Bioinformatics Core Facility at the University of California, Davis. SR50 reads were run on an Illumina HiSeq, with ~30 million reads per sample. Data analysis was performed by the UC Davis bioinformatics group using FastQC for read quality assessment, Sythe and Sickle for Illumina adapter and quality trimming, and Tophat2 for read alignment. Raw counts were derived from alignments using a STSeq-count python script (21). Tests of differential expression were conducted using a multifactorial model in edgeR/limma(voom). Data was uploaded to NCBI: http://www.ncbi.nlm.nih.gov/sra/SRP075696.

Glucose assays and Lactate Assays

Lactate accumulation in supernatants of BMDM was measured using the Lactate Assay Kit (MAK064, Sima-Aldritch, St Louis, MO) as described in the manufacturer's protocol. Glucose depletion from the media was measured using the Glucose (HK) assay kit (GAHK20, Sigma Aldrich, St Louis, MO). The protocol was modified to perform the assays in 96 well plates with 100uL reactions instead of 1mL reactions in cuvettes as described in the manufacturer's protocol. Glucose consumption was calculated by measuring glucose levels in the media after infection and subtracting from glucose measured from cell-free media.

ELISAs

For IL-1b ELISAs, supernatants from BMDM in 24 well plates were used. A mouse IL-1b ELISA kit (DY401, R&D systems, Minneapolis, MN) was used as described in the

manufacturer's protocol. For PGE2 ELISAs, the PGE2 EIA Kit (EA02, Oxford Biomedical Research, Rochester Hills, MI) was used as described in the manufacturer's protocol.

Metabolomic profiling by LC-MS/MS

Preparation of lysates for metabolomics profiling followed published protocols (22). In brief, $4x10^6$ BMDM were plated in 6 cm dishes in DMEM containing 10% FBS, 10 mM glucose, 4 mM L-glutamine, and 20 ng/mL recombinant GM-CSF (Cell Signaling Technologies, Danvers, MA). BMDM were infected at an MOI of 1 as described above. At 24h post infection, cells were washed with ice cold PBS and immediately lysed with ice cold 40:40:20 MeCN/MeOH/H_2O and immediately placed on ice. D_3-Serine (1 nmol) was added to each sample as an external standard. Samples were vigorously vortexed and sonicated and insoluble material was removed by centrifugation. An aliquot of the supernatant (20 µl) was analyzed by SRM-based LC/MS. Polar metabolite separation was achieved with a Luna normal-phase NH_2 column (50 × 4.6 mm, with 5-µm-diameter particles; Phenomenex, Torrance, CA). Mobile phase A was composed of 100% acetonitrile, and mobile phase B consisted of water and acetonitrile in a 95:5 ratio. Solvent modifier 0.2% ammonium hydroxide with 50 mM ammonium acetate was used to assist ion formation and to improve the LC resolution in negative ionization mode. The gradient started at 0% B and increased linearly to 100% B over the course of 30 min with a flow rate of 0.7 mL/min. MS analysis was performed with an electrospray ionization (ESI) source on an Agilent 6430 QQQ LC-MS/MS (Agilent Technologies, Santa Clara, CA). The capillary voltage was set to 3.0 kV, and the fragmentor voltage was set to 100 V. The drying gas temperature was 350^{o}C, the drying gas flow rate was 10 L/min, and the nebulizer pressure was 35 psi. Representative metabolites were quantified by SRM of the transition from precursor to product ions at associated optimized collision energies.

Results:

HIF-1α is required for IFN-γ mediated control of *M. tuberculosis* infection. To characterize the role of HIF-1α in macrophages during *M. tuberculosis* infection, HIF-1α protein levels were first assayed by western blot following infection with *M. tuberculosis*. Infection of bone marrow derived macrophages (BMDM) with *M. tuberculosis* resulted in accumulation of HIF-1α. However, the induction was weak and transient, with accumulation of HIF-1α that peaked at 4 hours after infection and was undetectable by 12 hours after infection (Figure 1A). This was surprising given that HIF-1α protein levels increase substantially in macrophages treated with LPS and during infection with several bacterial species (13, 15). However, in the context of IFN-γ stimulation, *M. tuberculosis* infection resulted in a substantially more robust and prolonged increase in HIF-1α protein levels (Figure 1A). The increase in HIF-1α protein levels observed with infection of IFN-γ activated macrophages is synergistic, as neither infection nor IFN-γ treatment alone induced substantial accumulation of HIF-1α (Figure S1A).

Next, growth of *M. tuberculosis* in wild-type and HIF-1α deficient macrophages BMDM was compared both in resting and IFN-γ activated macrophages. Bacterial numbers were enumerated by counting CFU at multiple time points after infection. After the initial phagocytosis period, CFU bacterial numbers were equivalent across all genotypes and conditions (Figure 1B). Over a 3 day timecourse, BMDM are a relatively restrictive environment for *M. tuberculosis* replication, with only a 2.5-fold increase in CFU observed, with wild-type and HIF-1α deficient BMDM able to restrict *M. tuberculosis* replication to the same degree in the absence of IFN-γ stimulation (Figure 1B). However, following IFN-γ stimulation, wild-type BMDM are able to kill *M. tuberculosis*, while bacterial numbers remain constant in the HIF-1α deficient BMDM (Figure 1B). HIF-1α therefore regulates processes in IFN-γ activated macrophages that enable bacterial killing.

HIF-1α is constitutively transcribed and translated and protein levels are governed by the activity of prolyl hydroxylases that mark HIF-1α for ubiquitination and degradation. Inhibition of prolyl hydroxlases by low oxygen, metabolic intermediates, or small molecule inhibitors causes HIF-1α stabilization and accumulation (23). To test whether pharmacological stabilization of HIF-1α in the absence of IFN-γ activation would impact *M. tuberculosis* replication in macrophages, BMDM were infected with *M. tuberculosis* and treated with the prolyl hydroxylase inhibitor DMOG. DMOG was tested in the presence of IFN-γ at both a standard activating concentration (1.25ng/mL), and at a subactivating concentration (0.05ng/mL). The addition of 200uM DMOG enhanced HIF-1α levels under both conditions, as well as in resting macrophages infected with *M. tuberculosis* (Figure S1B). To assess the impact on bacterial replication a reporter strain that constitutively expresses the bacterial luciferase encoding *luxCDABE* operon (TB-lux, gift from the Cox lab) was utilized. Luminescence from this strain was linear with bacterial number in axenic culture and during infection of macrophages and expression of the lux genes did not attenuate growth (Figure S1C,D). Exogenously stabilizing HIF-1α during *M. tuberculosis* infection of resting macrophages slightly reduced *M. tuberculosis* growth (Figure 1C). However, the addition of DMOG to IFN-γ activated macrophages resulted in a larger decrease in bacterial numbers (Figure 1C) indicating that pharmacological stabilization of HIF-1α can activate microbicidal

mechanisms effective against *M. tuberculosis* more robustly in the context of IFN-γ. The fact that the enhancement of bacterial restriction occurs both at effective IFN-γ concentrations as well as at lower, sub-activating IFN-γ concentrations suggests that artificial HIF-1α stabilization might be of therapeutic utility in the context of an insufficient IFN-γ response to *M. tuberculosis* infection.

HIF-1α is a key mediator of IFN-γ dependent gene expression

HIF-1α has a large number of potential target genes. A comprehensive analysis of HIF-1α target genes in the context of infection has not been performed. Therefore, RNA-seq was used to identify HIF-1α dependent changes in the macrophage transcriptome during infection with *M. tuberculosis* (data available at http://www.ncbi.nlm.nih.gov/sra/SRP075696). Infection of macrophages with *M. tuberculosis* resulted in changes in expression in 3330 genes, and the addition of IFN-γ to *M. tuberculosis* infected macrophages results in differential expression of 2595 genes relative to *M. tuberculosis* infection alone. In resting *M. tuberculosis* infected macrophages HIF-1α contributed to altered expression in only 118 genes, or 3.5% of all regulated genes. In IFN-γ activated macrophages, however, HIF-1α contributed to regulation of 1191 genes during infection, demonstrating that HIF-1α is responsible for approximately ~45% of IFN-γ induced alterations in the macrophage transcriptome 24 hours after *M. tuberculosis* infection.

Prominent among genes that were downregulated in HIF-1α deficient macrophages during infection with IFN-γ activation were inflammatory cytokines and chemokines including *Il1a*, *Il1b*, *Il6* and the neutrophil chemoattractant *Cxcl1* (Figure 2A). Loss of HIF-1α did not result in a global defect in transcription of cytokine and chemokine genes. Tnf levels were unaffected by HIF-1α deficiency, and IL10 levels were increased (Figure 2A). The cytokine IL-1 is essential for control of *M. tuberculosis* infection in mice. HIF-1α contributes to IL-1 transcription downstream of LPS activation (13), however a role for HIF-1α in expression of IL-1 during *M. tuberculosis* infection has not been demonstrated. Interestingly, levels of *Il1b* mRNA were dependent on HIF-1α in both resting and IFN-γ activated macrophages. This defect translated to a significant defect in pro-IL-1β protein production as assayed by western blotting from cell lysates (Figure 2C) and by ELISA from cell supernatants (Figure 2D). Furthermore, enhancing HIF-1α stabilization with DMOG further increased *Il1b* mRNA levels in *M. tuberculosis* infected and IFN-γ activated macrophages (Figure 2E). Of note, we observed that IFN-γ increased levels of pro-IL-1β in cell lysates and had no impact on IL-1β levels in cell supernatants. This contrasts with several reports that have demonstrated that IFN-γ suppresses IL-1β production in the context of TLR stimulation or *M. tuberculosis* infection (24, 25). Nevertheless, our data clearly indicate that HIF-1α is required for production of IL-1 during *M. tuberculosis* infection in both resting and IFN-γ activated macrophages. Thus, while HIF-1α only contributes to control of *M. tuberculosis* in infected macrophages in the context of IFN-γ activation, the low levels of HIF-1α observed in the absence of IFN-γ do promote transcription of a small number of immunologically important genes.

IL-6 expression was also found to be dependent on HIF-1α during *M. tuberculosis* infection (Figure 2F). To test whether the deficient expression of other cytokines and chemokines in the HIF-1α deficient macrophages was downstream of an autocrine effect

of IL-1 on macrophage activation, we tested whether IL-6 expression was altered in macrophages lacking IL1R. However, IL-6 levels were unaffected by the absence of IL1R (Figure 2G) supporting the hypothesis that HIF-1α plays a direct role in regulating the expression of cytokine and chemokine genes.

HIF-1α regulates production of prostaglandins and nitric oxide in *M. tuberculosis* infected macrophages

A recent study demonstrated that one important function of IL-1 during *M. tuberculosis* infection is to promote the production of prostaglandin E2 (PGE2) (26), a critical component of host immunity to *M. tuberculosis* (27-29). PGE2 is an eicosanoid derived from arachadonic acid via the enzymes COX2 and PGES. The defective IL-1 production in HIF-1α deficient macrophages suggests that there might also be a defect in PGE2 production in HIF-1α deficient macrophages. Eicosanoids have been shown to be important in macrophages for cell intrinsic control of *M. tuberculosis* replication and for productive and balanced inflammatory responses (28, 30, 31). However, eicosanoid production during *M. tuberculosis* infection of macrophages has only previously been characterized in the absence of IFN-γ. Interestingly, *Cox2* expression levels and PGE2 production in *M. tuberculosis* infected BMDM was dramatically enhanced by IFN-γ stimulation (Figure 3A, 3B). In addition, *Cox2* expression was partially dependent on HIF-1α in IFN-γ activated *M. tuberculosis* infected macrophages (Figure 3A). This decrease in Cox2 expression led to a significant defect in PGE2 production in HIF-1α deficient macrophages (Figure 3B). These data identify the production of enhanced levels of PGE2 as a potential mechanism of IFN-γ dependent control of *M. tuberculosis*, and demonstrate that HIF-1α is essential for PGE2 production.

Following IFN-γ activation and *M. tuberculosis* infection, HIF-1α deficient BMDM had lower levels of iNOS transcript (*Nos2)* than wild-type macrophages (Figure 3C). This observation is consistent with the observation that HIF-1α can bind at the *Nos2* promoter (32). This defect at the transcript level corresponded to a ~50% defect in NO production (Figure 3D) and was not a result of decreased cell viability of the HIF-1α deficient macrophages (Figure 3E). Finally, the addition of DMOG to resting and IFN-γ activated macrophages enhanced NO production, further confirming the importance of HIF-1α for functional responses of macrophages (Figure 3F). Taken together our results implicate HIF-1α as a crucial regulator of IFN-γ dependent inflammatory responses as well as cell intrinsic immune responses to *M. tuberculosis*.

Metabolic profiling during *M. tuberculosis* infection reveals increased levels of aerobic glycolysis in IFN-γ activated macrophages

RNA-seq revealed that infection of IFN-γ activated macrophages with *M. tuberculosis* causes a dramatic increase in expression of numerous glycolytic genes relative to the increase in gene expression observed with infection alone (Figure S2). We confirmed the increased expression of four of these genes, *Glut1*, *Hk2*, *Pfkfb3*, and *Mct4* by qPCR and found that the combination of IFN-γ and *M. tuberculosis* infection dramatically and synergistically increased expression of these glycolytic genes (Figure 4A). Aerobic glycolysis in resting macrophages infected with *M. tuberculosis* is thought to promote bacterial replication. Thus, the observation that glycolysis was further increased in IFN-γ activated macrophages, a bactericidal environment for *M. tuberculosis*, is unexpected. To

confirm these results, high-resolution tandem mass spectrometry was used to examine steady state levels of glycolytic intermediates in infected cells (33). *M. tuberculosis* infection of BMDM that had been activated with IFN-γ prior to infection resulted in a substantial increase in steady state levels of glycolytic intermediates compared to *M. tuberculosis* infection alone (Figure S3). Metabolic flux analysis using ^{13}C labeled glucose [U-^{13}C-glucose] demonstrated a modest increase in levels of ^{13}C pyruvate and lactate upon infection of resting macrophages with *M. tuberculosis* (Figure 4B, 4C). In agreement with previous work, this increase was partially dependent on the ESX-1 alternative secretion system (Figure 4B, 4C). However, analysis of ^{13}C labeled pyruvate and ^{13}C lactate levels confirmed that IFN-γ pre-activation resulted in greatly enhanced glycolytic flux relative to infection of resting macrophages (Figure 4B, 4C). Taken together these results demonstrate that increased glycolytic flux is associated with macrophages that are able to control infection with *M. tuberculosis*.

HIF-1α regulates metabolic transitions in IFN-γ activated and *M. tuberculosis* infected macrophages

In keeping with the known role of HIF-1α in regulating aerobic glycolysis, the majority of glycolytic genes had decreased expression in HIF-1α deficient BMDM relative to wild-type BMDM after *M. tuberculosis* infection of IFN-γ activated BMDM (Figure 4D). HIF-1α deficient BMDM also had significantly decreased glucose utilization during *M. tuberculosis* infection of IFN-γ activated macrophages (Figure 4E). Furthermore, HIF-1α deficient macrophages produced significantly less lactate upon infection (Figure 4F). The observation that HIF-1α deficient macrophages are not able to engage in aerobic glycolysis upon activation has previously been linked to a defect in ATP production in HIF-1α deficient peritoneal macrophages (18), which results in a defect in macrophage trafficking to sites of inflammation. A similar inability to produce ATP during infection could explain the defect in IFN-γ dependent control of *M. tuberculosis* infection observed in HIF-1α deficient BMDM. To test whether ATP production is compromised in HIF-1α deficient BMDM, ATP levels during *M. tuberculosis* infection in wild-type and HIF-1α deficient BMDM were measured. No difference in ATP levels between wild-type and HIF-1α deficient BMDM was observed in *M. tuberculosis* infected BMDM either in the presence or absence of IFN-γ (Figure 4G). This demonstrates that the observed defects in *M. tuberculosis* control in these macrophages does not result from major perturbations in cellular energetics.

HIF-1α is sensitive to changes in oxygen levels as well as changes in metabolite levels. HIF-1α stabilization is promoted by metabolites associated with aerobic glycolysis, including succinate and lactate (13, 34). 2-deoxyglucose (2-DG) is a glucose analog that is commonly used to inhibit or block flux through glycolysis. To test whether HIF-1α stabilization in *M. tuberculosis* infected and IFN-γ activated macrophages is promoted by flux through glycolysis, we treated macrophages with 2-DG and measured HIF-1α levels by western blotting. Limiting glycolytic flux dramatically reduced HIF-1α protein levels (Figure 4H). Thus, there is a positive feedback loop between HIF-1α and aerobic glycolysis which links aerobic glycolysis to IFN-γ dependent activation of macrophages. As expected, treatment of IFN-γ activated and *M. tuberculosis* infected macrophages with 2DG resulted in a significant decrease in glucose uptake from the culture media, confirming that 2DG limits glycolytic flux in this system (Figure 4I).

Flux through glycolysis supports IFN-γ dependent control of *M. tuberculosis* infection in macrophages

Previous reports have suggested that *M. tuberculosis* induces aerobic glycolysis in resting macrophages as a virulence strategy to promote bacterial growth (35, 36). Our data indicate that IFN-γ activation of macrophages, which restricts *M. tuberculosis* growth, also greatly enhances glycolytic flux. We therefore sought to determine whether the induction of aerobic glycolysis altered the ability of *M. tuberculosis* to replicate and/or survive in macrophages. To evaluate the role of aerobic glycolysis, resting and IFN-γ activated macrophages were infected with *M. tuberculosis* and treated with 2-DG and bacterial survival was assessed at 24 hours after infection. 2-DG treatment did not substantially alter *M. tuberculosis* growth or host control in resting BMDM (Figure 5A). In contrast, we found that the addition of 2-DG to IFN-γ activated BMDM resulted in enhanced bacterial survival, reversing IFN-γ dependent killing (Figure 5B). To confirm that the doses of 2-DG used had no impact on macrophage viability, microscopy was used to enumerate the number of cells surviving under each condition, a measurement of macrophage viability that is not confounded by possible alterations in metabolism (Figure 5C). To confirm that aerobic glycolysis is necessary for IFN-γ dependent killing, the capacity for cells to enhance glycolytic flux was also limited by culturing the macrophages on galactose rather than glucose as the carbon source in the media (37, 38). Macrophages cultured in galactose were unable to restrict the growth of *M. tuberculosis* in an IFN-γ dependent manner (Figure 5D). However culturing macrophages on galactose did not impact infection in resting macrophages (Figure 5D). Although macrophage viability was not impacted by 24h of culture with 2DG or galactose, by 48h we observed differences in macrophage survival that precluded analysis of bacterial loads at later timepoints. To circumvent this issue, and validate the importance of flux through glycolysis, we treated macrophages for 24h with 2DG followed by restoration of standard glucose containing media. We then measured bacterial loads at three days after infection, a time point at which we see a large difference in bacterial numbers between resting and IFN-γ activated macrophages, compared with the only two fold difference at 24h post infection. In addition, three days post infection is the timepoint at which the defect in HIF-1α deficient macrophages is most apparent. We found that 2DG treatment in the first 24h after infection resulted in impaired IFN-γ dependent control at 3d after infection. The effect of 2DG was dose dependent, with the maximal concentration of 2DG used resulting in a defect of IFN-γ dependent control that was equivalent to that found in HIF-1α deficient macrophages (Figure 5E). Interestingly, treatment with 2DG did not further impair the microbicidal activity of HIF-1α deficient macrophages (Figure 5F). Taken together, these findings demonstrate that macrophages infected with *M. tuberculosis* increase rates of glycolysis, that IFN-γ addition enhances this effect, and that aerobic glycolysis is necessary for IFN-γ dependent restriction of *M. tuberculosis*.

HIF-1α is crucial for control of *M. tuberculosis* infection *in vivo*

To assess the role of HIF-1α during *M. tuberculosis* infection *in vivo*, mice deficient for HIF-1α in the myeloid lineage (*Hif1a*$^{fl/fl}$*LysMcre*$^{+/+}$ [hereafter *Hif1a*$^{-/-}$]) and wild-type mice were infected with *M. tuberculosis* via the aerosol route. *Hif1a*$^{-/-}$ mice exhibited rapid weight loss, with ~75% of the *Hif1a*$^{-/-}$ mice succumbing to infection within 30 days

(Figure 6A). The increased susceptibility of *Hif1a*$^{-/-}$ mice was also reflected in bacterial burden in the lungs. The earliest timepoint with a difference in bacterial burden was 14 days after infection, with a small but statistically significantly higher bacterial burden in the *Hif1a*$^{-/-}$ mice compared to wild-type. By 22 days after infection there was more than 10-fold higher bacterial burden in the *Hif1a*$^{-/-}$ mice (Figure 6B). Additionally, *Hif1a*$^{-/-}$ mice had higher burdens in spleens at 22 days after infection (Figure 6C). Histological analysis was also performed on lungs and spleens from wild-type and *Hif1a*$^{-/-}$ mice 22 days after infection. Both wild-type and HIF-1α deficient mice exhibited acute to subacute neutrophilic and histiocytic inflammation, peribronchiolar to perivascular pneumonia, and lymphocytic perivascular cuffing (Figure 6D). The HIF-1α deficient lungs had a more necrotizing character and slightly more area affected (42.6% vs 32.3%), however the differences were relatively modest despite the ~1 log increased bacterial burden in the lungs at this timepoint. Interestingly, the HIF-1α deficient mice do not have large necrotic lesions, as has been reported for IFN-γ deficient mice (39). No differences were observed in HIF-1α deficient spleens compared with wild type. Taken together, these data support the idea that there is not a major defect in immune recruitment to the lungs in *Hif1a*$^{-/-}$ mice, but rather there is a defect in control of bacterial replication in infected macrophages.

HIF-1α regulates expression of immunologically important genes *in vivo*

Our *in vitro* data suggests that HIF-1α activity is enhanced in the context of IFN-γ stimulation of macrophages. To test whether this is also true *in vivo* we isolated CD11b+ macrophages from lungs of infected mice and examined the expression of HIF-1α target genes over time. *Bnip3* is a canonical HIF-1α target gene. We found that *Bnip3* expression increased between day 11 after infection and day 22 after infection, a timing that mirrors the development of the IFN-γ dependent T cell response (Figure 7A). As expected, macrophages from *Hif1a*$^{-/-}$ mice had much lower levels of *Bnip3* that did not increase with the onset of IFN-γ signaling (Figure 7A). Expression of iNOS increased over time in a partially HIF-1α dependent manner (Figure 7B). Furthermore, HIF-1α deficient CD11b+ cells plated *ex vivo* were deficient for NO production (Figure 7C). In addition, we confirmed that inflammatory cytokines and regulators of aerobic glycolysis were dependent on HIF-1α for expression *in vivo*. At 21d after infection we found that expression of glycolytic enzymes (*Pfkfb3, Hk2)*, inflammatory cytokines (*Il1a, Il1b, Il6)* and *Cox2* were all significantly lower in HIF-1α deficient CD11b+ cells than wild type (Figure 7D-7I). Furthermore, we found that expression of these genes was largely independent of HIF-1α until ~18d after infection, coinciding with the onset of IFN-γ dependent immunity (Figure S4). These results confirm that RNA-seq profiling of HIF-1α deficient macrophages *in vitro* is predictive of HIF-1α activity *in vivo,* and that IFN-γ activation enhances HIF-1α activity both *in vitro* and *in vivo*.

Discussion:

In this report we identify HIF-1α as an essential mediator of IFN-γ dependent immunity to *M. tuberculosis*. We find that *Hif1a*$^{-/-}$ mice are strikingly susceptible to *M. tuberculosis* infection *in vivo*. This places HIF-1α among a surprisingly short list of genes essential for control of *M. tuberculosis* infection *in vivo.* We find that in macrophages HIF-1α is required for the production of immune effectors including NO, IL-1 and PGE2. In addition, we demonstrate that HIF-1α is required for a transition to aerobic glycolysis in IFN-γ activated and *M. tuberculosis* infected macrophages and that aerobic glycolysis is crucial for IFN-γ dependent control of *M. tuberculosis* replication. Finally, we find that the immune effectors regulated by HIF-1α *in vitro* are also regulated by HIF-1α *in vivo* during infection with *M. tuberculosis*.

HIF-1α is emerging as an important regulator of immune responses to and defense against bacterial infection. In particular, two recent studies using different mycobacterial pathogens raised the possibility that HIF-1α might be required for defense against *M. tuberculosis* infection. First, it was demonstrated that pharmacological stabilization of HIF-1α during infection of zebrafish embryos with *M. marinum* leads to a reduced bacterial burden at early timepoints (19). Second, HIF-1α was found to play a role in a mouse model of granuloma caseation in livers of mice infected with *M. avium* (20). This granuloma formation depends upon hypoxia but is independent of effectors of IFN-γ based immunity, including NO. In this model, the lack of HIF-1α leads to more rapid necrosis of granulomatous lesions and a modest increase in bacterial numbers in livers and spleens that emerged by around 60 days after infection. Interestingly, our data indicate that HIF-1α is much more important for defense against *M. tuberculosis* than might have been predicted from these studies as we observed a dramatic susceptibility to aerosol infection with most HIF-1α deficient mice succumbing to infection within 30 days. As mouse lungs are not hypoxic during infection with *M. tuberculosis* (40-42) our data demonstrate that HIF-1α is not simply required for defense in areas of hypoxic inflammation, but is a mediator of IFN-γ dependent immunity regardless of oxygen availability. In addition, our data support the hypothesis that pharmacological stabilization of HIF-1α might be beneficial in clinical settings where IFN-γ production is impaired.

HIF-1α has been identified as important for control of Group A *Streptococcus* (GAS), *Pseudomonas aeruginosa,* and uropathogenic *E. coli* (15-17). For these infections HIF-1α has been described to regulate innate responses of macrophages, and is crucial for the production of NO and antimicrobial peptides by infected macrophages. Although several antimicrobial peptides have been proposed to contribute to host defense against *M. tuberculosis*, we did not observe that expression of these antimicrobial peptides was dependent on HIF-1α (not shown). Furthermore, our data indicate that HIF-1α is primarily important for control of *M. tuberculosis* in IFN-γ activated macrophages, thus extending the role of HIF-1α to a mediator of adaptive immunity. In this context, HIF-1α regulates both cell intrinsic and inflammatory responses of IFN-γ activated macrophages. The production of NO is a critical mediator of IFN-γ dependent control, and we find that maximal production of NO requires HIF-1α. Interestingly, we also find that the production of the prostaglandin PGE2 is dramatically increased by IFN-γ stimulation of *M. tuberculosis* infected macrophages. PGE2 is known to mediate cell

intrinsic control of *M. tuberculosis* infection in the absence of IFN-γ stimulation, however a possible role for PGE2 in cell intrinsic control of infection in IFN-γ activated macrophages has not been established. We find that HIF-1α is required for PGE2 production, potentially due to a defect in *Cox2* expression in HIF-1α deficient macrophages. We also find that HIF-1α is important for expression of numerous cytokines and chemokines in IFN-γ activated macrophages including *Il1a*, *Il1b* and *Il6*. Interestingly, IL-1 is one of the few cytokines that appear to be regulated by HIF-1α in both resting and IFN-γ activated macrophages infected with *M. tuberculosis*. In summary, our data suggests that HIF-1α plays a far more important role in the expression of important immune defenses against bacterial pathogens than has been previously appreciated. Determining the relative importance of each of these factors to the dramatic susceptibility of HIF-1α deficient mice will be the subject of future studies.

We also identify aerobic glycolysis as a novel component of IFN-γ dependent immunity. It was recently published that infection of unstimulated macrophages with *M. tuberculosis* induces aerobic glycolysis, and that this is a pathogenesis strategy employed by *M. tuberculosis* (35, 36). We also find that infection with *M. tuberculosis* induces a modest increase in glycolytic flux and lactate production in macrophages in the absence of IFN-γ, and that this is indeed ESX-1 dependent. However, we observe a much more dramatic shift to aerobic glycolysis in the presence of IFN-γ. In previous studies, treatment of macrophages with glycolytic inhibitors caused a decrease in *M. tuberculosis* replication in resting macrophages (35, 36). In contrast, we observed that glycolytic inhibition with 2-DG reversed control of *M. tuberculosis* replication in the context of IFN-γ activation, but had no impact in the absence of IFN-γ. One possible explanation for the different observations include the use of primary murine cells in our study as opposed to transformed human cell lines that have metabolic perturbations at baseline. An additional possibility is our use of significantly lower 2-DG concentrations that limit flux through glycolysis without impacting macrophage viability. It is also possible that in the context of a permissive growth environment *M. tuberculosis* actively induces and perhaps slightly benefits from heightened flux through glycolysis and concomitant nutrient availability, but when an infected macrophage is also activated with IFN-γ as part of an adaptive immune response, the immunometabolic program it adopts includes and is dependent upon aerobic glycolysis to differentiate into an effective microbicidal cell.

Our data supports a model in which HIF-1α contributes to a shift to aerobic glycolysis in *M. tuberculosis* infected and IFN-γ activated macrophages. However, as yet unidentified mechanisms also promote glycolysis, as the defect in HIF-1α deficient macrophages is only partial. Furthermore the fact that HIF-1α stabilization requires aerobic glycolysis suggests that a HIF-1α independent mechanism initially induces enhanced glycolytic flux, leading to stabilization of HIF-1α, which further promotes aerobic glycolysis by enhancing expression of glycolytic genes. The importance of aerobic glycolysis for IFN-γ dependent control of *M. tuberculosis* is likely at least partially explained by a positive feedback loop between glycolytic flux and HIF-1α that we identify in which aerobic glycolysis supports the immune effector functions mediated by HIF-1α. However, it is possible that aerobic glycolysis also mediates HIF-1α independent functions in IFN-γ dependent control of *M. tuberculosis* infection and gene expression in activated macrophages, for example via regulation of translation (38, 43).

In conclusion, we identify HIF-1α as an essential component of immunity to *M. tuberculosis in vitro* and *in vivo*. We further find that HIF-1α coordinates an immunometabolic program in IFN-γ activated and *M. tuberculosis* infected macrophages required for the transition to aerobic glycolysis and the production of numerous immune effectors including NO, IL-1 and PGE2. Finally, we demonstrate that aerobic glycolysis also contributes to HIF-1α stabilization, suggesting that positive feedback amplifies IFN-γ dependent activation of macrophages during *M. tuberculosis* infection.

Acknowledgements:
The authors gratefully acknowledge Tim Eubank for the kind gift of *Hif1a*$^{-/-}$ macrophages; Russell Vance for *LysMcre* and *Nos2*$^{-/-}$ mice; Jeffrey Cox and Paolo Manzanillo for the TB-lux strain; Russell Vance, Daniel Portnoy, and Jordan Price for helpful discussions; Katherine Chen for technical assistance. We thank Lutz Froenicke (DNA Technologies and Expression Analysis Core, UC Davis) and Monica Britton, Joseph Fass and Blythe Durbin (Genome Center and Bioinformatics Core Facility, UC Davis) for RNA-seq and data analysis. We thank Denise M. Imai-Leonard, DVM, PhD, DACVP (UC Davis Comparative Pathology Laboratory) for histological analysis.

References:

1. Floyd, K. 2012. *Global Tuberculosis Report 2012*, (World Health Organization, ed). WHO Press; :1–100.
2. Abel, L., and J.-L. Casanova. 2000. Genetic predisposition to clinical tuberculosis: bridging the gap between simple and complex inheritance. *American journal of human genetics* 67: 274.
3. Flynn, J. L., J. Chan, K. J. Triebold, D. K. Dalton, T. A. Stewart, and B. R. Bloom. 1993. An essential role for interferon gamma in resistance to Mycobacterium tuberculosis infection. *J. Exp. Med.* 178: 2249–2254.
4. Cooper, A. M., D. K. Dalton, T. A. Stewart, J. P. Griffin, D. G. Russell, and I. M. Orme. 1993. Disseminated tuberculosis in interferon gamma gene-disrupted mice. *J. Exp. Med.* 178: 2243–2247.
5. Zhang, Y. J., M. C. Reddy, T. R. Ioerger, A. C. Rothchild, V. Dartois, B. M. Schuster, A. Trauner, D. Wallis, S. Galaviz, C. Huttenhower, J. C. Sacchettini, S. M. Behar, and E. J. Rubin. 2013. Tryptophan biosynthesis protects mycobacteria from CD4 T-cell-mediated killing. *Cell* 155: 1296–1308.
6. Alonso, S., K. Pethe, D. G. Russell, and G. E. Purdy. 2007. Lysosomal killing of Mycobacterium mediated by ubiquitin-derived peptides is enhanced by autophagy. *Proc. Natl. Acad. Sci. U.S.A.* 104: 6031–6036.
7. Fabri, M., S. Stenger, D. M. Shin, J. M. Yuk, P. T. Liu, S. Realegeno, H. M. Lee, S. R. Krutzik, M. Schenk, P. A. Sieling, R. Teles, D. Montoya, S. S. Iyer, H. Bruns, D. M. Lewinsohn, B. W. Hollis, M. Hewison, J. S. Adams, A. Steinmeyer, U. Zugel, G. Cheng, E. K. Jo, B. R. Bloom, and R. L. Modlin. 2011. Vitamin D Is Required for IFN- -Mediated Antimicrobial Activity of Human Macrophages. *Sci Transl Med* 3: 104ra102–104ra102.
8. Gutierrez, M. G., S. S. Master, S. B. Singh, G. A. Taylor, M. I. Colombo, and V. Deretic. 2004. Autophagy is a defense mechanism inhibiting BCG and Mycobacterium tuberculosis survival in infected macrophages. *Cell* 119: 753–766.
9. MacMicking, J. D. 2003. Immune Control of Tuberculosis by IFN- -Inducible LRG-47. *Science* 302: 654–659.
10. Kim, B. H., A. R. Shenoy, P. Kumar, R. Das, S. Tiwari, and J. D. MacMicking. 2011. A Family of IFN- -Inducible 65-kD GTPases Protects Against Bacterial Infection. *Science* 332: 717–721.
11. Chan, J., Y. Xing, R. S. Magliozzo, and B. R. Bloom. 1992. Killing of virulent Mycobacterium tuberculosis by reactive nitrogen intermediates produced by activated murine macrophages. *J. Exp. Med.* 175: 1111–1122.
12. MacMicking, J. D., R. J. North, R. LaCourse, J. S. Mudgett, S. K. Shah, and C. F. Nathan. 1997. Identification of nitric oxide synthase as a protective locus against tuberculosis. *Proc. Natl. Acad. Sci. U.S.A.* 94: 5243–5248.
13. Tannahill, G. M., A. M. Curtis, J. Adamik, E. M. Palsson-McDermott, A. F. McGettrick, G. Goel, C. Frezza, N. J. Bernard, B. Kelly, N. H. Foley, L. Zheng, A. Gardet, Z. Tong, S. S. Jany, S. C. Corr, M. Haneklaus, B. E. Caffrey, K. Pierce, S. Walmsley, F. C. Beasley, E. Cummins, V. nizet, M. Whyte, C. T. Taylor, H. Lin, S. L.

Masters, E. Gottlieb, V. P. Kelly, C. Clish, P. E. Auron, R. J. Xavier, and L. A. J. O'Neill. 2013. Succinate is an inflammatory signal that induces IL-1β through HIF-1α. *Nature* 496: 238–242.
14. Shalova, I. N., J. Y. Lim, M. Chittezhath, A. S. Zinkernagel, F. Beasley, E. Hernández-Jiménez, V. Toledano, C. Cubillos-Zapata, A. Rapisarda, J. Chen, K. Duan, H. Yang, M. Poidinger, G. Melillo, V. Nizet, F. Arnalich, E. López-Collazo, and S. K. Biswas. 2015. Human monocytes undergo functional re-programming during sepsis mediated by hypoxia-inducible factor-1α. *Immunity* 42: 484–498.
15. Peyssonnaux, C., V. Datta, T. Cramer, A. Doedens, E. A. Theodorakis, R. L. Gallo, N. Hurtado-Ziola, V. Nizet, and R. S. Johnson. 2005. HIF-1alpha expression regulates the bactericidal capacity of phagocytes. *J. Clin. Invest.* 115: 1806–1815.
16. Lin, A. E., F. C. Beasley, J. Olson, N. Keller, R. A. Shalwitz, T. J. Hannan, S. J. hultgren, and V. nizet. 2015. Role of Hypoxia Inducible Factor-1α (HIF-1α) in Innate Defense against Uropathogenic Escherichia coli Infection. *PLOS Pathogens* 11: e1004818.
17. Berger, E. A., S. A. McClellan, K. S. Vistisen, and L. D. Hazlett. 2013. HIF-1α Is Essential for Effective PMN Bacterial Killing, Antimicrobial Peptide Production and Apoptosis in Pseudomonas aeruginosa Keratitis. *PLOS Pathogens* 9: e1003457.
18. Cramer, T., Y. Yamanishi, B. E. Clausen, I. Förster, R. Pawlinski, N. Mackman, V. H. Haase, R. Jaenisch, M. Corr, and V. Nizet. 2003. HIF-1α is essential for myeloid cell-mediated inflammation. *Cell* 112: 645–657.
19. Elks, P. M., S. Brizee, M. van der Vaart, S. R. Walmsley, F. J. van Eeden, S. A. Renshaw, and A. H. Meijer. 2013. Hypoxia Inducible Factor Signaling Modulates Susceptibility to Mycobacterial Infection via a Nitric Oxide Dependent Mechanism. *PLOS Pathogens* 9: e1003789.
20. Cardoso, M. S., T. M. Silva, M. Resende, R. Appelberg, and M. Borges. 2015. Lack of the transcription factor hypoxia-inducible factor (HIF)-1α in macrophages accelerates the necrosis of Mycobacterium avium-induced granulomas. *Infect. Immun.*
21. Anders, S., P. T. Pyl, and W. Huber. 2015. HTSeq--a Python framework to work with high-throughput sequencing data. *Bioinformatics* 31: 166–169.
22. Benjamin, D. I., A. Cozzo, X. Ji, L. S. Roberts, S. M. Louie, M. M. Mulvihill, K. Luo, and D. K. Nomura. 2013. Ether lipid generating enzyme AGPS alters the balance of structural and signaling lipids to fuel cancer pathogenicity. *Proc. Natl. Acad. Sci. U.S.A.* 110: 14912–14917.
23. Lee, J.-W., S.-H. Bae, J.-W. Jeong, S.-H. Kim, and K.-W. Kim. 2004. Hypoxia-inducible factor (HIF-1)alpha: its protein stability and biological functions. *Exp. Mol. Med.* 36: 1–12.
24. Mishra, B. B., V. A. K. Rathinam, G. W. Martens, A. J. Martinot, H. Kornfeld, K. A. Fitzgerald, and C. M. Sassetti. 2013. Nitric oxide controls the immunopathology of tuberculosis by inhibiting NLRP3 inflammasome-dependent processing of IL-1β. *Nat. Immunol.* 14: 52–60.
25. Eigenbrodm T, Bode K.A., Dalpke, A.H. 2013. Early inhibition of IL-1β expression by IFN-γ is mediated by impaired binding of NF-κB to the IL-1β promoter but is independent of nitric oxide. *J. Immunol.* 190: 6533–6541.
26. Mayer-Barber, K. D., B. B. Andrade, S. D. Oland, E. P. Amaral, D. L. Barber, J. Gonzales, S. C. Derrick, R. Shi, N. P. Kumar, W. Wei, X. Yuan, G. Zhang, Y. Cai, S.

Babu, M. Catalfamo, A. M. Salazar, L. E. Via, C. E. Barry, and A. Sher. 2014. Host-directed therapy of tuberculosis based on interleukin-1 and type I interferon crosstalk. *Nature* 511: 99–103.
27. Divangahi, M., D. Desjardins, C. Nunes-Alves, H. G. Remold, and S. M. Behar. 2010. Eicosanoid pathways regulate adaptive immunity to Mycobacterium tuberculosis. *Nat. Immunol.* 11: 751–758.
28. Chen, M., M. Divangahi, H. Gan, D. S. J. Shin, S. Hong, D. M. Lee, C. N. Serhan, S. M. Behar, and H. G. Remold. 2008. Lipid mediators in innate immunity against tuberculosis: opposing roles of PGE2 and LXA4 in the induction of macrophage death. *J. Exp. Med.* 205: 2791–2801.
29. Divangahi, M., M. Chen, H. Gan, D. Desjardins, T. T. Hickman, D. M. Lee, S. Fortune, S. M. Behar, and H. G. Remold. 2009. Mycobacterium tuberculosis evades macrophage defenses by inhibiting plasma membrane repair. *Nat. Immunol.* 10: 899–906.
30. Tobin, D. M., J. C. Vary, J. P. Ray, G. S. Walsh, S. J. Dunstan, N. D. Bang, D. A. Hagge, S. Khadge, M.-C. King, T. R. Hawn, C. B. Moens, and L. Ramakrishnan. 2010. The lta4h locus modulates susceptibility to mycobacterial infection in zebrafish and humans. *Cell* 140: 717–730.
31. Tobin, D. M., F. J. Roca, S. F. Oh, R. McFarland, T. W. Vickery, J. P. Ray, D. C. Ko, Y. Zou, N. D. Bang, T. T. H. Chau, J. C. Vary, T. R. Hawn, S. J. Dunstan, J. J. Farrar, G. E. Thwaites, M.-C. King, C. N. Serhan, and L. Ramakrishnan. 2012. Host genotype-specific therapies can optimize the inflammatory response to mycobacterial infections. *Cell* 148: 434–446.
32. Jung, F., L. A. Palmer, N. Zhou, and R. A. Johns. 2000. Hypoxic regulation of inducible nitric oxide synthase via hypoxia inducible factor-1 in cardiac myocytes. *Circ. Res.* 86: 319–325.
33. Kopp, F., T. Komatsu, D. K. Nomura, S. A. Trauger, J. R. Thomas, G. Siuzdak, G. M. Simon, and B. F. Cravatt. 2010. The Glycerophospho Metabolome and Its Influence on Amino Acid Homeostasis Revealed by Brain Metabolomics of GDE1(−/−) Mice. *Chemistry & Biology* 17: 831–840.
34. Colegio, O. R., N.-Q. Chu, A. L. Szabo, T. Chu, A. M. Rhebergen, V. Jairam, N. Cyrus, C. E. Brokowski, S. C. Eisenbarth, G. M. Phillips, G. W. Cline, A. J. Phillips, and R. Medzhitov. 2014. Functional polarization of tumour-associated macrophages by tumour-derived lactic acid. *Nature* 513: 559–563.
35. Singh, V., S. Jamwal, R. Jain, P. Verma, R. Gokhale, and K. V. S. Rao. 2012. Mycobacterium tuberculosis-Driven Targeted Recalibration of Macrophage Lipid Homeostasis Promotes the Foamy Phenotype. *Cell Host Microbe* 12: 669–681.
36. Mehrotra, P., S. V. Jamwal, N. Saquib, N. Sinha, Z. Siddiqui, V. Manivel, S. Chatterjee, and K. V. S. Rao. 2014. Pathogenicity of Mycobacterium tuberculosis is expressed by regulating metabolic thresholds of the host macrophage. *PLOS Pathogens* 10: e1004265.
37. Rossignol, R., R. Gilkerson, R. Aggeler, K. Yamagata, S. J. Remington, and R. A. Capaldi. 2004. Energy substrate modulates mitochondrial structure and oxidative capacity in cancer cells. *Cancer Research* 64: 985–993.
38. Chang, C.-H., J. D. Curtis, L. B. Maggi Jr, B. Faubert, A. V. Villarino, D. O'Sullivan, S. C.-C. Huang, G. J. van der Windt, J. Blagih, and J. Qiu. 2013. Posttranscriptional Control of T Cell Effector Function by Aerobic Glycolysis. *Cell* 153: 1239–1251.

39. Nandi, B., and S. M. Behar. 2011. Regulation of neutrophils by interferon-γ limits lung inflammation during tuberculosis infection. *Journal of Experimental Medicine* 208: 2251–2262.
40. Via, L. E., P. L. Lin, S. M. Ray, J. Carrillo, S. S. Allen, S. Y. Eum, K. Taylor, E. Klein, U. Manjunatha, J. Gonzales, E. G. Lee, S.-K. Park, J. A. Raleigh, S.-N. Cho, D. N. McMurray, J. L. Flynn, and C. E. Barry. 2008. Tuberculous granulomas are hypoxic in guinea pigs, rabbits, and nonhuman primates. *Infect. Immun.* 76: 2333–2340.
41. Aly, S., K. Wagner, C. Keller, S. Malm, A. Malzan, S. Brandau, F.-C. Bange, and S. Ehlers. 2006. Oxygen status of lung granulomas in Mycobacterium tuberculosis-infected mice. *J. Pathol.* 210: 298–305.
42. Klinkenberg, L. G., L. A. Sutherland, W. R. Bishai, and P. C. Karakousis. 2008. Metronidazole lacks activity against Mycobacterium tuberculosis in an in vivo hypoxic granuloma model of latency. *The Journal of Infectious Diseases* 198: 275–283.
43. Su, X., Y. Yu, Y. Zhong, E. G. Giannopoulou, X. Hu, H. Liu, J. R. Cross, G. Rätsch, C. M. Rice, and L. B. Ivashkiv. 2015. Interferon-γ regulates cellular metabolism and mRNA translation to potentiate macrophage activation. *Nat. Immunol.* 16: 838–849.

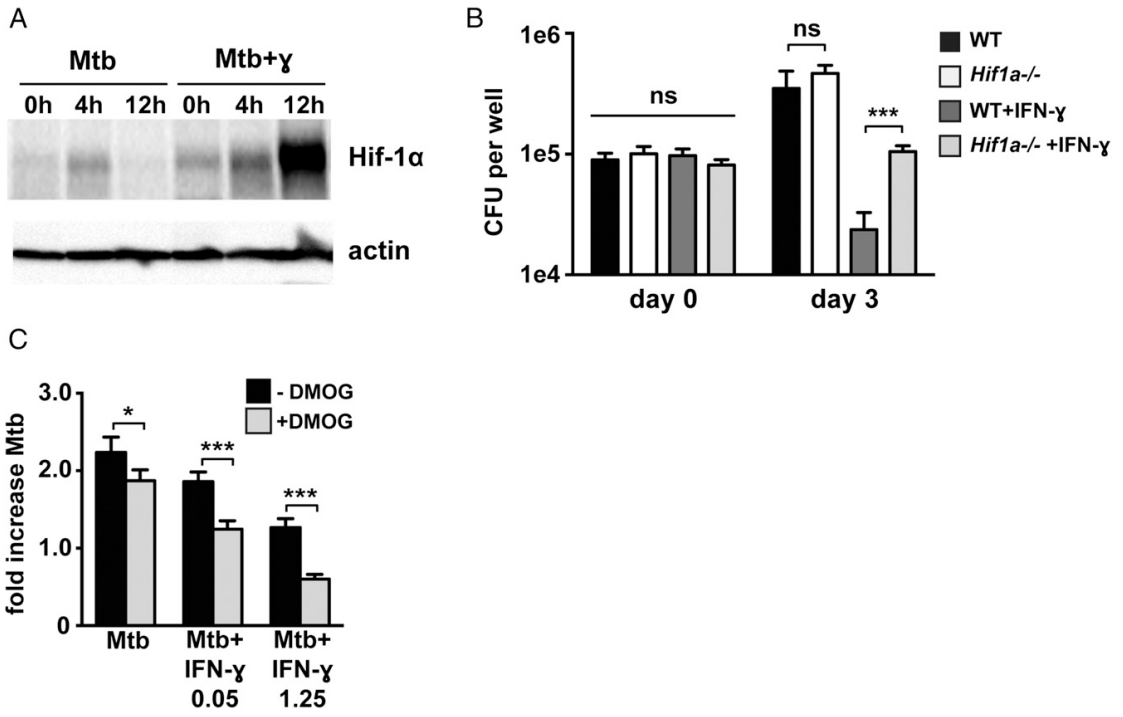

Figure 1. HIF-1α is required for IFN-γ based control of *M. tuberculosis* replication in macrophages. (A) Timecourse of HIF-1α protein stabilization by western blotting after infection of resting and IFN-γ activated WT BMDM with *M. tuberculosis* at MOI=5 with the 0h timepoint reflecting the end of the 4h phagocytosis period. (B) WT and Hif1a-/- BMDM were infected with *M. tuberculosis* at MOI=5 and bacterial replication was monitored with and without IFN-γ treatment by plating for CFU. CFU on day 0 and day 3 are shown. (C) Resting and IFN-γ activated WT BMDM were infected with the TB-lux strain of *M. tuberculosis* and treated with 200 μM DMOG after phagocytosis of bacteria. Bacterial growth was assessed by reading RLU immediately after phagocytosis and at 72h after infection and fold change is shown. For all experiments error bars represent the standard deviation of a minimum of quadruplicate wells and a representative experiment of a minimum of 3 is shown. p-values were determined using an unpaired t-test. ***$p \leq 0.001$, *$p \leq 0.05$.

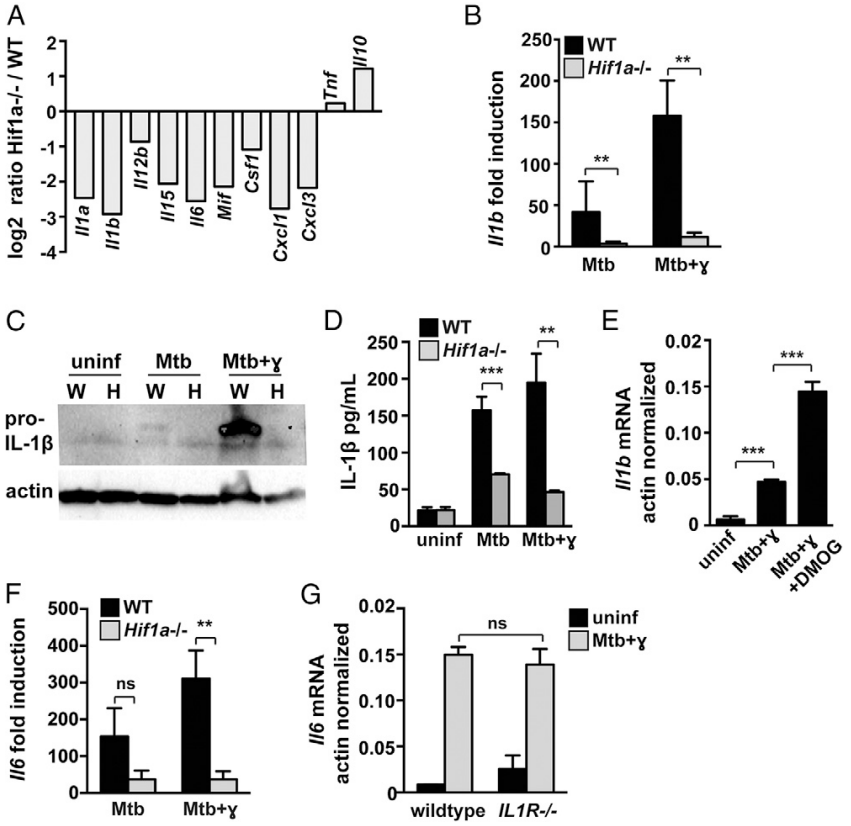

Figure 2. HIF-1α regulates cytokine and chemokine production. Resting and IFN-γ activated WT and *Hif1a*-/- BMDM were infected with *M. tuberculosis* at MOI=5. RNA was prepared for RNA-seq at 24h post infection. (A) RNA-seq data showing transcript levels of cytokines and chemokines in *Hif1a*-/- BMDM relative to WT BMDM on a log2 scale. Data shown is from macrophages treated with IFN-γ and infected with *M. tuberculosis*. (B) RNA-seq data showing fold induction of *Il1b* transcript over untreated macrophages in WT and *Hif1a*-/- BMDM (C) Western blotting for pro-IL-1b from cell lysates at 12h after infection in wild-type [W] and *Hif1a*-/- [H] macrophages. (D) ELISA for IL1b from cell supernatants at 36h after infection. (E) qPCR data showing actin normalized *Il1b* transcript in WT BMDM with DMOG treatment. (F) RNAseq data showing fold induction of *Il6* transcript over untreated macrophages in WT and *Hif1a*-/- BMDM (G) qPCR data showing actin normalized *Il6* transcript levels in WT and IL1R deficient BMDM. For RNA-seq, RNA was prepared from 3 independent infections. All other experiments were repeated 2-3 times and representative experiments are shown. Error bars represent standard deviation. p values were determined using an unpaired t-test. ***p≤0.001, **p≤0.01, *p≤0.05.

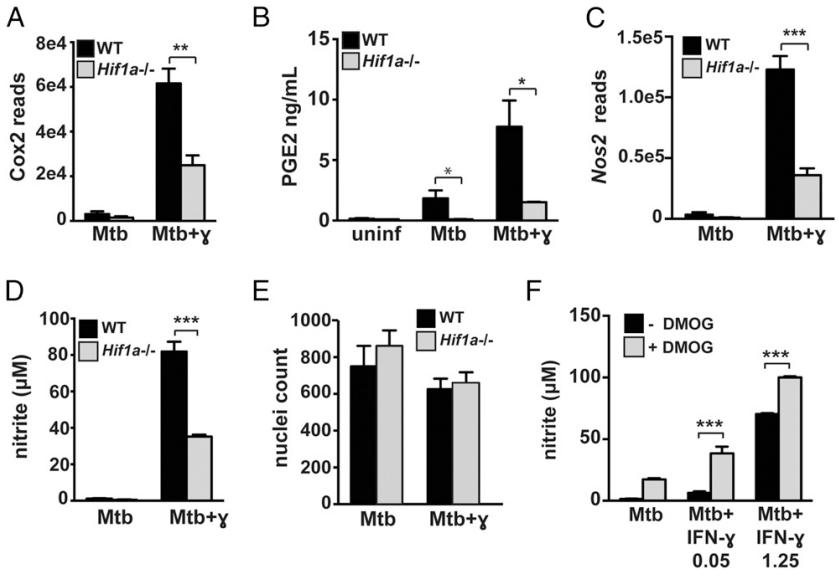

Figure 3. HIF-1α is required for full activation of IFN-γ dependent cell intrinsic immune responses. Resting and IFN-γ activated WT and *Hif1a*-/- BMDM were infected with *M. tuberculosis* at MOI=5. RNA was prepared for RNA-seq at 24h post infection. (A) RNA-seq data showing expression levels of *Cox2* (official name *Ptgs2*) in WT and *Hif1a*-/- BMDM. (B) PGE2 ELISA from macrophage supernatants at 36h after infection. (C) RNA-seq data showing expression levels of *Nos2* in WT and *Hif1a*-/- BMDM (D) Griess assay for nitric oxide production in WT and *Hif1a*-/- BMDM. (E) Nuclei counts after DAPI staining in WT and *Hif1a*-/- BMDM 24h after infection. (F) Resting and IFN-γ activated BMDM were infected with *M. tuberculosis* and treated with 200 μM DMOG after phagocytosis of bacteria and a Griess assay was performed 72h after infection. For RNA-seq, RNA was prepared from 3 independent infections. All other experiments are representative of 3 or more. Error bars represent standard deviation. p-values were determined using an unpaired t-test. ***p≤0.001, **p≤0.01, *p≤0.05.

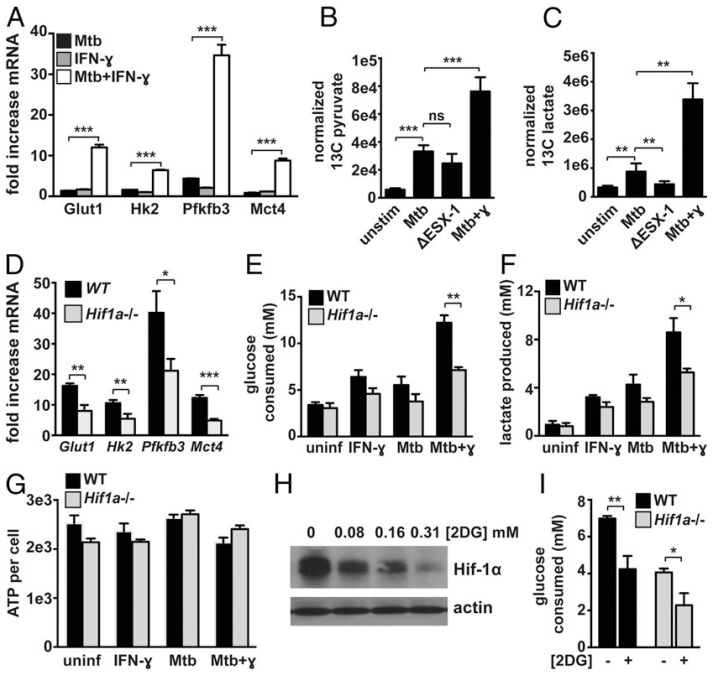

Figure 4. HIF-1α mediates the transition to aerobic glycolysis in *M. tuberculosis* infected macrophages but is not required for maintenance of ATP production. (A) Fold increase in transcript levels over resting BMDM for the glycolytic genes *Glut1*, *Hk2, Pfkfb3*, and *Mct4* were measured by qPCR in WT BMDM. (B and C) BMDM infected with *M. tuberculosis* were cultured in media containing 13C labeled glucose for 24h at which time lysates were prepared and 13C labeled pyruvate (B) and lactate (C) were detected by LC-MS/MS. Values represent the average of quintuplicate wells and error is standard deviation. (D) RNAseq data showing fold increase over resting BMDM of glycolytic genes in WT and *Hif1a*-/- BMDM treated with IFN-γ and infected with M. tuberculosis. (E) Glucose consumption after 36h by WT and *Hif1a*-/- BMDM. (F) Lactate production after 24h by WT and Hif1a-/- BMDM. (G) ATP levels were measured using a luciferase based assay (CellTiter-Glo) and were normalized to cell number measured by DAPI staining and counting of nuclei. (H) HIF-1α western blot 12h after *M. tuberculosis* infection of IFN-γ treated BMDM, treated with increasing dose of 2-DG following 4h phagocytosis period. (I) Glucose consumption 24h post infection of WT and *Hif1a*-/- BMDM with and without 2DG treatment. Data in (A),(D),(E),(F) and (H) are representative of 3 or more experiments, data in (G) and (I) are representative of 2 experiments. Error bars represent standard deviation. p-values were determined using an unpaired t-test. ***p≤0.001, **p≤ 0.01, *p≤0.05

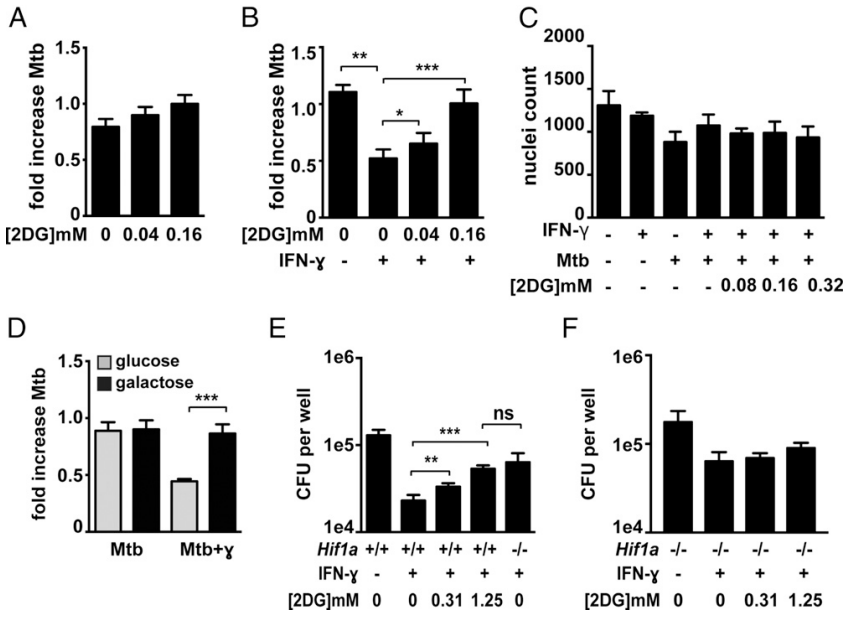

Figure 5. Enhanced flux through glycolysis is required for IFN-γ dependent control of *M. tuberculosis* infection. Resting (A) and IFN-γ activated (B) BMDM were infected with the TB-lux strain *of M. tuberculosis* and treated with 2DG immediately after the 4h phagocytosis period. Bacterial growth was assessed by reading RLU immediately after phagocytosis and at 24h after infection and fold change is shown. (C) Macrophage viability was assessed using DAPI staining of nuclei and microscopy 24h after infection. (D) Resting and IFN-γ activated macrophages were infected with the TB-lux strain of *M. tuberculosis* and were switched to glucose free media containing galactose immediately after the 4h phagocytosis period and fold growth was determined at 24h after infection. (E and F) WT and *Hif1a*-/- BMDM were infected with *M. tuberculosis* at MOI=5 and bacterial replication was monitored by plating for CFU. 2DG treatment at the indicated concentrations began after the 4h phagocytosis and 2DG was washed out 24h later. CFU 72h post infection is shown. Representative experiments of 3 or more are shown for (A-D) and representative of 2 experiments for (E) and (F). Error bars are standard deviation from 3-6 replicate wells for TB-lux data, 3 replicate wells for nuclei counts, and 5 replicate wells for CFU. p-values were determined using an unpaired t-test, ***p≤ 0.001, **p≤0.01, *p≤0.05

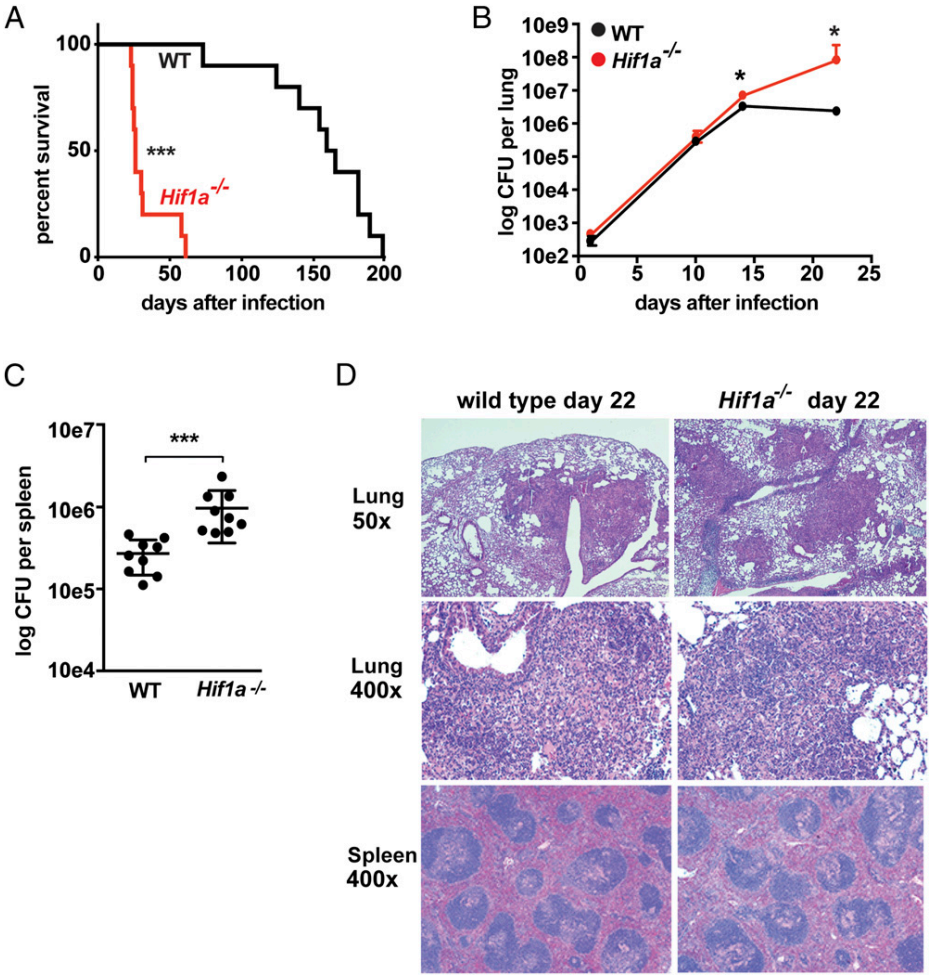

Figure 6. HIF-1α is required for control of *M. tuberculosis* infection in vivo. WT and *Hif1a*-/- mice on the C57BL/6 background were infected with ~400 CFU of the virulent *M. tuberculosis* strain Erdman via the aerosol route. (A) Survival following aerosol infection is shown for WT and *Hif1a*-/- mice. Experiment shown is representative of three experiments using 10-12 mice per genotype. (B) Bacterial loads in the lungs of WT and *Hif1a*-/- mice were enumerated by plating for CFU. Timecourse is representative of 3 experiments with 4-5 mice used per group at each timepoint. (C) Bacterial loads in the spleens at 21d after infection. Data from two pooled experiments are shown. (D) Lung tissues were fixed, embedded in paraffin, sectioned, and stained with haematoxylin and eosin. Images were obtained at 50x and 400x magnification. Error bars represent standard deviation. For survival curves p values were determined using the Mantel-Cox log. For CFU, p-values were determined using Mann-Whitney U. ***$p<0.001$, *$p\leq0.05$.

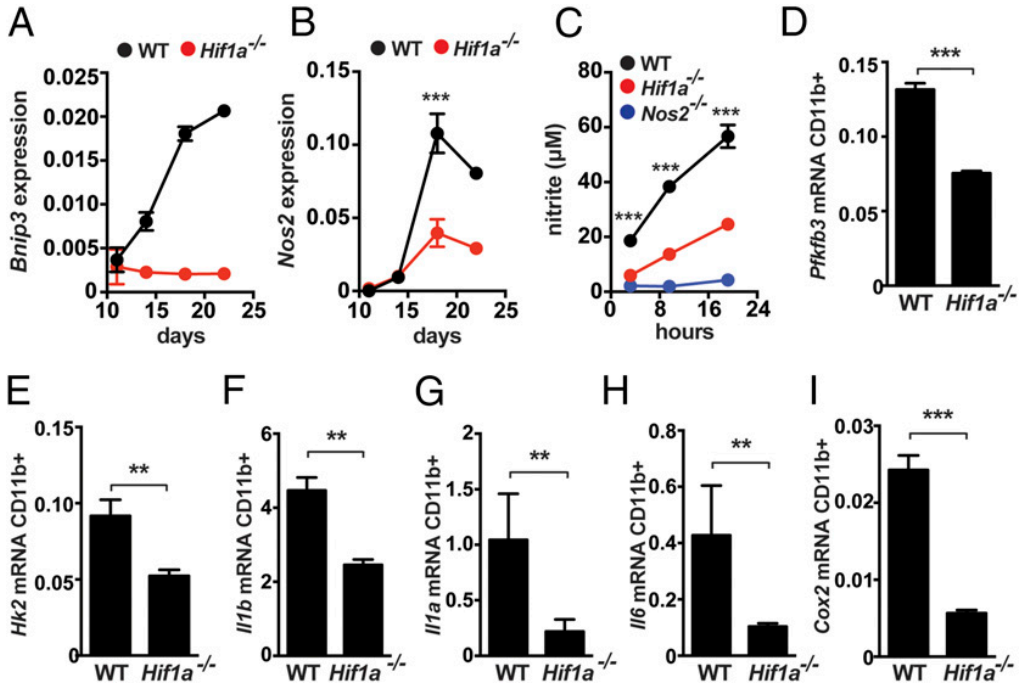

Figure 7. HIF-1α regulates immune effectors in vivo. WT and *Hif1a*-/- mice on the C57BL/6 background were infected with ~400 CFU of the virulent *M. tuberculosis* strain Erdman via the aerosol route. CD11b+ cells were isolated from lungs of infected mice at the indicated timepoints and analyzed by qPCR for expression of *Bnip3* (A) and *Nos2* (B). (C) isolated CD11b+ cells were plated and the supernatants were assayed for nitric oxide production by Griess assay at the indicated timepoints. (D-I) qPCR from isolated from CD11b+ cells at 21 days post-infection in WT and Hif1a-/- mice. Data shown in (C-I) is representative of 2-3 experiments. p-values were determined using an unpaired t-test, ***p≤ 0.001, **p≤0.01.

Figure S1

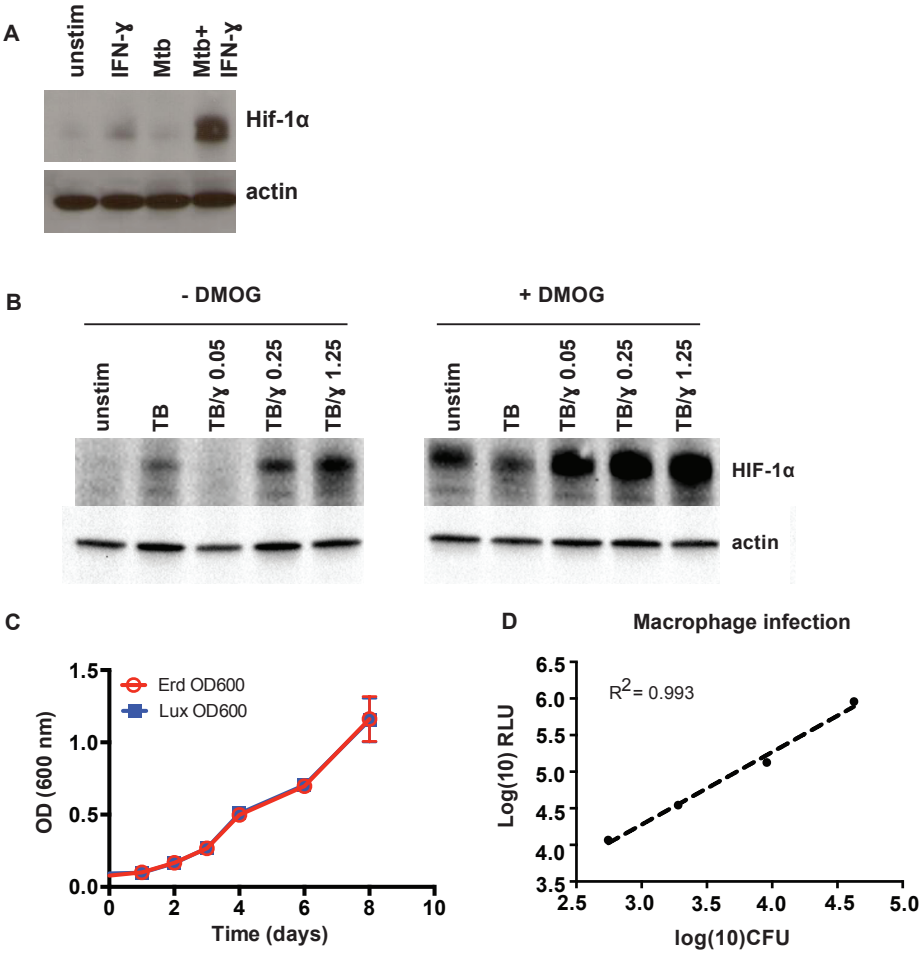

Figure S1. Characterization of DMOG treatment of BMDM and characterization of TB-lux expressing the *luxCDABE* operon. (A) HIF-1α western blot at 12h post infection. IFN-γ is at 1.25ng/ml (B) HIF-1α western blot 12h post-infection of WT BMDM with IFN-γ dose response (.05-1.25ng/ml) with and without addition of 200uM DMOG at the end of the 4hr phagocytosis (C) wildtype (Erdman) *M. tuberculosis* was compared to Erdman carrying a plasmid that constitutively expresses the *luxCDABE* operon. Bacteria were seeded into 7H9 at an OD600 of 0.05. OD600 measurements were taken daily to demonstrate that expression of the *luxCDABE* operon does not inhibit growth. (D) BMDM were infected with different MOIs of bacteria expressing the *luxCDABE* operon. After a 4h phagocytosis, the infected macrophages were washed and media was replaced. Luminescence was measured, and subsequently the infected monolayers were lysed and plated for CFU.

Figure S2

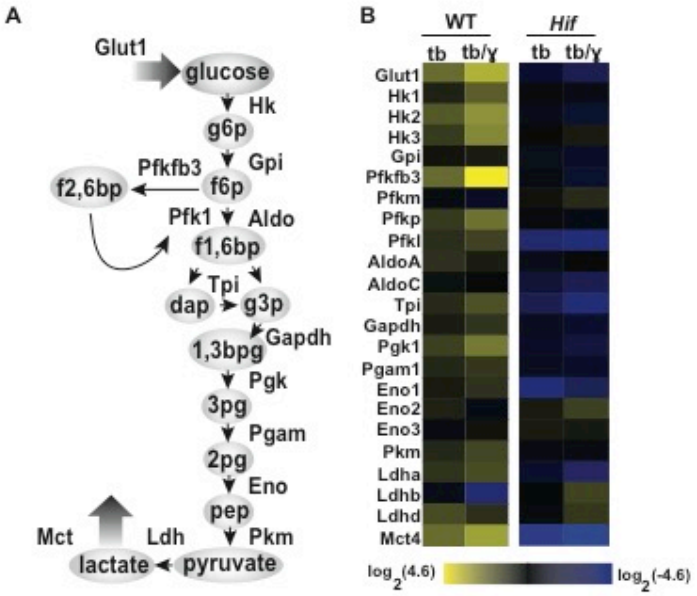

Figure S2. HIF-1α activates expression of glycolytic genes in *M. tuberculosis* infected macrophages. (A) Glycolysis pathway depicting metabolites (grey bubbles) and enzymes. (B) Heat map depicting relative expression data from RNA-seq. Wild-type (WT) is relative to uninfected; HIF-1α deficient (Hif) is relative to the same condition in WT. glucose 6 phosphate (g6p), fructose 6 phosphate (f6p), fructose 2,6 bisphosphate (f2,6bp), fructose 1,6 bisphosphate (f1,6bp), dihydroxyacetone phosphate (dap), glyceraldehyde 3 phosphate (g3p) 1,3 bisphosphoglycerate (1,3bpg), 3-phosphoglycerate (3pg), 2-phosphoglycerate (2pg), phosphoenoylpyruvate (pep).

Figure S3

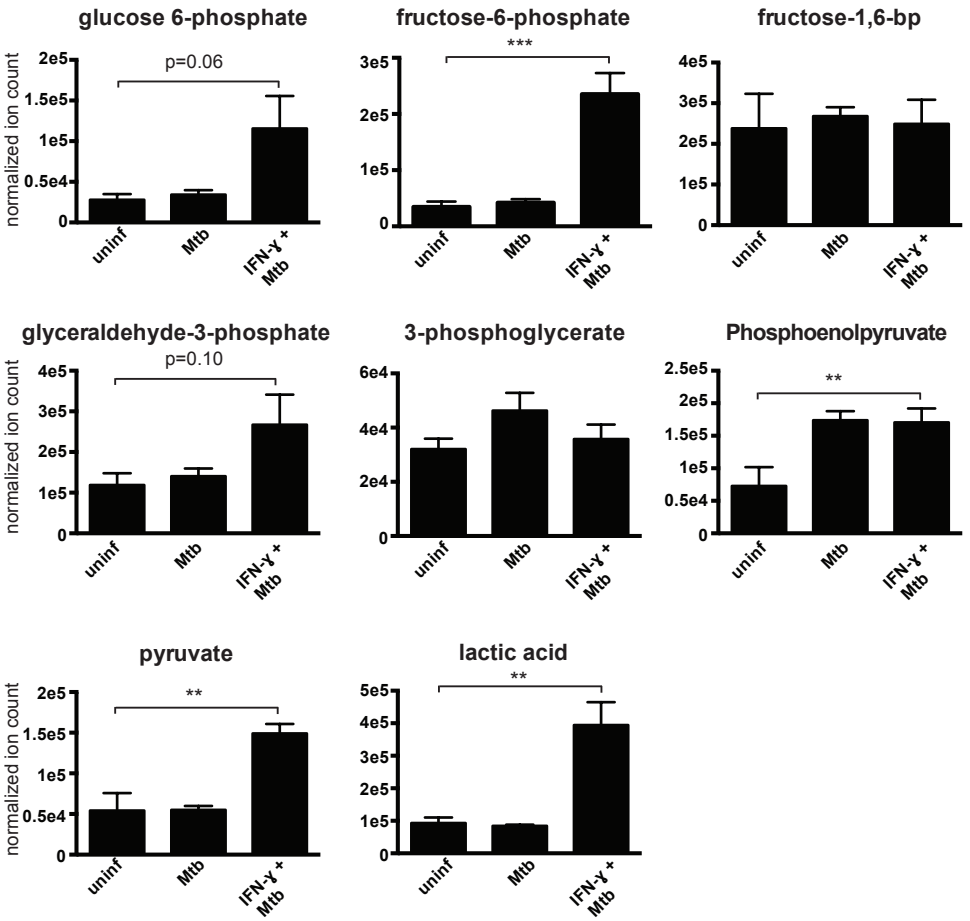

Figure S3. Steady state levels of glycolytic intermediates in cells infected with *M. tuberculosis*. Resting and IFN-γ activated WT BMDM were infected with *M. tuberculosis* at MOI=1. Metabolite levels were measured using high-resolution tandem mass spectrometry in quintuplicate samples 24h post-infection and were normalized to an external control. Dihydroxyacetone phosphate (DHAP) and glyceraldehyde-3-P are isomers that are indistinguishable by mass spectrometry and are represented as glyceraldehyde-3-P. Error bars represent SEM. p-values were determined by unpaired t-test ***p≤0.001, **p≤ 0.01.

Figure S4

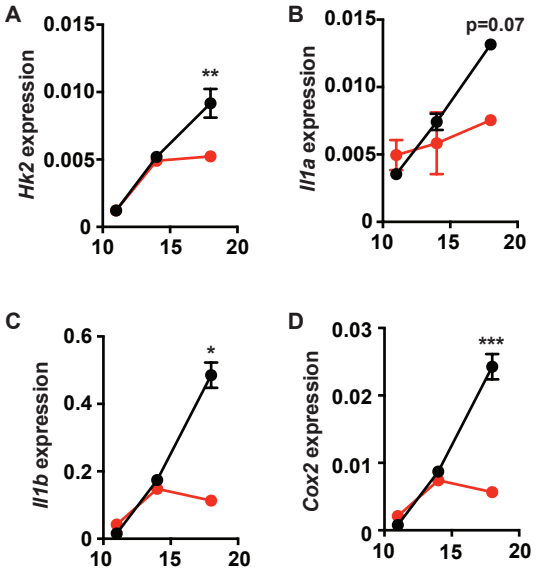

Figure S4. HIF-1α target genes are regulated *in vivo* after the onset of IFN-γ. CD11b+ cells were isolated from lungs of infected mice as in Figure 7 and analyzed by qPCR. (A-D) Timecourse of actin normalized expression of the indicated genes. WT is in black and HIF-1α-/- is in red. p-values were determined using an unpaired t-test, ***p≤ 0.001, **p≤0.01, *p≤0.05.

Chapter Two: Nitric Oxide Modulates Macrophage Responses to *Mycobacterium tuberculosis* Infection Through Activation of HIF-1α and Repression of NF-kB

This work is currently under review at the Journal of Immunology
Jonathan Braverman and Sarah A. Stanley

Abstract:
IFN-γ is essential for control of *Mycobacterium tuberculosis* infection *in vitro* and *in vivo*. However, the mechanisms by which IFN-γ controls infection remain only partially understood. One of the crucial IFN-γ target genes required for control of *M. tuberculosis* is Inducible nitric oxide synthase (iNOS). While nitric oxide (NO) produced by iNOS is thought to have direct bactericidal activity against *M. tuberculosis*, the role of NO as a signaling molecule has been poorly characterized in the context *M. tuberculosis* infection. Here, we find that iNOS broadly regulates the macrophage transcriptome during *M. tuberculosis* infection, activating antimicrobial pathways while also limiting inflammatory cytokine production. The transcription factor Hypoxia inducible factor-1α (HIF-1α) was recently shown to be critical for IFN-γ mediated control of *M. tuberculosis* infection. We find that HIF-1α function requires NO production, and that HIF-1α and iNOS are linked by a positive feedback loop that amplifies macrophage activation. Furthermore, we find that NO inhibits NF-kB activity to prevent hyper-inflammatory responses. Thus, NO activates robust microbicidal programs while at the same time limiting damaging inflammation. IFN-γ signaling must carefully calibrate an effective immune response that does not cause excessive tissue damage, and this work identifies NO as a key player in establishing this balance during *M. tuberculosis* infection.

Introduction:

Mycobacterium tuberculosis infection is responsible for an enormous burden of morbidity and mortality worldwide, causing ~1.5 million deaths annually (1). Successful immunity to *M. tuberculosis* infection requires the cytokine Interferon-γ (IFN-γ) (2, 3). The dependence on IFN-γ for control of *M. tuberculosis* infection can be seen both in cell culture and mouse models of infection, and patients lacking components of the IFN-γ signaling pathway are extremely susceptible to mycobacterial infections (4). While the essentiality of IFN-γ activation to successful control of *M. tuberculosis* infection is well established, the mechanisms through which this occur remain poorly understood. IFN-γ activation of macrophages is thought to control infection by transforming infected macrophages into a microbicidal environment, while also limiting damaging inflammation caused by recruitment of neutrophils (5-7).

Multiple IFN-γ dependent mechanisms of cell intrinsic control of *M. tuberculosis* have been proposed, including restriction of nutrient availability, enhanced production of antimicrobial peptides, induction of autophagy, and the production of nitric oxide (NO) by Inducible nitric oxide synthase (iNOS) (8-13). Mice deficient for iNOS are extremely susceptible to *M. tuberculosis* infection (13), accounting for a substantial portion of the susceptibility of IFN-γ deficient mice. While the role of NO as a second messenger that regulates mammalian signaling is well known, in the context of *M. tuberculosis* infection the possible regulatory roles of NO have been mostly overlooked. Instead, the susceptibility of iNOS deficient mice has long been attributed to direct bactericidal activity of NO (5, 14). However, several lines of evidence suggest that this model is incomplete. First, a study using microarrays to examine the transcriptional response to *M. tuberculosis* infection in the context of IFN-γ activation demonstrated that a large proportion of the gene expression changes observed under these conditions require expression of iNOS and/or phagosome oxidase (phox) (15). Although this study made the important point that NO likely modulates signaling during *M. tuberculosis* infection, a mechanistic basis for the impact of NO on the macrophage transcriptome was not identified. More recently, it was shown that the ability of NO to suppress inflammasome dependent production of IL-1 is important to prevent excessive inflammation that contributes to immune pathology independent of bacterial growth in mice infected with *M. tuberculosis* (16).

In this study, we demonstrate that NO has a broad impact on the macrophage transcriptome during *M. tuberculosis* infection and identify key regulatory pathways through which this occurs. We find that during *M. tuberculosis* infection NO is required for IFN-γ dependent stabilization of HIF-1α, a transcription factor we have recently shown to be critical for control of *M. tuberculosis* infection (17). Interestingly, we find that HIF-1α and iNOS are linked in a positive feedback loop during IFN-γ activation of *M. tuberculosis* infected macrophages. RNAseq profiling reveals that HIF-1α and iNOS regulate a largely overlapping set of genes, suggesting that iNOS plays an unexpectedly broad role in mediating antibacterial responses of macrophages, via the activation of HIF-1α. Surprisingly, we also find that HIF-1α and iNOS antagonistically regulate a small but critical set of inflammatory cytokines and chemokines that are positively regulated by HIF-1α but negatively regulated by iNOS. We find that iNOS suppresses prolonged nuclear localization of the NF-kB family member RelA and that this activity at least partially explains the divergent functions of iNOS that allow both an enhancement of

antimicrobial responses and suppression of excessive inflammatory cytokine and chemokine production. These findings fit with an emerging understanding that IFN-γ signaling must carefully calibrate an effective immune response that does not cause excessive tissue damage, and provide further support for the hypothesis that NO is a key player in establishing this balance.

Materials and Methods:

Ethics Statement
All procedures involving the use of mice were approved by the University of California, Berkeley IACUC, the Animal Care and Use Committee (protocol number R353-1113B). All protocols conform to federal regulations, the National Research Council's *Guide for the Care and Use of Laboratory Animals* and the Public Health Service's (PHS's) *Policy on Humane Care and Use of Laboratory Animals*.

Reagents
Recombinant mouse IFN-γ (485 MI/CF) was obtained from R&D systems. 1400W, and Dimethyloxalylglycine (DMOG) were obtained from Cayman Chemical. Pam3CysK4 (PAM) was obtained from EMC Microcollections. Ascorbate and S-Nitroso-N-acetylpenicillamine (SNAP) were obtained from Sigma-Aldrich. The following primary antibodies were used: HIF-1α (NB100-479, Novus Biologicals), IL-1b (AF-401-NA, R&D systems), and the following Cell Signaling Technology antibodies: HIF-1α (D2U3T), RelA (D14E12), RelB (C1E4), NF-kB1 (D4P4D), IkBa (L35A5), α/β-Tubulin (2148), Histone H3 (D1H2), and β-actin (13E5).

Mice
Wildtype mice were C57BL/6, were obtained from Jackson Laboratory, and then bred in house. All knockout mice are on the C57BL/6 background. B6.129-*Hif1a*^{tm3Rsjo}*/J* (HIF1α^{flox}) mice were obtained from the Jackson Laboratory and were crossed with B6.129P2-*Lyz2*$^{tm1(cre)Ifo}$*/J* (LysMcre) to generate *Hif1a*$^{flox/flox}$,LysMcre$^{+/+}$ mice that had *Hif1a* deletion targeted to the myeloid lineage. B6.129P2-*Nos2*^{tm1Lau}*/J* (iNOS-) mice were obtained from the Jackson Laboratory and were bred in house, and also crossed to *Hif1a*$^{flox/flox}$,LysMcre$^{+/+}$ mice to generate *Hif1a*$^{flox/flox}$, LysMcre$^{+/+}$, Nos2$^{-/-}$ mice. NFkB-RE-luc mice (10499, Taconic) on the BALB/c background were obtained and BMDM were prepared from these mice for NFkB-luciferase experiments.

Cell Culture
Macrophages were derived from bone marrow of wildtype, Nos2$^{-/-}$, *Hif1a*$^{flox/flox}$,LysMcre$^{+/+}$, and *Hif1a*$^{flox/flox}$, LysMcre$^{+/+}$, Nos2$^{-/-}$ by culturing in DMEM with 10% FBS, 2 mM L-glutamine and 10% supernatant from 3T3-M-CSF cells for 6 days with feeding on day 3. After differentiation, macrophages were cultured in DMEM supplemented with 10% FBS, 2mM GlutaMAX, and 10% supernatant from 3T3-M-CSF cells (BMDM media).

Bacterial culture
The *M. tuberculosis* strain Erdman was used for all experiments. *M. tuberculosis* was grown in Middlebrook 7H9 liquid media supplemented with 10% ADS (albumin-dextrose-saline), 0.4% glycerol, and 0.05% Tween-80. The fluorescent mCherry strain used for microscopy was derived from an Erdman strain, with episomal PMV261 containing Zeo-mCherry under the GroEL promoter.

***In vitro* infections**

BMDM were plated into 96-well or 24-well plates with $5x10^4$ and $3x10^5$ macrophages per well respectively, and were allowed to adhere and rest for 24 hours. For all experiments where IFN-γ was used, BMDM were pretreated with IFN-γ overnight (at 6.25ng/ml unless otherwise indicated) and then infected in DMEM supplemented with 5% horse serum and 5% FBS at MOI=5. After a 4-hour phagocytosis period, infected BMDM were washed with PBS before replacing with BMDM media. For experiments with 1400W or DMOG, these reagents were added to the BMDM media after the 4-hour phagocytosis. For IFN-γ pretreated wells, IFN-γ was also added after infection at the same concentration. For enumeration of CFU, infected BMDM were washed with PBS, lysed in water with 0.5% Triton-X for ten minutes at 37C, and serial dilutions were prepared in PBS with 0.05% Tween-80 and plated onto 7H10 plates.

For experiments using the RAW-NF-κB luciferase reporter cells (a kind gift from Greg Barton), cells were plated and infections were performed once cells reached ~75% confluence. Complete RPMI media was used, and infections were performed as described above with the following difference: IFN-γ was only added post-infection. For conditions with 1400W, it was added the same time as IFN-γ, immediately following the 4-hour phagocytosis. To measure luciferase reporter activity, the Dual-Luciferase Reporter Assay Sytem (E1910, Promega) was used as per the manufacturer's protocol.

Glucose assays

Glucose depletion from the media was measured using the Glucose (HK) assay kit (GAHK20, Sigma Aldrich). The protocol was modified to perform the assays in 96 well plates with 100uL reactions instead of 1mL reactions in cuvettes as described in the manufacturer's protocol. Glucose consumption was calculated by measuring glucose levels in the media after infection and subtracting from glucose measured in cell-free media.

ELISAs

For IL-1β ELISAs, supernatants from BMDM in 24 well plates were used. A mouse IL-1 β ELISA kit (DY401, R&D systems) was used as per the manufacturer's protocol.

Western blots. BMDM were washed with PBS, lysed in 1x SDS-PAGE buffer on ice, and heat sterilized for 20 min at 100°C before removal from the BSL3 facility. Total protein lysates were analyzed by SDS-PAGE using pre-cast Tris-HCl criterion gels (Bio-Rad). HRP conjugated secondary antibodies were used. Western Lightning Plus-ECL chemiluminescence substrate (PerkinElmer) was used and blots were developed on film or using a ChemiDoc MP System (Bio-Rad).

qRT-PCR and RNA-seq. For q-RT-PCR, $3x10^5$ BMDM were seeded in 24-well dishes and infected as described. At 24h post-infection, cells were washed with room temperature PBS and lysed in 1 mL TRIzol (Invitrogen Life Technologies). Total RNA was extracted using chloroform (200 μL) and the aqueous layer was further purified using RNeasy spin columns (Qiagen). For qPCR, cDNA was generated from 1 μg of RNA using Superscript III (Invitrogen Life Technologies) and Oligo-dT primers. Select genes were analyzed using Maxima SYBR green qPCR master mix (Thermo Scientific). Each sample was analyzed in triplicate on a CFX96 Real-time PCR detection system (Bio-

Rad). C_Q values were normalized to values obtained for actin and relative changes in gene expression were calculated using the $\Delta\Delta C_Q$ method. All methods for iNOS RNA-seq were performed as previously described (17). Although the iNOS dataset was not previously reported, the data was collected simultaneously with the wildtype and HIF-1α datasets. Data for selected genes from the wildtype and HIF-1α deficient macrophages was depicted in a previous publication (17). RNAseq data is from three independent infections, and all error bars represent the SD between the three independent infections. RNA-seq was performed at the Genome Center and Bioinformatics Core Facility at the University of California, Davis.

Microscopy

BMDM were plated on glass coverslips in 24 well plates at $3x10^5$ per coverslip, and infected with *M. tuberculosis* Erdman-mCherry. 24h post-infection, coverslips were fixed in formalin, and stained for RelA. Microscopy was performed on a Carl Zeiss LSM710 confocal microscope. Images shown were taken with a 63x objective. For quantification, larger fields were taken with a 20x objective. Nuclear fluorescence from RelA staining was quantified from a minimum of 800 cells for each condition. Microscopy was performed at The CNR Biological Imaging Facility at The University of California, Berkeley. Research reported in this publication was supported in part by the National Institutes of Health S10 program under award number 1S10RR026866-01.

Transcription factor prediction

oPOSSUM, a tool for identification of over-represented transcription factor binding sites in co-expressed genes (18) was used to predict transcription factors regulated by NO. To identify transcription factors activated by NO, oPOSSUM analysis was run on all genes found to be lower in the $Nos2^{-/-}$ BMDM during *M. tuberculosis* infection with IFN-γ activation in our RNAseq data. To identify transcription factors inhibited by NO, oPPOSSUM analysis was run all genes found to be 4-fold or more elevated in the $Nos2^{-/-}$ BMDM during *M. tuberculosis* infection with IFN-γ activation.

Ingenuity IPA analysis, which utilizes curated experimental data to predict transcription factor regulation was also performed. To predict transcription factors both activated and inhibited by NO, analysis was performed on all genes 2fold or more upregulated or downregulated and statistically significant ($p<.05$) in the $Nos2^{-/-}$ BMDM during *M. tuberculosis* infection with IFN-γ activation in our RNAseq data.

***In vivo* infections**

Cohorts of age and sex matched wild-type and $Nos2^{-/-}$ mice were infected by aerosol route with *M. tuberculosis* strain Erdman at a dose of ~300 CFU. All mice were on the C57BL/6 background, and were 7-12 weeks of age when infected. Aerosol infection was done using a Nebulizer and Full Body Inhalation System (Glas-Col). Mice were weighed the day of infection, and weights were followed until a humane 15% weight loss cutoff was reach at which point the mice were euthanized. Neutrophil depletions were performed as described in (7), using the anti-Ly6G mAb (clone 1A8, BioXcell) or an isotype control (clone 2A3, BioXcell). 200ug antibody was injected every other day starting 10 days post-infection. Alternatively, the anti-Ly6G/Ly6C mAb (clone RB6-

8C5, BioXcell) was used, with 250ug antibody or isotype control injected every other day starting 10 days post-infeciton.

Results:

Nitric oxide shapes the macrophage transcriptome during infection

To identify potential signaling roles for nitric oxide (NO) during *M. tuberculosis* infection, we performed RNAseq on wildtype and iNOS deficient (*Nos2*$^{-/-}$) bone marrow derived macrophages (BMDM). We found that upon infection of IFN-γ activated BMDM with *M. tuberculosis*, over 1500 genes were differentially expressed in *Nos2*$^{-/-}$ BMDM compared with wildtype (Figure 1A, Dataset S1). A much smaller number of genes were differentially expressed upon infection with *M. tuberculosis* in the absence of IFN-γ activation, and the transcriptome of resting wildtype and *Nos2*$^{-/-}$ BMDM were essentially identical (Figure 1A, Dataset S1). This correlates with NO production, which is undetectable in resting BMDM, very low with *M. tuberculosis* infection alone, and robust with IFN-γ activation combined with *M. tuberculosis* infection (Figure 1B). The NO dependent alterations to the macrophage transcriptome are extensive, and comprise 32% of all IFN-γ regulated genes during *M. tuberculosis* infection (Figure 1C).

The large number of genes dependent on NO production for expression suggests that NO might impact the function of global transcriptional regulators. To identify candidate transcription factors regulated by NO during *M. tuberculosis* infection, we applied two bioinformatic methods to our RNA-seq dataset. First, we used Ingenuity IPA analysis, which utilizes curated experimental data to predict transcription factor regulation. Transcription factors predicted to be activated by NO, and transcription factors predicted to be inactivated by NO are listed in (Table S1A). Second, we used oPOSSUM, a tool for identification of over-represented transcription factor binding sites in co-expressed genes (18). Analysis of genes positively regulated by NO (downregulated in *Nos2*$^{-/-}$ BMDM) using both IPA and oPOSSUM identified HIF-1α (Figure 1D, Table S1A, Table S1B), which we have recently identified as a key mediator of IFN-γ dependent control of *M. tuberculosis* infection (17).

iNOS activates HIF-1α signaling

As HIF-1α was identified in our analysis as a potential NO regulated transcription factor, and has been shown to be important for control of *M. tuberculosis* infection, we selected this transcription factor for further analysis. The genes *Egln3* and *Bnip3* are canonical HIF-1α dependent target genes (19). In *M. tuberculosis* infected macrophages where production of NO is low, we observed low levels of *Egln3* and *Bnip3* expression that are HIF-1α dependent but NO independent (Figure 2A, 2B). However, in IFN-γ stimulated and *M. tuberculosis* infected BMDM, where NO production is high, we observed an upregulation of *Egln3* and *Bnip3* that is strongly dependent on both HIF-1α and iNOS (Figure 2A, 2B). In resting macrophages, HIF-1α is constitutively transcribed and translated, but kept at low levels by constitutive proteasomal degradation (20, 21). While HIF-1α protein levels are primarily regulated at the level of protein stability, HIF-1α can also be transcriptionally regulated (22). We first tested whether NO impacts transcription of the *Hif1a* gene, and found that transcript levels were equivalent or higher in *Nos2*$^{-/-}$ BMDM relative to wildtype (Figure 2C), indicating that NO dependent upregulation of HIF-1α target genes is unlikely to be due to NO dependent upregulation of *Hif1a* transcript. Next, HIF-1α protein accumulation during *M. tuberculosis* infection with IFN-γ activation was assessed in wildtype and *Nos2*$^{-/-}$ BMDM. In wildtype BMDM HIF-1α protein levels rise, peaking at 12h post infection (Figure 2D). In contrast, iNOS

deficient macrophages have a weak and transient accumulation of HIF-1α (Figure 2D), indicating that the large accumulation of HIF-1α that occurs after 4h is dependent on the production of NO. The addition of ascorbate, a reducing agent that reverses S-nitrosylation (16), inhibited HIF-1α stabilization in wildtype BMDM, suggesting the possibility that protein S-nitrosylation by NO contributes to HIF-1α stabilization (Figure S1A).

To identify a threshold of NO production required for HIF-1α stabilization, BMDM were treated with a dose response of the iNOS inhibitor 1400W following infection with *M. tuberculosis* and activation with IFN-γ. Even a modest inhibition (~50%) of NO production completely reverses NO dependent HIF-1α stabilization (Figure 2E). Additionally, the addition of the exogenous NO donor S-Nitroso-N-acetylpenicillamine (SNAP) is able to rescue this 1400W dependent abrogation of HIF-1α stabilization (Figure 2F), confirming that NO itself is responsible for the defect in HIF-1α stabilization in *Nos2*$^{-/-}$ BMDM. Finally, we tested whether this signaling role for NO is specific to *M. tuberculosis* infection of macrophages, or whether it is a more general feature of IFN-γ activation. Wildtype and *Nos2*$^{-/-}$ BMDM were treated with the TLR1/2 agonist PAMCysK4 and IFN-γ, and probed for HIF-1α by Western blot 12h post-treatment. We observed a similar result in the context of sterile stimulation of BMDM as with *M. tuberculosis* infection, with *Nos2*$^{-/-}$ BMDM exhibiting a strong defect in HIF-1α stabilization (Figure S1B). This suggests that NO stabilizing HIF-1α is a general feature of IFN-γ activation of macrophages.

iNOS and HIF-1α are linked in a positive feedback loop, and regulate aerobic glycolysis

We have previously shown that HIF-1α is required for maximal production of NO in BMDM activated with IFN-γ and infected with *M. tuberculosis* (17). The dependence of NO production on HIF-1α is observable across a wide range of IFN-γ concentrations (Figure 3A). Furthermore, treatment with the HIF-1α stabilizer dimethyloxalylglycine (DMOG) enhances NO production in wildtype but not HIF-1α deficient (*Hif1a*$^{-/-}$) BMDM (Figure 3A). Thus, iNOS and HIF-1α positively regulate each other, with NO being required for IFN-γ dependent HIF-1α stabilization, and HIF-1α being required for maximal NO production. We next compared genes differentially expressed in *Hif1a*$^{-/-}$ BMDM with genes differentially expressed in *Nos2*$^{-/-}$ BMDM. During *M. tuberculosis* infection with IFN-γ, we identified ~1700 genes in *Hif1a*$^{-/-}$ BMDM and ~1600 genes in *Nos2*$^{-/-}$ BMDM that had altered expression levels compared to wildtype BMDM. Approximately 40% of these regulated genes overlapped (Figure 3B), indicating that NO dependent regulation of HIF-1α activity accounts for a substantial portion of the HIF-1α dependent transcriptional response in IFN-γ activated macrophages during *M. tuberculosis* infection.

This overlapping gene regulation includes regulation of aerobic glycolysis, which we and others have previously shown to be a key function required for control of *M. tuberculosis* in macrophages (17, 23, 24). RNAseq data indicates that *Nos2*$^{-/-}$ and *Hif1a*$^{-/-}$ BMDM have a defect in transcription of genes that are induced as a part of the program of aerobic glycolysis, including *glut1, ldha,* and *pfkfb3* (Figure 3C). Consistent with this observation, glucose assays indicate that both *Nos2*$^{-/-}$ and *Hif1a*$^{-/-}$ BMDM are deficient for glucose uptake during *M. tuberculosis* infection with IFN-γ activation (Figure 3D).

iNOS and HIF-1α have opposing roles in the regulation of inflammation

Our finding that NO positively regulates HIF-1α stabilization suggests a role for NO in positively regulating inflammatory gene expression, as we and others have shown HIF-1α to be a key transcriptional regulator of inflammatory cytokines during bacterial infection (17, 25, 26). However, an excessive inflammatory response has been suggested to contribute to the susceptibility of both *Nos2*$^{-/-}$ and IFN-γ deficient mice, suggesting that in fact NO acts as an anti-inflammatory mediator (7, 16).

Analysis of our RNAseq data indicated that of the nearly 700 genes that are regulated by both iNOS and HIF-1α, only ~5% are regulated in opposite directions (increased expression in one genotype and decreased expression in the other genotype for a single gene). Interestingly, this subset is highly enriched for inflammatory cytokines and chemokines. Surprisingly, given the positive feedback relationship between HIF-1α and NO, HIF-1α broadly upregulates inflammatory cytokines and chemokines, while NO strongly suppresses mRNA abundance of a key subset of cytokines and chemokines (Figure 4A). We examined the *Il1a and Il1b* transcripts in more detail, as IL-1 is essential for control of *M. tuberculosis* infection (27). Levels of IL-1 produced during *M. tuberculosis* infection must be carefully balanced to protect the host; IL-1 is required for the protective immune response to *M. tuberculosis* but excessive IL-1 leads to host pathology and death (16). For *Il1a* and *Il1b*, a nearly identical transcriptional phenotype was observed, with *Hif1a* $^{-/-}$ BMDM having substantially lower levels during *M. tuberculosis* infection both in the presence and absence of IFN-γ, while *Nos2*$^{-/-}$ BMDM have much higher transcript levels than WT, but only in the context of IFN-γ activation (Figure 4B, 4C). Analysis of intracellular pro-IL-1β by western blot indicates that during *M. tuberculosis* infection with IFN-γ activation, *Nos2*$^{-/-}$ BMDM have markedly higher levels than wildtype BMDM, while pro-IL-1β is barely detectable in *Hif1a* $^{-/-}$ BMDM (Figure 4D). Similarly, ELISAs for IL-1β from supernatants of *M. tuberculosis* infected BMDM recapitulate the transcriptional phenotype, with markedly higher levels of IL-1β detected in *Nos2*$^{-/-}$ BMDM and dramatically lower levels detected in *Hif1a* $^{-/-}$ BMDM (Figure 4E). Thus while HIF-1α and iNOS are regulated by positive feedback, and coordinately regulate hundreds of genes, they have antagonistic roles with regard to inflammatory cytokine production. Interestingly, mRNA levels of IL-1 and CXCL1, which both play a role in recruitment of neutrophils, are elevated in *Nos2*$^{-/-}$ BMDM. This raises the possibility that NO is the IFN-γ dependent effector responsible for restricting destructive inflammation resulting from excessive neutrophil recruitment. Depleting neutrophils from IFN-γ deficient mice extends the survival time of these mice (7). We tested whether depleting neutrophils from *Nos2*$^{-/-}$ mice is also protective. We independently tested two antibodies for neutrophil depletion and found that under these experimental conditions, depleting neutrophils did not extend the life of *Nos2*$^{-/-}$ mice, but instead slightly exacerbated infection (Figure 4F,G).

iNOS suppresses NF-kB activity during *M. tuberculosis* infection

NO has been demonstrated to regulate NF-kB signaling via S-nitrosylation of NF-kB family members, including p50 and p65 (28, 29). However, depending on the context, NO can either inhibit or enhance NF-kB dependent transcriptional responses (30). Indeed, increased activation of NF-kB by NO has been observed in multiple

inflammatory settings (31, 32). Our bioinformatic analyses suggest that in *M. tuberculosis* infected and IFN-γ activated macrophages, NO suppresses NF-kB dependent signaling. Indeed, both IPA and oPOSSUM transcription factor prediction analysis identify NF-kB family members as top hits for transcription factors inhibited by NO (Figure 5A, Table S1A, Table S1B). We hypothesized that this activity of NO might explain the hyper-inflammatory phenotype of *Nos2*$^{-/-}$ BMDM, and the divergent phenotypes of *Hif1a* $^{-/-}$ and *Nos2*$^{-/-}$ BMDM for a subset of inflammatory cytokines (Figure 4A).

To experimentally determine whether NO inhibits NF-kB activity in IFN-γ activated and *M. tuberculosis* infected macrophages we first examined the effect of NO on a NF-kB dependent firefly luciferase reporter gene in both the RAW cell line and primary BMDM. Inhibition of NO production with 25uM 1400W (Figure 5B) led to an increase in reporter activity in RAW cells at 36h after infection (Figure 5C), suggesting that NO may suppress NF-kB dependent signaling at late timepoints after macrophage activation. However, it was surprising that even without inhibition of NO production, there were high levels of activation of NF-kB in *M. tuberculosis* infected and IFN-γ activated macrophages 36h after infection. We therefore sought to test whether a similar effect was observed in primary cells, and utlilized BMDM prepared from a mouse expressing an NF-kB luciferase reporter in all cells (33). We found that 12h after infection NF-kB signaling in *M. tuberculosis* infected and IFN-γ activated BMDM was comparable to that found in resting macrophages. However, using a dose response of 1400W to titrate NO levels, we found that inhibition of NO production caused prolonged NF-kB activity at later time-points in a dose dependent manner (Figure 5D, 5E). We next sought to identify which NF-kB family members contribute to the prolonged NF-kB activity observed. Increased mRNA levels were observed for *Rel, Relb, Nfkb1*, and *Nfkb2* in *Nos2*$^{-/-}$ BMDM relative to wildtype BMDM infected with *M. tuberculosis* and activated with IFN-γ (Figure S2A-E). To determine whether the enhanced levels of mRNA translated to increased protein levels and increased activation of NF-kB family members, western blotting was performed in whole cell lysates and nuclear extracts for all NF-kB family members 24h post-infection. While whole cell and nuclear levels of RelB increased with *M. tuberculosis* infection of IFN-γ treated BMDM, there was no clear difference between wildtype and *Nos2*$^{-/-}$ BMDM (Figure 6A). There was also no clear difference between wildtype and *Nos2*$^{-/-}$ BMDM for NF-kB1 (Figure 6A). We were unable to detect nuclear c-Rel or any NF-kB2 protein under the conditions examined (data not shown). Also, as expected, IkBa levels were reduced with infection, but there was no obvious difference between wildtype and *Nos2*$^{-/-}$ BMDM (Figure 6A). The only NF-kB family member for which there was a clear difference in *Nos2*$^{-/-}$ BMDM was the RelA/p65 subunit. While total levels of RelA remained unchanged across all conditions, there was markedly more nuclear RelA in *Nos2*$^{-/-}$ BMDM than in wildtype BMDM after infection (Figure 6A). This result was confirmed by confocal immunofluorescence microscopy for RelA/p65. In resting BMDM, staining is predominantly cytoplasmic, but upon *M. tuberculosis* infection of IFN-γ activated BMDM there is a relocalization of RelA to the nucleus in iNOS deficient BMDM that is observable at 24h after infection (Figure 6B). Quantification of RelA positive nuclei shows that ~3x as many nuclei are RelA positive in *Nos2*$^{-/-}$ BMDM relative to wildtype (Figure 6C). Taken together, this supports the hypothesis that NO deficiency causes prolonged nuclear localization of RelA

with a concomitant increase in the expression of specific inflammatory cytokines, including IL-1.

As NO is reported to play an anti-inflammatory role during *M. tuberculosis* infection by inhibiting NLRP3 dependent IL1b processing (16), we sought to test whether the upregulation of NF-kB activity in NO deficient BMDM that we observed might be a secondary effect following IL-1 autocrine or paracrine signaling between macrophages. RNAseq data suggests that this is unlikely, as the IL1 receptor antagonist (*Il1rn*) is ~100x more highly expressed than then IL1 receptor (*Il1r1*) during *M. tuberculosis* infection with and without IFN-γ activation (Figure 6D). To functionally assess whether IL-1 autocrine/paracrine signaling plays a role, the iNOS inhibitor 1400W was used in wildtype, *Nos2*$^{-/-}$ and *IL1R*$^{-/-}$ BMDM infected with *M. tuberculosis* and activated with IFN-γ. As expected, 1400W treatment increased *Il1b* expression in wildtype macrophages, recapitulating a *Nos2*$^{-/-}$ phenotype (Figure 6E). However, In *IL1R*$^{-/-}$ BMDM, 1400W treatment enhanced *Il1b* transcription to the same level as in wildtype BMDM (Figure 6E), indicating that signaling through the IL-1 receptor is not required for *Il1b* upregulation, and suggesting that the broad transcriptional repression of cytokines by NO occurs by more direct modulation of NF-kB.

Simultaneous deletion of HIF-1α and iNOS from macrophages balances inflammatory cytokine production, but does not restore control of infection

To further characterize the role of iNOS and its interactions with HIF-1α in the regulation of IFN-γ dependent transcriptional responses and cell intrinsic control of *M. tuberculosis*, we examined BMDM lacking both HIF-1α and iNOS. *Nos2*$^{-/-}$ BMDM are known to be defective in IFN-γ dependent control of *M. tuberculosis* infection, and we have shown that *Hif1a*$^{-/-}$ BMDM are also defective in control of *M. tuberculosis* specifically in the context of IFN-γ activation (17). First, we compared *Nos2*$^{-/-}$, *Hif1a*$^{-/-}$, and *Hif1a*$^{-/-}$ *Nos2*$^{-/-}$ double knockout BMDM for their ability to control infection. We observed no differences in bacterial growth in the absence of IFN-γ between any of the genotypes tested (Figure 7A). In the context of IFN-γ activation we found that *Nos2*$^{-/-}$, *Hif1a*$^{-/-}$, and *Hif1a*$^{-/-}$ *Nos2*$^{-/-}$ BMDM all had significantly elevated CFU relative to wildtype BMDM (Figure 7B). Interestingly, all three mutant genotypes had a remarkably similar defect in IFN-γ dependent restriction of bacterial growth, and the *Hif1a*$^{-/-}$ *Nos2*$^{-/-}$ double knockout BMDM had no further loss of control relative to the individual knockouts (Figure 7B). This result suggests that iNOS and HIF-1α are acting through the same cell intrinsic pathway for control of *M. tuberculosis* infection. We next compared cytokine expression by qPCR in *Nos2*$^{-/-}$, *Hif1a*$^{-/-}$, and *Hif1a*$^{-/-}$ *Nos2*$^{-/-}$ BMDM following *M. tuberculosis* infection and IFN-γ activation. *Hif1a*$^{-/-}$ BMDM have a strong defect in *Il1a, Il1b* and *Il6* transcript levels while *Nos2*$^{-/-}$ BMDM have highly increased levels (Figure 7C, 7D, 7E). Interestingly, the *Hif1a*$^{-/-}$ *Nos2*$^{-/-}$ BMDM balance out these hyper-inflammatory and hypo-inflammatory phenotypes and have intermediate *Il1a, Il1b* and *Il6* transcript levels, similar to that of wildtype BMDM (Figure 7C, 7D, 7E). Thus, NO appears to be required for cell intrinsic control of *M. tuberculosis* infection via activation of HIF-1α, while at the same time iNOS and HIF-1α antagonistically regulate inflammatory cytokine production to produce a properly calibrated inflammatory response.

Discussion:

In this report, we identify two key signaling roles for iNOS during *M. tuberculosis* infection. First, we find that NO mediates stabilization of HIF-1α, a transcription factor that is required for optimal expression of both pro-inflammatory cytokines and antimicrobial effectors. Second, we find that NO represses NF-kB signaling, and prevents nuclear RelA localization. Additionally, we find that iNOS and HIF-1α are linked by a positive feedback loop while at the same time they antagonistically regulate inflammatory cytokine production. Thus, we find that iNOS promotes the microbicidal functions of the pro-inflammatory transcription factor HIF-1α while simultaneously preventing excessive inflammatory responses via suppression of the NF-kB family member RelA/p65 (Figure S3).

NO is produced in macrophages in response to a diverse array of microbial pathogens and has been found to be protective in most infection models (34). In the case of *M. tuberculosis* infection, NO is produced following the onset of adaptive immunity and IFN-γ signaling (5). It has long been known that *Nos2*$^{-/-}$ mice are extremely susceptible to *M. tuberculosis* infection, accounting for much of the susceptibility of IFN-γ$^{-/-}$ mice (13). It has been assumed that the predominant mechanism by which NO controls infection in macrophages is via direct killing of *M. tuberculosis*. However, the need for re-examination of this hypothesis has been raised by several key observations. First, the isolation of *M. tuberculosis* mutants that are dramatically more susceptible to nitrosative stress can be interpreted as evidence that *M. tuberculosis* has evolved resistance mechanisms to direct NO dependent killing (14). Second, part of the susceptibility phenotype of IFN-γ deficient mice has been attributed to an excessive inflammatory response caused by a failure to suppress the recruitment of neutrophils to sites of infection (7). Finally, an intriguing paper demonstrated that NO prevents immunopathology during *M. tuberculosis* infection independent of bacterial replication, providing the first concrete evidence that NO contributes to control of *M. tuberculosis* infection through a mechanism other than direct bacterial toxicity (16).

While the role of NO as a second messenger that regulates mammalian signaling is well known (35), in the context of *M. tuberculosis* infection the potential regulatory roles of NO have not been well defined. In addition to its well-studied role in regulating cyclic GMP (cGMP) dependent kinases, NO has broad effects on signaling via NO-induced post translational modifications including S-nitrosylation, S-glutathionylation and tyrosine nitration (36). In addition, NO can inhibit the function of iron dependent proteins (37). The role of NO in regulating inflammation is complex, and can either be pro-inflammatory or anti-inflammatory depending on the context (30, 32).

We identified HIF-1α as a key transcription factor that is activated by NO production during *M. tuberculosis* infection. RNAseq profiling of *Nos2*$^{-/-}$ and *Hif1a*$^{-/-}$ macrophages indicates that there is a large overlap of genes regulated by both HIF-1α and NO. We have recently shown that HIF-1α is a key mediator of IFN-γ mediated control of *M. tuberculosis* infection *in vitro* and *in vivo*. This implies that NO may have a broader role in mediating IFN-γ dependent antibacterial defense against *M. tuberculosis* than was previously appreciated, and may do so in large part through the activation of HIF-1α dependent bactericidal effectors.

Aerobic glycolysis is associated with M1 polarized bactericidal macrophages (38) and we have recently shown that in the context that *M. tuberculosis* infection, aerobic

glycolysis is required for IFN-γ dependent control of infection in macrophages (17). We find that the metabolic program of aerobic glycolysis in *M. tuberculosis* infected and IFN-γ activated macrophages requires both iNOS and HIF-1α. Thus, NO may contribute to control of *M. tuberculosis* infection by regulating aerobic glycolysis. Although NO positively regulates both HIF-1α and aerobic glycolysis during *M. tuberculosis* infection, the mechanism by which this occurs remains an open question. The observation that ascorbate treatment abrogates HIF-1α stabilization under these conditions suggests that S-nitrosylation of a protein involved in HIF-1α regulation may be involved. Direct S-nitrosylation and activation of HIF-1α has been reported to lead to PHD independent stabilization of HIF1 (39). Similarly, NO could interfere with PHD function either by nitrosylation or via disruption of the catalytic site via iron binding (40). An additional possibility is that the NO dependent upregulation of HIF-1α is indirect, and downstream of an upregulation of aerobic glycolysis, which we have shown to be required for HIF-1α stabilization during *M. tuberculosis* infection (17). Finally, because the reaction catalyzed by iNOS requires the use of molecular oxygen, it is possible that consumption of O_2 by iNOS creates a locally hypoxic environment that results in stabilization of HIF-1α.

Interestingly, while there is broad overlap in HIF-1α and iNOS regulated genes, there is a small but critical set of inflammatory cytokines and chemokines that are dramatically upregulated in *Nos2*$^{-/-}$ macrophages and downregulated in *Hif1a* $^{-/-}$ macrophages. This suggests that in addition to enhancing antimicrobial and inflammatory activity via HIF-1α, NO production is also profoundly anti-inflammatory in the context of *M. tuberculosis* infection. This is a somewhat surprising result given the positive feedback between HIF-1α and iNOS, but implies that NO serves as an important braking mechanism to prevent excessive inflammation at the transcriptional level. It has been demonstrated that NO specifically nitrosylates and inactivates the NLRP3 inflammasome, thus limiting IL-1β processing, and that *Nos2*$^{-/-}$ mice have a striking hyper-inflammatory response to *M. tuberculosis* infection *in vivo* (16). We find that the immunosuppressive functions of NO are broader than just the inactivation of the NLRP3 inflammasome. Our RNA-seq data reveals that in *M. tuberculosis* infected, IFN-γ activated macrophages, NO represses not only IL-1α and IL-1β at the transcriptional level, but also many other inflammatory cytokines and chemokines including CXCL1. Interestingly, IL1 and CXCL1 both promote the recruitment of neutrophils, suggesting that NO might function to suppress the recruitment of neutrophils to the site of infection thereby preventing the excessive inflammatory response that can be mediated by neutrophils. Although we find that NO negatively regulates the transcription of neutrophil attractant chemokines *in vitro*, we did not observe an increased survival time in Nos2$^{-/-}$ mice following neutrophil depletion *in vivo*. However, the dose we used for infection is 2-4 fold higher than the dose used to observe the protective effect in IFN-γ$^{-/-}$ mice upon neutrophil depletion (7). It is possible that the aerosol infection model we use results in a hyperinflammation via multiple mechanisms, thereby masking a protective effect of neutrophil depletion.

To identify effectors of the broad transcriptional upregulation of inflammatory cytokines and chemokines we observe in Nos2$^{-/-}$ macrophages, we performed a bioinformatic analysis of genes found to be upregulated in Nos2$^{-/-}$ macrophages, and identified NF-kB family members as the best candidates. We experimentally validated

this bioinformatic prediction, and found that the p65/RelA subunit of NF-kB is inhibited by NO production during IFN-γ activation of *M. tuberculosis* infected macrophages. This result fits with the known role of NO in nitrosylating and inhibiting multiple NF-kB family members including both the p50 and p65 NF-kB monomers (28, 29). Thus, while iNOS activates HIF-1α dependent cell intrinsic bactericidal mechanisms, it also counterbalances HIF-1α dependent upregulation of inflammatory mediators by inhibiting pro-inflammatory cytokine transcription by NF-kB. We propose that this dual role for NO allows for robust activation of IFN-γ dependent cell intrinsic bactericidal effectors via HIF-1α while also suppressing excessive production of inflammatory cytokines that would result from activation of both NF-kB and HIF-1α, presumably to preclude excessive tissue damage during an effective IFN-γ mediated response to infection.

To further characterize role of iNOS in mediating both control of bacterial growth and preventing excessive inflammatory cytokine production, we utilized *Hif1a*$^{-/-}$ *Nos2*$^{-/-}$ macrophages. We assessed their ability to regulate inflammatory cytokine production and their ability to control *M. tuberculosis* infection relative to *Nos2*$^{-/-}$ macrophages *and* *Hif1a*$^{-/-}$ macrophages. We found that *Hif1a*$^{-/-}$ *Nos2*$^{-/-}$ macrophages have inflammatory cytokine transcription that is intermediate between the hyperinflammatory *Nos2*$^{-/-}$ macrophages and hypoinflammatory *Hif1a*$^{-/-}$ macrophages, closely matching wildtype cytokine transcription. This result indicates that NO is both activating cytokine production via HIF-1α while also potently inhibiting cytokine production by inactivating NF-kB activity. This result also indicates that although HIF-1α protein levels and transcriptional activity are reduced in *Nos2*$^{-/-}$ macrophages, there is still some HIF-1α activity in the *Nos2*$^{-/-}$ macrophages that further contributes to the hyperinflammatory phenotype caused by NO deficiency.

Although we find that *Hif1a*$^{-/-}$ *Nos2*$^{-/-}$ macrophages have wildtype levels of cytokine transcript, this does not lead to effective control of *M. tuberculosis* in macrophages, implying that NO is required for cell intrinsic control independent of cytokine production. Indeed we find that *Nos2*$^{-/-}$ macrophages, *Hif1a*$^{-/-}$ macrophages, and *Hif1a*$^{-/-}$ *Nos2*$^{-/-}$ macrophages have an identical defect in IFN-γ dependent killing of *M. tuberculosis*. This result implies that HIF-1α and iNOS act through the same pathway to effect cell intrinsic control of *M. tuberculosis* infection. Although we have recently identified a variety of effector functions that are impaired in HIF-1α deficient macrophages during *M. tuberculosis* infection (17), it remains an open question as to what specifically mediates HIF-1α dependent killing of *M. tuberculosis* in macrophages.

In conclusion, we demonstrate that iNOS dependent NO production is responsible for broad regulation of the macrophage transcriptome during *M. tuberculosis* infection, and we identify two key transcription factors that are regulated by NO production in the context of IFN-γ activation. We identify HIF-1α as a key transcription factor that is activated by NO and supports cell intrinsic bacterial restriction, and we identify NF-kB as a key transcription factor inhibited by NO that prevents excessive inflammatory cytokine production.

Acknowledgments. The authors thank Lutz Froenicke (DNA Technologies and Expression Analysis Core, UC Davis) and Monica Britton, Joseph Fass and Blythe Durbin (Genome Center and Bioinformatics Core Facility, UC Davis), for RNA-seq and data analysis; Russell Vance, Jeffrey Cox, Bennett Penn, Kim Sogi and Katie Lien for helpful discussions. This work was supported by National Institutes of Health grant 1R01AI113270-01A1 and the Searle Funds at the Chicago Community Trust.

References:

1. Floyd, K. (World Health Organization, ed). WHO Press; :1–100.
2. Cooper, A. M., D. K. Dalton, T. A. Stewart, J. P. Griffin, D. G. Russell, and I. M. Orme. Disseminated tuberculosis in interferon gamma gene-disrupted mice. *J. Exp. Med.* 178: 2243–2247.
3. Flynn, J. L., J. Chan, K. J. Triebold, D. K. Dalton, T. A. Stewart, and B. R. Bloom. An essential role for interferon gamma in resistance to Mycobacterium tuberculosis infection. *J. Exp. Med.* 178: 2249–2254.
4. Abel, L., and J.-L. Casanova. Genetic predisposition to clinical tuberculosis: bridging the gap between simple and complex inheritance. *American journal of human genetics* 67: 274.
5. Chan, J., Y. Xing, R. S. Magliozzo, and B. R. Bloom. Killing of virulent Mycobacterium tuberculosis by reactive nitrogen intermediates produced by activated murine macrophages. *J. Exp. Med.* 175: 1111–1122.
6. Desvignes, L., and J. D. Ernst. 2009. Interferon-γ-Responsive Nonhematopoietic Cells Regulate the Immune Response to Mycobacterium tuberculosis. *Immunity* 31: 974–985.
7. Nandi, B., and S. M. Behar. Regulation of neutrophils by interferon-γ limits lung inflammation during tuberculosis infection. *Journal of Experimental Medicine* 208: 2251–2262.
8. Zhang, Y. J., M. C. Reddy, T. R. Ioerger, A. C. Rothchild, V. Dartois, B. M. Schuster, A. Trauner, D. Wallis, S. Galaviz, C. Huttenhower, J. C. Sacchettini, S. M. Behar, and E. J. Rubin. Tryptophan biosynthesis protects mycobacteria from CD4 T-cell-mediated killing. *Cell* 155: 1296–1308.
9. Alonso, S., K. Pethe, D. G. Russell, and G. E. Purdy. Lysosomal killing of Mycobacterium mediated by ubiquitin-derived peptides is enhanced by autophagy. *Proc. Natl. Acad. Sci. U.S.A.* 104: 6031–6036.
10. MacMicking, J. D. Immune Control of Tuberculosis by IFN- -Inducible LRG-47. *Science* 302: 654–659.
11. Singh, S. B., A. S. Davis, G. A. Taylor, and V. Deretic. Human IRGM induces autophagy to eliminate intracellular mycobacteria. *Science* 313: 1438–1441.
12. MacMicking, J. D., R. J. North, R. LaCourse, J. S. Mudgett, S. K. Shah, and C. F. Nathan. Identification of nitric oxide synthase as a protective locus against tuberculosis. *Proc. Natl. Acad. Sci. U.S.A.* 94: 5243–5248.
13. MacMicking, J. D., R. J. North, R. LaCourse, J. S. Mudgett, S. K. Shah, and C. F. Nathan. 1997. Identification of nitric oxide synthase as a protective locus against tuberculosis. *Proceedings of the National Academy of Sciences* 94: 5243–5248.
14. Darwin, K. H. 2003. The Proteasome of Mycobacterium tuberculosis Is Required for Resistance to Nitric Oxide. *Science* 302: 1963–1966.
15. Ehrt, S., D. Schnappinger, S. Bekiranov, J. Drenkow, S. Shi, T. R. Gingeras, T. Gaasterland, G. Schoolnik, and C. Nathan. 2001. Reprogramming of the Macrophage Transcriptome in Response to Interferon-γ and Mycobacterium tuberculosis. *Journal of Experimental Medicine* 194: 1123–1140.
16. Mishra, B. B., V. A. K. Rathinam, G. W. Martens, A. J. Martinot, H. Kornfeld, K. A. Fitzgerald, and C. M. Sassetti. 2012. Nitric oxide controls the immunopathology of tuberculosis by inhibiting NLRP3 inflammasome–dependent processing of IL-1β. *Nat. Immunol.* 14: 52–60.

17. Braverman, J., K. M. Sogi, D. Benjamin, D. K. Nomura, and S. A. Stanley. 2016. HIF-1α Is an Essential Mediator of IFN-γ-Dependent Immunity to Mycobacterium tuberculosis. *J. Immunol.* 197: 1287–1297.
18. Ho Sui, S. J., J. R. Mortimer, D. J. Arenillas, J. Brumm, C. J. Walsh, B. P. Kennedy, and W. W. Wasserman. oPOSSUM: identification of over-represented transcription factor binding sites in co-expressed genes. *Nucleic Acids Research* 33: 3154–3164.
19. Benita, Y., H. Kikuchi, A. D. Smith, M. Q. Zhang, D. C. Chung, and R. J. Xavier. 2009. An integrative genomics approach identifies Hypoxia Inducible Factor-1 (HIF-1)-target genes that form the core response to hypoxia. *Nucleic Acids Research* 37: 4587–4602.
20. Salceda, S., and J. Caro. 1997. Hypoxia-inducible factor 1alpha (HIF-1alpha) protein is rapidly degraded by the ubiquitin-proteasome system under normoxic conditions. Its stabilization by hypoxia depends on redox-induced changes. *Journal of Biological Chemistry* 272: 22642–22647.
21. Maxwell, P. H., M. S. Wiesener, G. W. Chang, S. C. Clifford, E. C. Vaux, M. E. Cockman, C. C. Wykoff, C. W. Pugh, E. R. Maher, and P. J. Ratcliffe. 1999. The tumour suppressor protein VHL targets hypoxia-inducible factors for oxygen-dependent proteolysis. *Nature* 399: 271–275.
22. Bárdos, J. I., and M. Ashcroft. 2005. Negative and positive regulation of HIF-1: a complex network. *Biochimica et Biophysica Acta* 1755: 107–120.
23. Gleeson, L. E., F. J. Sheedy, E. M. Palsson-McDermott, D. Triglia, S. M. O'Leary, M. P. O'Sullivan, L. A. J. O'Neill, and J. Keane. 2016. Cutting Edge: Mycobacterium tuberculosis Induces Aerobic Glycolysis in Human Alveolar Macrophages That Is Required for Control of Intracellular Bacillary Replication. *J. Immunol.* 196: 2444–2449.
24. Shi, L., H. Salamon, E. A. Eugenin, R. Pine, A. Cooper, and M. L. Gennaro. 2015. Infection with Mycobacterium tuberculosis induces the Warburg effect in mouse lungs. *Sci. Rep.* 5: 18176.
25. Tannahill, G. M., A. M. Curtis, J. Adamik, E. M. Palsson-McDermott, A. F. McGettrick, G. Goel, C. Frezza, N. J. Bernard, B. Kelly, N. H. Foley, L. Zheng, A. Gardet, Z. Tong, S. S. Jany, S. C. Corr, M. Haneklaus, B. E. Caffrey, K. Pierce, S. Walmsley, F. C. Beasley, E. Cummins, V. nizet, M. Whyte, C. T. Taylor, H. Lin, S. L. Masters, E. Gottlieb, V. P. Kelly, C. Clish, P. E. Auron, R. J. Xavier, and L. A. J. O'Neill. Succinate is an inflammatory signal that induces IL-1β through HIF-1α. *Nature* 496: 238–242.
26. Peyssonnaux, C., V. Datta, T. Cramer, A. Doedens, E. A. Theodorakis, R. L. Gallo, N. Hurtado-Ziola, V. Nizet, and R. S. Johnson. 2005. HIF-1α expression regulates the bactericidal capacity of phagocytes. *J. Clin. Invest.* 115: 1806–1815.
27. Mayer-Barber, K. D., D. L. Barber, K. Shenderov, S. D. White, M. S. Wilson, A. Cheever, D. Kugler, S. Hieny, P. Caspar, G. Nunez, D. Schlueter, R. A. Flavell, F. S. Sutterwala, and A. Sher. 2010. Cutting Edge: Caspase-1 Independent IL-1 Production Is Critical for Host Resistance to Mycobacterium tuberculosis and Does Not Require TLR Signaling In Vivo. *The Journal of Immunology* 184: 3326–3330.
28. delaTorre, A., R. A. Schroeder, C. Punzalan, and P. C. Kuo. 1999. Endotoxin-mediated S-nitrosylation of p50 alters NF-kappa B-dependent gene transcription in ANA-1 murine macrophages. *The Journal of Immunology* 162: 4101–4108.
29. Kelleher, Z. T., A. Matsumoto, J. S. Stamler, and H. E. Marshall. 2007. NOS2

regulation of NF-kappaB by S-nitrosylation of p65. *Journal of Biological Chemistry* 282: 30667–30672.
30. Marshall, H. E., D. T. Hess, and J. S. Stamler. S-nitrosylation: physiological regulation of NF-kappaB. *Proc. Natl. Acad. Sci. U.S.A.* 101: 8841–8842.
31. Yakovlev, V. A., I. J. Barani, C. S. Rabender, S. M. Black, J. K. Leach, P. R. Graves, G. E. Kellogg, and R. B. Mikkelsen. 2007. Tyrosine nitration of IkappaBalpha: a novel mechanism for NF-kappaB activation. *Biochemistry* 46: 11671–11683.
32. Connelly, L., M. Palacios-Callender, C. Ameixa, S. Moncada, and A. J. Hobbs. 2001. Biphasic regulation of NF-kappa B activity underlies the pro- and anti-inflammatory actions of nitric oxide. *The Journal of Immunology* 166: 3873–3881.
33. Carlsen, H., J. Ø. Moskaug, S. H. Fromm, and R. Blomhoff. 2002. In vivo imaging of NF-kappa B activity. *The Journal of Immunology* 168: 1441–1446.
34. MacMicking, J., Q. W. Xie, and C. Nathan. 1997. Nitric oxide and macrophage function. *Annu. Rev. Immunol.* 15: 323–350.
35. Francis, S. H., J. L. Busch, J. D. Corbin, and D. Sibley. 2010. cGMP-dependent protein kinases and cGMP phosphodiesterases in nitric oxide and cGMP action. *Pharmacol. Rev.* 62: 525–563.
36. Martínez-Ruiz, A., and S. Lamas. 2009. Two decades of new concepts in nitric oxide signaling: from the discovery of a gas messenger to the mediation of nonenzymatic posttranslational modifications. *IUBMB Life* 61: 91–98.
37. Cooper, C. E. 1999. Nitric oxide and iron proteins. *Biochimica et Biophysica Acta* 1411: 290–309.
38. Galván-Peña, S., and L. A. J. O'Neill. 2014. Metabolic reprograming in macrophage polarization. *Front Immunol* 5: 420.
39. Li, F., P. Sonveaux, Z. N. Rabbani, S. Liu, B. Yan, Q. Huang, Z. Vujaskovic, M. W. Dewhirst, and C.-Y. Li. Regulation of HIF-1alpha stability through S-nitrosylation. *Mol. Cell* 26: 63–74.
40. Metzen, E. 2003. Nitric Oxide Impairs Normoxic Degradation of HIF-1 by Inhibition of Prolyl Hydroxylases. *Molecular Biology of the Cell* 14: 3470–3481.

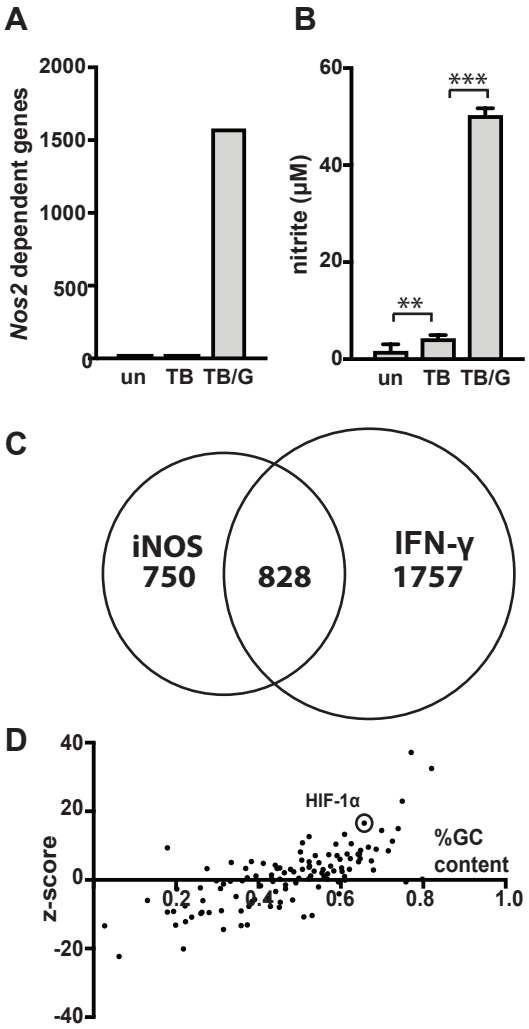

Figure 1. NO has large effects on the macrophage transcriptome. (A) Total number of differentially expressed genes between wildtype and *Nos2*$^{-/-}$ BMDM in untreated [un], *M. tuberculosis* infected [TB], and M. tuberculosis infected and IFN-γ treated [TB/G] BMDM 24h post-infection. For this analysis, statistical significance ($p<.05$) and a 2-fold or greater difference in expression was used as a cutoff. For RNAseq data and all other *in vitro* infections, the *M. tuberculosis* strain Erdman was used at an MOI of 5. (B) Griess assay measuring NO production 24h post-infection of wildtype BMDM with and without IFN-γ. (C) Venn diagram showing overlap of iNOS regulated genes during *M. tuberculosis* infection with IFN-γ treatment, and genes differentially expressed between *M. tuberculosis* infected wildtype macrophages with and without IFN-γ (D) Bioinformatic prediction (using oPOSSUM) of transcription factors responsible for regulation of all genes found to be expressed at a lower level in *Nos2*$^{-/-}$ BMDM during *M. tuberculosis* infection with IFN-γ treatment. RNAseq data is from 3 independent infections. (B) is representative of >5 experiments. The p values were determined using an unpaired t test. **$p<.01$, ***$p<.001$

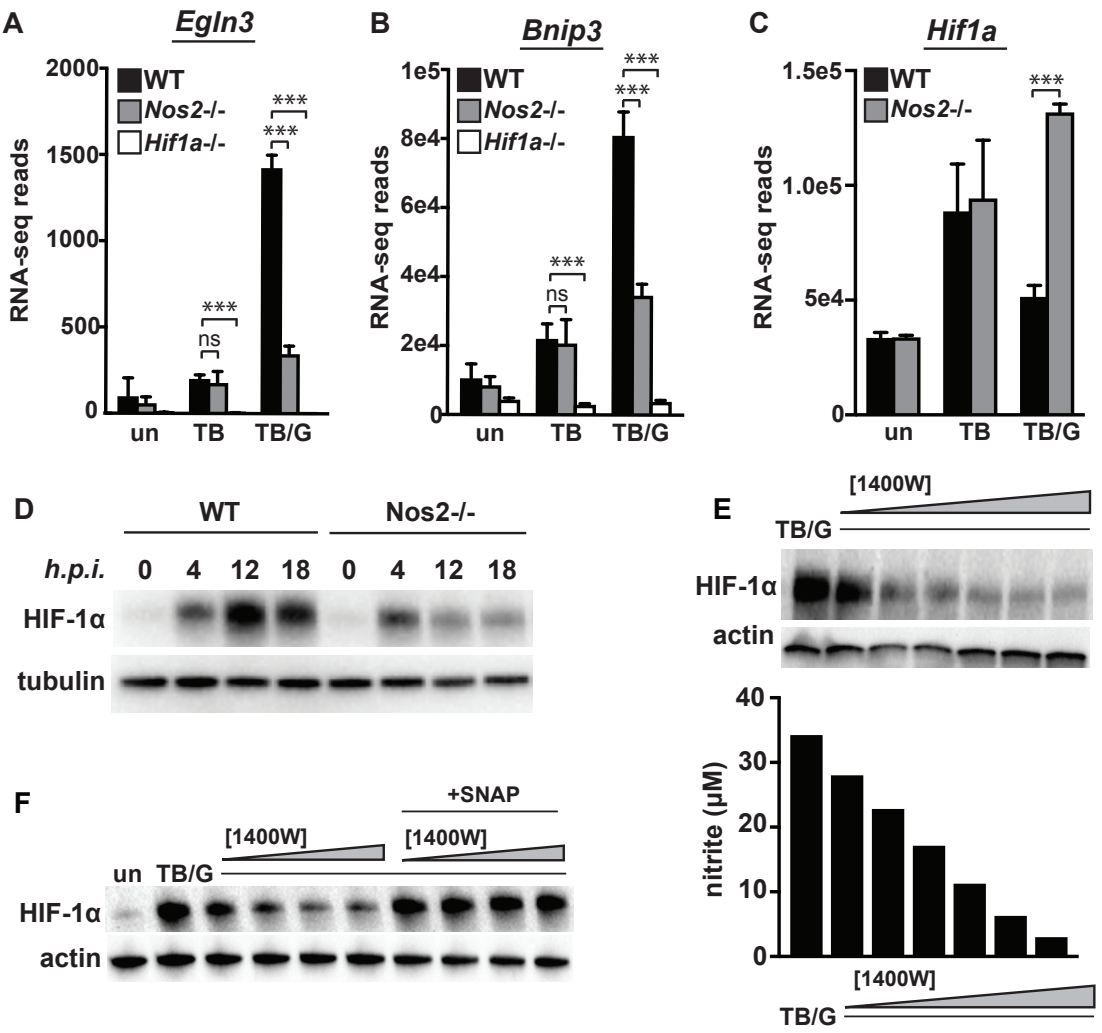

Figure 2. iNOS is required for HIF-1α stabilization and transcriptional activity. (A,B,C) RNAseq reads 24h post-infection in wildtype, *Nos2*$^{-/-}$, and *Hif1a*$^{-/-}$ BMDM in untreated [un], *M. tuberculosis* infected [TB], and *M. tuberculosis* infected with IFN-γ activation [TB/G] for HIF-1α target genes *Egln3, Bnip3,* and for *Hif1a.* (D) Western blot for HIF-1α in *M. tuberculosis* infected, IFN-γ activated BMDM at 0,4,12 and 18h post-infection in wildtype and *Nos2*$^{-/-}$ BMDM. (E) Western blot for HIF-1α in *M. tuberculosis* infected, IFN-γ activated BMDM with a dose response of the iNOS inhibitor 1400W [.625, 1.25, 2.5, 5, 10, 25uM]. Griess assay for NO production was done on the supernatant of the cells used for the western blot. (F) Western blot for HIF-1α in *M. tuberculosis* infected, IFN-γ activated BMDM with a dose response of 1400W [.625, 1.25, 2.5, 5uM] with and with addition of the NO donor SNAP [250uM]. RNAseq data is from 3 independent experiments. (D,E,F) are representative of 2 or more experiments. Error bars represent the SD from 3 independent experiments. The p values were determined using an unpaired t test. ***p<.001

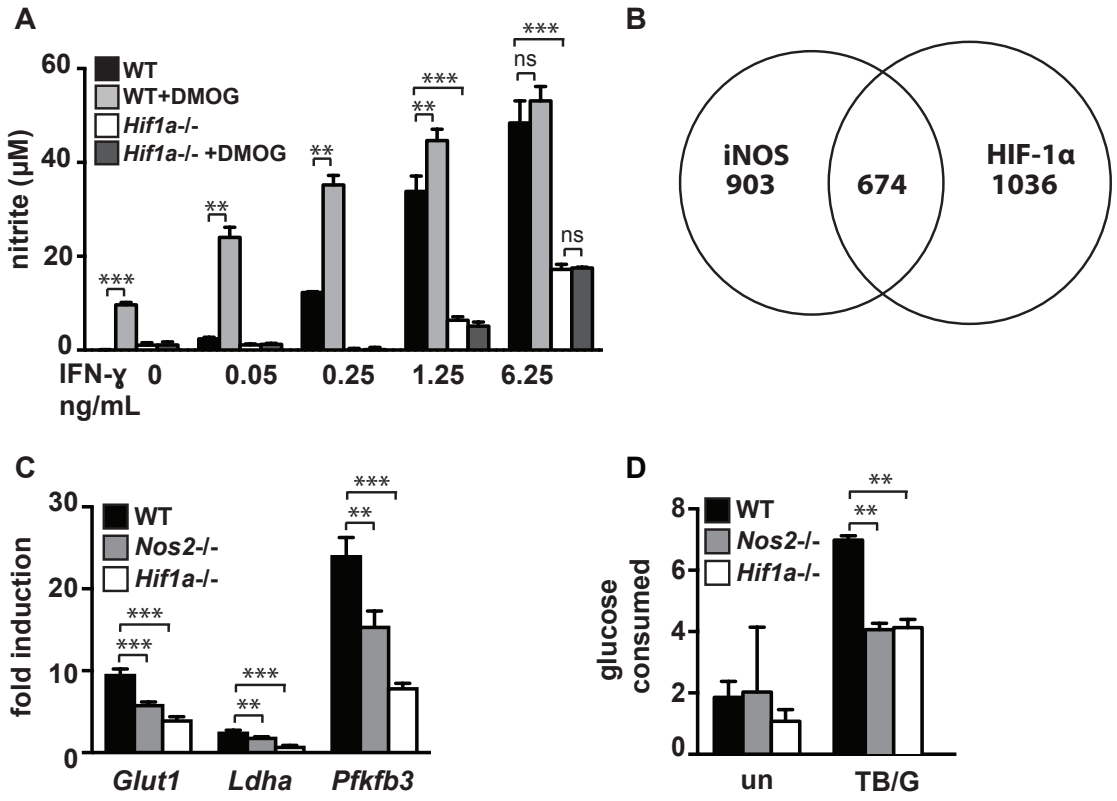

Figure 3. iNOS and HIF-1α are linked by positive feedback, and regulate aerobic glycolysis. (A) Griess assay measuring NO production 24h post-infection of *M. tuberculosis* infected wildtype and *Hif1a*$^{-/-}$ BMDM, with a dose response of IFN-γ. The HIF-1α stabilizer DMOG [200uM] increases NO production in a HIF-1α dependent manner. (B) Venn diagram of RNAseq data showing overlap of genes differentially expressed in *Nos2*$^{-/-}$ vs wildtype and *Hif1a*$^{-/-}$ vs wildtype BMDM during *M. tuberculosis* infection with IFN-γ activation. (C) RNAseq data showing fold induction of the glycolytic genes *Glut1, Ldha,* and *Pfkfb3* during *M. tuberculosis* infection with IFN-γ activation in wildtype, *Nos2*$^{-/-}$, *Hif1a*$^{-/-}$ BMDM relative to untreated. (D) Measurement of glucose uptake in wildtype, *Nos2*$^{-/-}$ and *Hif1a*$^{-/-}$ BMDM either untreated [un] or *M. tuberculosis* infected and IFN-γ activated [TB/G]. RNAseq data is from 3 independent experiments. (A,D) are representative of 2 or more experiments. Error bars represent SD from 3 or more wells (A,D) or 3 independent experiments (C). The p values were determined using an unpaired t test. **p<.01, ***p<.001

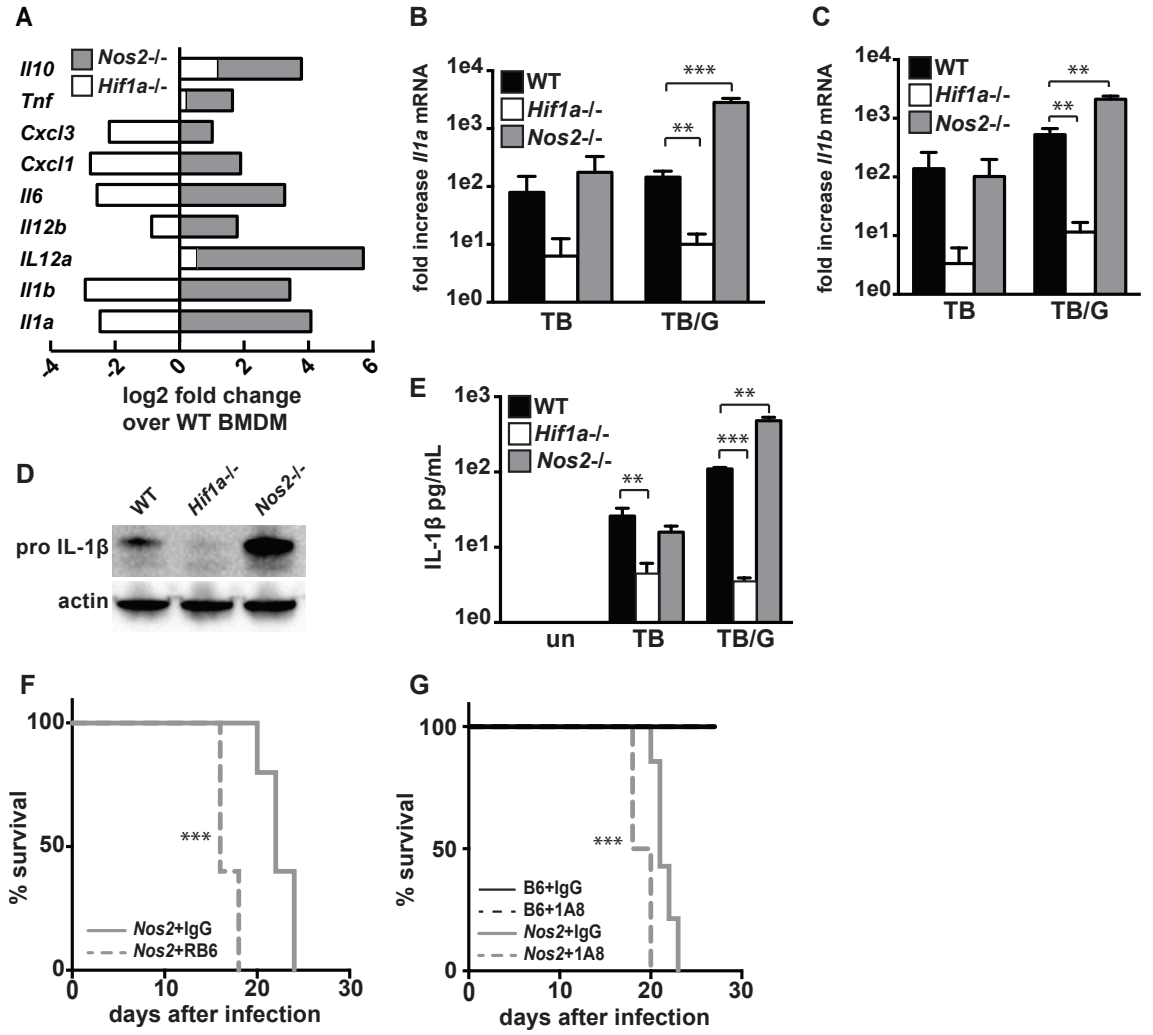

Figure 4. iNOS and HIF-1α antagonistically regulate inflammatory cytokine production. (A) RNAseq data showing fold difference in cytokines and chemokines in *Nos2*$^{-/-}$ and *Hif1a*$^{-/-}$ BMDM relative to wildtype during *M. tuberculosis* infection with IFN-γ activation. (B,C) RNAseq data from wildtype, *Hif1a*$^{-/-}$, and *Nos2*$^{-/-}$ BMDM showing fold change over uninfected for *Il1a* and *Il1b* with either *M. tuberculosis* infection [TB] or *M. tuberculosis* infection with IFN-γ activation [TB/G]. (D) Western blot for pro-IL-1B from wildtype, *Hif1a*$^{-/-}$ and *Nos2-/-* BMDM 24h post-infection with *M. tuberculosis* and IFN-γ activation. (E) ELISA for IL1B from supernatants of wildtype, *Hif1a*$^{-/-}$ and *Nos2*$^{-/-}$ BMDM 36h post-infection with and without IFN-γ activation. (F,G) Survival of *Nos2*$^{-/-}$ mice following aerosol infection with the virulent *M. tuberculosis* strain Erdman, with antibody mediated neutrophil depletion or with control IgG treatment. Mice injected with antibody every other day beginning 10 days post-infection. RNAseq data is from 3 independent experiments. (D,E) representative of 2 or more experiments. (F) representative of 2 independent infections. The p values were determined using an unpaired t test for (B,C,E), and using the Log-rank Mantel-Cox test for (F and G). **p<.01, ***p<.001

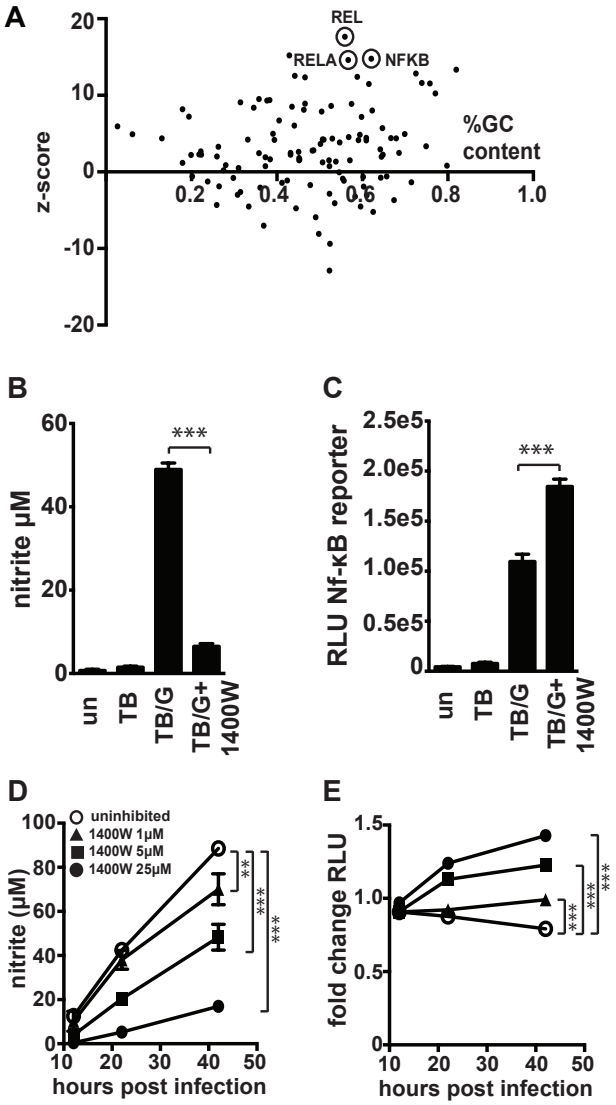

Figure 5. iNOS suppresses NF-kB activity. (A) Bioinformatic analysis of RNAseq data using oPOSSUM to predict transcription factors regulating the subset of genes found to be 4-fold or more upregulated in *Nos2*$^{-/-}$ BMDM relative to wildtype BMDM during *M. tuberculosis* infection with IFN-γ activation. (B) Griess assay measuring NO production 24h post-infection in RAW macrophages carrying an NF-kB luciferase reporter, with *M. tuberculosis* infection without IFN-γ [TB], with IFN-γ activation [TB/G], and with IFN-γ activation and addition of 25uM 1400W [TB/G+1400W]. (C) Luciferase assay 24h post-infection for the same cells as in (B) to measure NF-kB activity. (D) Griess assays measuring NO production over a timecourse in *M. tuberculosis* infected, IFN-γ activated BMDM (carrying an NF-kB luciferase reporter) with a dose response of 1400W. (E) Luciferase assay for NF-kB activity from the same cells as in (D). (B,C) representative of 3 experiments, (D,E) representative of 2 experiments. The p values were determined using an unpaired t test. **p<.01, ***p<.001

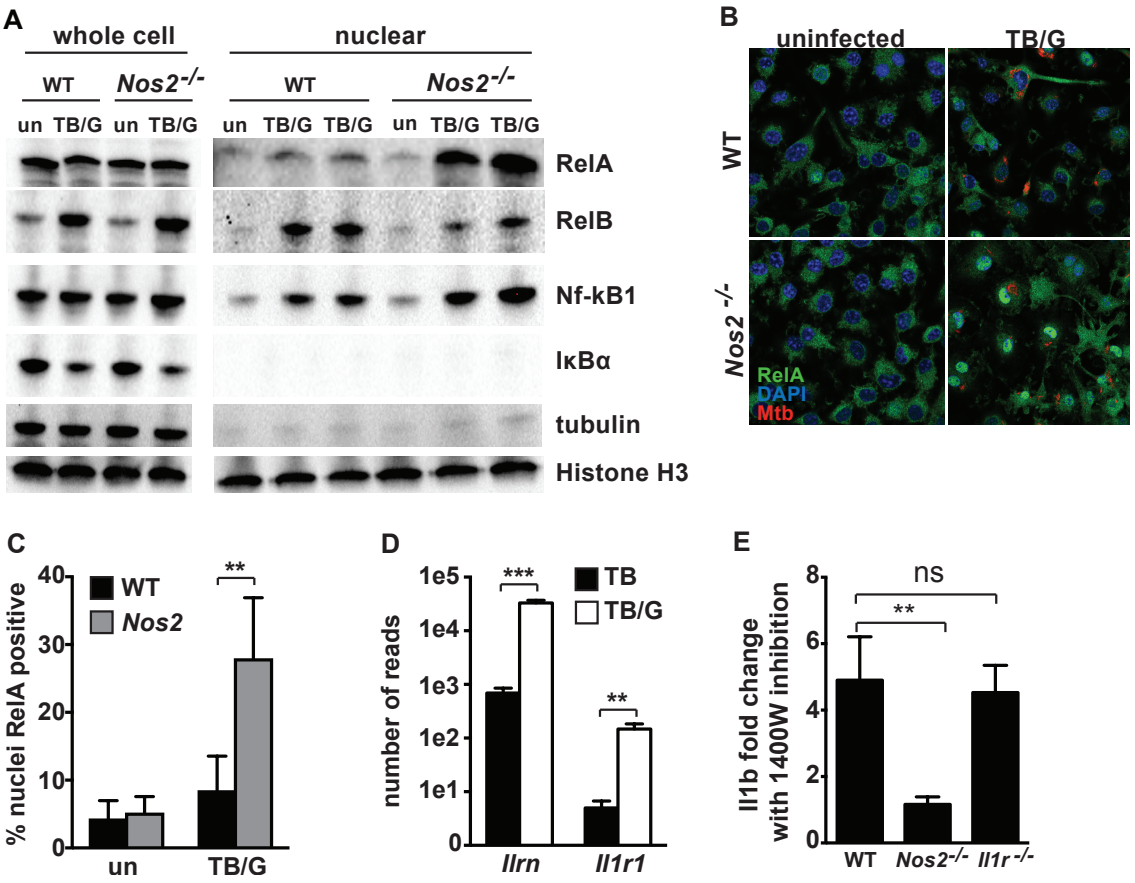

Figure 6. iNOS deficiency leads to aberrantly high nuclear RelA. (A) Western blots 24h post-infection from whole cell lysates and nuclear extracts for RelA, RelB, NF-kB1, and IkBa, with tubulin as a cytoplasmic marker and Histone H3 as a nuclear marker. Western blots with wildtype and *Nos2*$^{-/-}$ BMDM either uninfected [un] or *M. tuberculosis* infected with IFN-γ activation [TB/G]. For nuclear extracts, [TB/G] performed in biological duplicate for each repeat. (B) Confocal microscopy at 63x for RelA 24h post-infection in wildtype and *Nos2*$^{-/-}$ BMDM, uninfected or during *M. tuberculosis* infection with IFN-γ activation [TB/G]. For microscopy, the *M. tuberculosis* strain Erdman, carrying a fluorescent mCherry was utilized. (C) Quantification of p65 positive nuclei from the same samples as in (B), but from 20x images. >800 nuclei were analyzed for each condition, error bars represent SD between 5 fields. (D) RNAseq data showing number of reads for the IL1R antagonist (*Ilrn)* and IL1R (*Il1r1)* in wildtype BMDM infected with *M. tuberculosis* [TB] or *M. tuberculosis* with IFN-γ activation [TB/G]. (E) qPCR for *Il1b* transcript in wildtype, *Nos2*$^{-/-}$ and *Il1r*$^{-/-}$ BMDM, during *M. tuberculosis* infection with IFN-γ activation. Data shown is fold change in transcript level with iNOS inhibition using 25uM 1400W. The p values were determined using an unpaired t test. **p<.01, ***p<.001

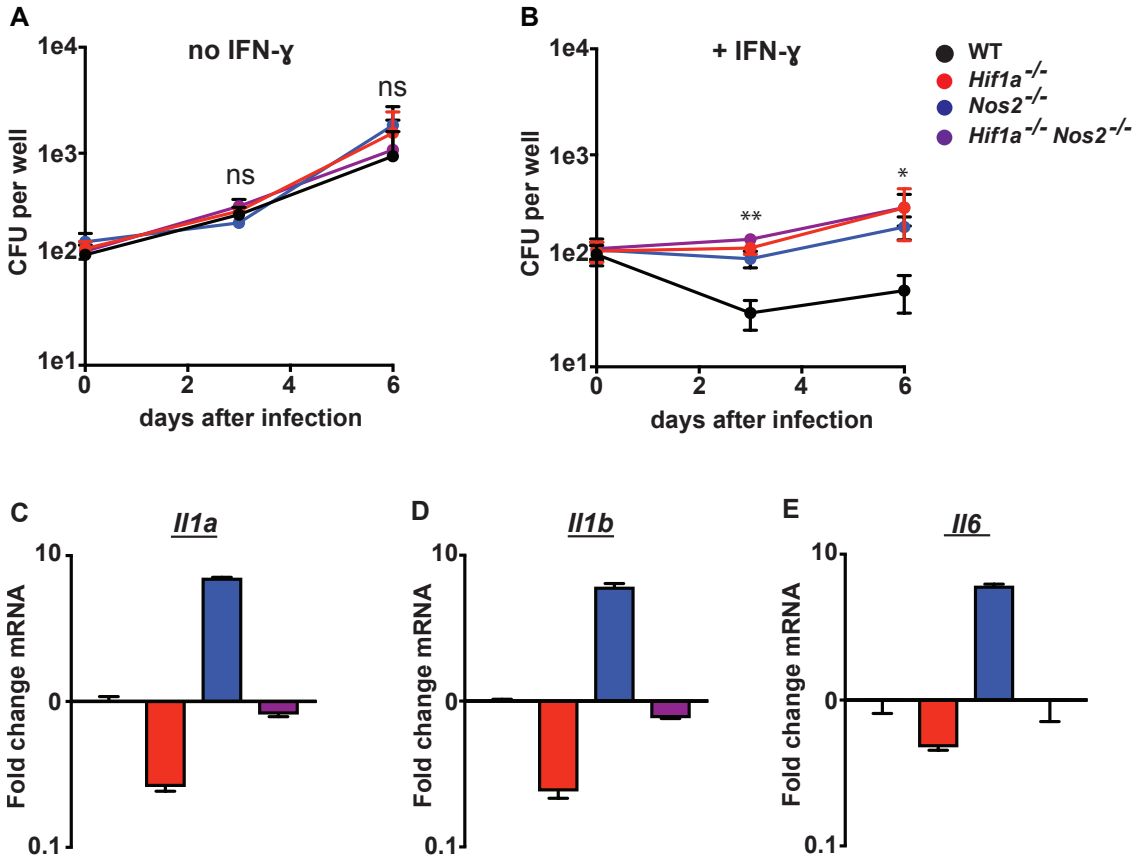

Figure 7. Double knockout of iNOS and HIF-1α balances inflammation. Wildtype, *Nos2*$^{-/-}$, *Hif1a*$^{-/-}$, and *Nos2*$^{-/-}$ *Hif1a*$^{-/-}$ BMDM were infected with *M. tuberculosis* without IFN-γ (A) and with IFN-γ (B). CFU was enumerated immediately following phagocytosis of bacteria, and again 3d and 6d post-infection. (C,D,E) wildtype, *Nos2*$^{-/-}$, *Hif1a*$^{-/-}$, and *Nos2*$^{-/-}$ *Hif1a*$^{-/-}$ BMDM were treated with IFN-γ and infected with *M. tuberculosis*. qPCR for *Il1a, Il1b,* and *Il6* was performed on RNA isolated from BMDM 24h post-infection. (A-E) representative of 3 or more independent experiments. The p values were determined using an unpaired t test. *p<.05, **p<.01

Figure S1

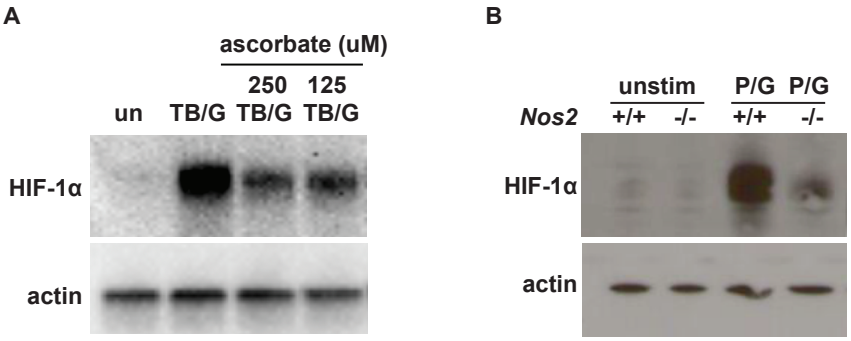

Figure S1
(A) Western blot for HIF-1α in untreated [un] and *M. tuberculosis* infected, IFN-γ activated [TB/G] wildtype BMDM 12h post infection, with and without ascorbate treatment at indicated concentrations. (B) Western blot for HIF-1α in wildtype and Nos2-/- BMDM either unstimulated or stimulated with Pam3CsyK4 (50ng/ml) and IFN-γ (6.25ng/ml) [P/G] for 12h. (A) representative of 2 experiments, (B) representative of 3 experiments.

Figure S2

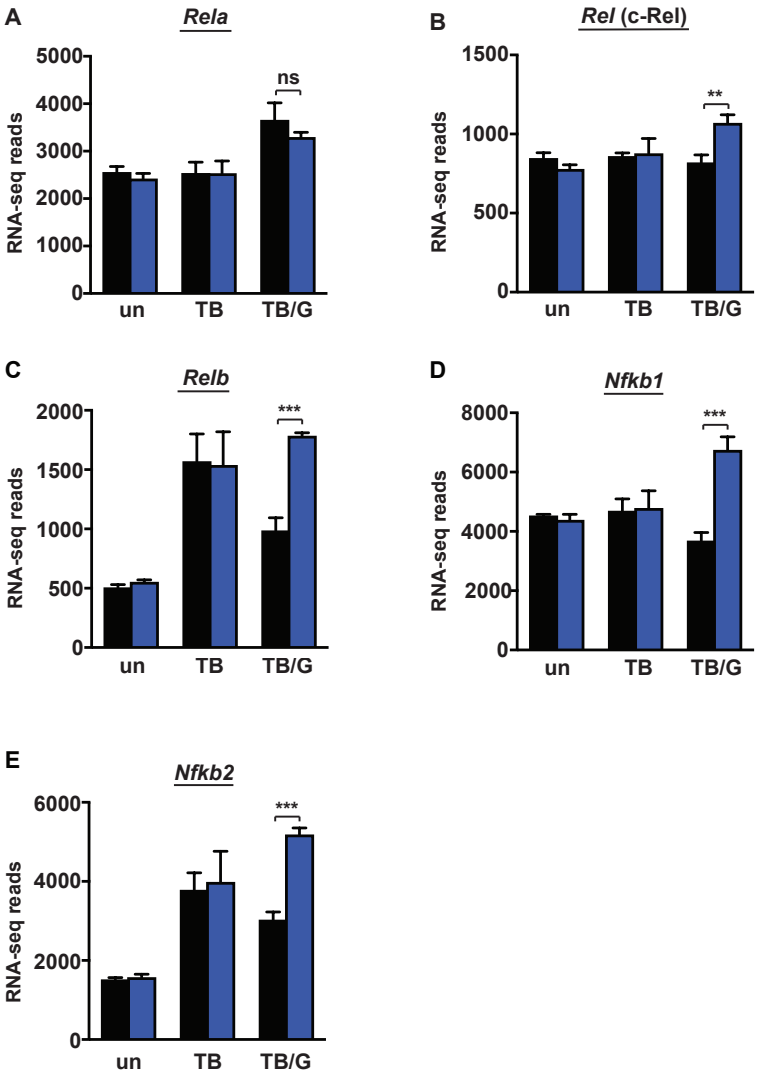

Figure S2
RNAseq data showing total reads for NF-kB family members (Rela, Rel, Relb, Nfkb1, and Nfkb2) in wildtype BMDM [black bars] and Nos2-/- BMDM [blue bars] in uninfected [un], *M. tuberculosis* infected [TB], and *M. tuberculosis* infected and IFN-γ treated [TB/G] BMDM. RNAseq data is from 3 independent infections. The p values were determined using an unpaired t test. **p<.01, ***p<.001

Figure S3

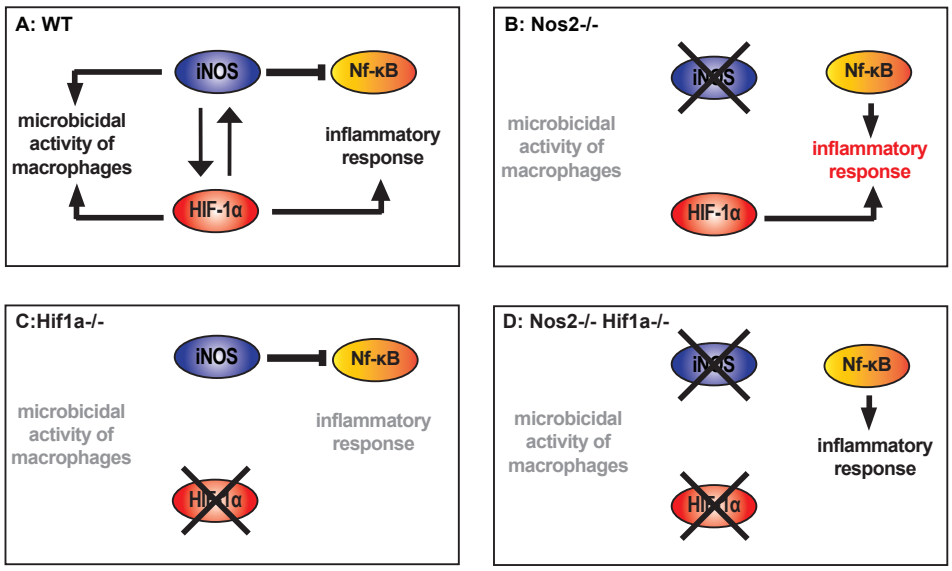

Figure S3
Model for the interactions between iNOS, HIF-1α, and NF-kB during M. tuberculosis infection of IFN-γ activated macrophages
(A) In wildtype macrophages during *M. tuberculosis* infection, both iNOS and the transcription factor HIF-1α are robustly induced, and are linked by a positive feedback loop. HIF-1α contributes to microbicidal activity through mechanisms that remain to be fully elucidated, and also upregulates a broad array of inflammatory cytokines and chemokines. At the same time, iNOS is enhancing microbicidal activity via activation of HIF-1 α, while also suppressing the inflammatory response by repressing NF-kB activity. Nitric oxide (NO) produced by macrophages may also be directly killing *M. tuberculosis* in wildtype macrophages. (B) In Nos2-/- macrophages, microbicidal activity of macrophages is impaired, and there is a dramatic hyper-inflammatory phenotype. NF-kB activity is aberrantly high, and HIF-1α levels and activity are low. However, HIF-1α activity is not completely gone, and still contributes to inflammatory cytokine production, leading to a hyper-inflammatory response driven by both NF-kB and HIF-1α. (C) In Hif1a-/- macrophages, there is impaired microbicidal activity, a hypo-inflammatory response and reduced NO production. However, NO production is not fully eliminated, and the remaining NO is sufficient to inhibit NF-kB activity. Our data suggests that the reduced level of NO produced in HIF-1α knockouts is not directly microbicidal, as the Nos2-/- Hif1a-/- double knockout (which eliminates this remnant NO production) shows no additional loss of bacterial control relative to the HIF-1α-/-. (D) Nos2-/- Hif1a-/- double knockout macrophages have impaired microbicidal activity, but normal levels of inflammatory cytokine production. The observation that these double knockout macrophages have the same defect in control of *M. tuberculosis* as the individual Hif1a-/- or Nos2-/- macrophages suggests that HIF-1α and iNOS are acting through the same pathway for cell autonomous control of infection. Although the levels of cytokine production Nos2-/- Hif1a-/- double knockout macrophages is similar to wildtype macrophages, our data suggests that expression is being driven by NF-kB instead of HIF-1α.

Table S1

(A) Ingenuity IPA analysis of transcription factors predicted to be activated or inhibited by NO during *M. tuberculosis* infection of IFN-γ activated macrophages.

Upstream Regulator	Predicted Activation State	Activation z-score	p-value of overlap
ZFP36	Activated	-3.639	1.65E-09
HSF1	Activated	-2.838	1.01E-01
FOXA2	Activated	-2.619	1.36E-01
HIF1A	Activated	-2.573	6.41E-10
STAT4	Activated	-2.524	7.30E-12
NCOA3	Activated	-2.423	1.92E-01
FOXA1	Activated	-2.422	1.00E+00
BCL3	Activated	-2.24	1.25E-04
RCAN1	Activated	-2.17	1.91E-02
MECP2	Activated	-2.117	4.77E-02
NCOA2	Activated	-2.047	1.88E-05
MYCN	Inhibited	6.09	9.63E-28
CEBPB	Inhibited	4.226	5.33E-16
MYC	Inhibited	4.08	3.39E-24
STAT3	Inhibited	3.568	5.47E-22
RELA	Inhibited	3.362	1.17E-13
IRF6	Inhibited	3.361	1.54E-10
REL	Inhibited	3.221	3.99E-05
HMGB1	Inhibited	3.209	1.37E-05
NFKB1	Inhibited	2.937	4.42E-11
CEBPE	Inhibited	2.936	2.20E-07
JUN	Inhibited	2.818	1.45E-17
IRF8	Inhibited	2.754	4.75E-09
FOXO1	Inhibited	2.747	1.33E-09
TBX2	Inhibited	2.646	2.01E-01
JUND	Inhibited	2.61	5.96E-08
ANKRD42	Inhibited	2.433	4.42E-07
PYCARD	Inhibited	2.39	1.19E-03
SP1	Inhibited	2.372	2.04E-11
RUNX2	Inhibited	2.356	2.38E-04
MYBL2	Inhibited	2.236	4.43E-02
TFAP4	Inhibited	2.236	8.42E-02
FOXL2	Inhibited	2.212	2.88E-09
BCL10	Inhibited	2.195	1.84E-03
CARM1	Inhibited	2.155	9.35E-06
IFI16	Inhibited	2.101	4.03E-05
ID1	Inhibited	2.097	1.70E-03
ID3	Inhibited	2.091	3.89E-03
EP300	Inhibited	2.074	6.39E-05

(B) oPOSSUM analysis of transcription factors predicted to be activated or inhibited by NO during *M. tuberculosis* infection of IFN-γ activated macrophages.

Transcription factor	Predicted Activation score	GC Content	z-score
Klf4	Activated	0.771	37.15
SP1	Activated	0.82	32.48
Zfx	Activated	0.749	22.997
HIF1A::ARNT	Activated	0.657	16.586
Egr1	Activated	0.739	14.985
Mycn	Activated	0.699	14.417
Tcfcp2l1	Activated	0.609	13.304
NFYA	Activated	0.523	12.6
MZF1_1-4	Activated	0.725	11.307
Hand1::Tcfe2a	Activated	0.507	10.845
E2F1	Activated	0.625	10.534
MZF1_5-13	Activated	0.588	10.456
INSM1	Activated	0.667	9.573
MEF2A	Activated	0.179	9.372
Myc	Activated	0.686	8.981
EBF1	Activated	0.648	8.602
Arnt::Ahr	Activated	0.715	8.477
REL	Inhibited	0.559	17.65
ELF5	Inhibited	0.429	15.224
NF-kappaB	Inhibited	0.621	14.792
RELA	Inhibited	0.567	14.606
SP1	Inhibited	0.82	13.35
MZF1_1-4	Inhibited	0.725	12.848
FEV	Inhibited	0.442	12.543
MZF1_5-13	Inhibited	0.588	12.4
SPIB	Inhibited	0.466	12.355
Egr1	Inhibited	0.739	11.611
NFKB1	Inhibited	0.758	11.565
ZNF354C	Inhibited	0.615	11.496
Klf4	Inhibited	0.771	10.25
CEBPA	Inhibited	0.358	9.516
IRF1	Inhibited	0.383	9.378
TBP	Inhibited	0.377	9.328
HOXA5	Inhibited	0.315	9.094
SRF	Inhibited	0.466	8.911
Pax5	Inhibited	0.575	8.879
RXRA::VDR	Inhibited	0.527	8.632
SPI1	Inhibited	0.435	8.532
NFATC2	Inhibited	0.346	8.394
MEF2A	Inhibited	0.179	8.189

Chapter Three: Conclusion and Future Directions

The role of IFN-γ during *M. tuberculosis* infection remains unclear:

When I began my thesis work, one of my goals was to identify novel IFN-γ dependent pathways required for control of *M. tuberculosis* infection. At the time, there were two major pathways that were thought to largely account for this bacterial control. Accepted mechanisms of IFN-γ dependent control of *M. tuberculosis* infection included enhancement of bacterial targeted autophagy, and induction of iNOS to directly kill bacteria via nitric oxide toxicity. The genetic evidence for the roles of autophagy and iNOS seemed solid when I began my thesis work; iNOS deficient mice have long been known to be extraordinarily susceptible to *M. tuberculosis* infection, explaining a substantial portion of IFN-γ dependent control of infection (1), and Atg5 deficient mice had been recently shown to die rapidly following *M. tuberculosis* infection (2).

However, the role of autophagy during *M. tuberculosis* infection has recently been called into question by a thorough report examining the susceptibility of a variety of autophagy mutant mice (3). The primary conclusion of this report is that only Atg5 deficient mice manifest an extreme susceptibility to *M. tuberculosis* infection. Furthermore, it was demonstrated that the susceptibility of Atg5 deficient mice is largely due to a lack of Atg5 in neutrophils, not the macrophages thought to be the primary host/pathogen interface during *M. tuberculosis* infection. This throws quite a bit of cold water on the notion that direct bacterial targeted autophagy is a key mechanism of IFN-γ dependent (or independent) control of infection. Furthermore, our lab has been unable to recapitulate the result that IFN-γ activation of macrophages enhances bacterial targeted autophagy *in vitro*. Thus, while the role of autophagy during *M. tuberculosis* remains somewhat unclear, and the mechanisms by which *M. tuberculosis* can successfully evade autophagy remain intriguing and important open questions, it is unlikely that bacterial targeted autophagy is a major explanatory mechanism of IFN-γ dependent control of *M. tuberculosis*.

While macrophage production of nitric oxide has been presumed to be important for control of infection due to direct bacterial toxicity, this has never been clearly demonstrated, and the identification of *M. tuberculosis* mutants with high susceptibility to nitrosative stress (4) can be interpreted as evidence that wildtype *M. tuberculosis* has robust protective mechanisms against nitric oxide toxicity. More directly challenging the model that *in vivo* susceptibility of iNOS deficient mice is due primarily to a loss of direct bacterial toxicity are some clever experiments employing a streptomycin dependent strain of *M. tuberculosis*. This strain can only replicate in the presence of streptomycin, which can be administered to mice, allowing the bacteria to replicate in mice. Upon withdrawal of streptomycin from infected mice, the bacteria are no longer able to replicate (but are not effectively cleared). Intriguingly, while wildtype mice do not display any lung pathology in this infection model, iNOS deficient mice have extensive lung pathology and wasting even in the absence of bacterial replication (5). This is excellent evidence that the loss of nitric oxide leads to immunopathology and suggests an anti-inflammatory role for nitric oxide during *M. tuberculosis* infection *in vivo*.

Thus, a satisfactory explanation for the observation that IFN-γ activation of macrophages *in vitro* allows macrophages to kill *M. tuberculosis* is still lacking. During my thesis work, I have identified HIF-1α stabilization and the metabolic program of

aerobic glycolysis as IFN-γ dependent responses required for control of *M. tuberculosis*, as well as characterized some of the signaling roles of nitric oxide in macrophages during *M. tuberculosis* infection. This has added to the understanding of how IFN-γ activates macrophages during *M. tuberculosis* infection, but definitive mechanisms for how these pathways lead to bacterial killing remain elusive.

HIF-1α, iNOS, and aerobic glycolysis constitute a mutually reinforcing, IFN-γ dependent immunometabolic program required for control of *M. tuberculosis*:

When I began my thesis work, I was interested in characterizing IFN-γ dependent metabolic changes occurring in macrophages during *M. tuberculosis* infection. It had been reported that infection of macrophages leads to a metabolic shift to aerobic glycolysis, and that this was a bacterial driven process requiring the ESX-1 secretion system (6,7). However, it was also reported that a transition to aerobic glycolysis can be triggered by LPS stimulation of macrophages, and that this response is mediated by HIF-1α (8). This suggested that this metabolic program was a more general feature of activated macrophages, and not something induced by specific *M. tuberculosis* effectors.

I first compared IFN-γ activation alone, *M. tuberculosis* infection alone, and *M. tuberculosis* infection of IFN-γ activated macrophages. I found that neither *M. tuberculosis* infection nor IFN-γ activation led to robust increases in transcription of glycolytic genes, and only led to small increases in glucose consumption. However, IFN-γ and *M. tuberculosis* infection appeared to be synergistic stimuli inducing robust increases in glycolytic gene transcription (5-30 fold increases), glucose consumption, and lactate production. Interestingly, these phenotypes were largely recapitulated with the combination of Pam3CysK4 (a TLR1/2 agonist) and IFN-γ, suggesting that this was a host driven pathway, and not something that *M. tuberculosis* was actively inducing the macrophages to engage in.

I first assessed whether aerobic glycolysis was required for IFN-γ dependent killing of *M. tuberculosis* in macrophages by utilizing two strategies to limit glycolytic flux. The first was to add the glycolytic inhibitor 2DG, and the second was to limit glycolytic flux by switching macrophages from glucose to galactose following infection. Both of these perturbations prevented IFN-γ dependent killing of *M. tuberculosis* in macrophages. This implied that the transition to aerobic glycolysis was not only an IFN-γ dependent host response to infection, but that it was also necessary for killing of *M. tuberculosis*. This finding stands in contrast to the previous model that aerobic glycolysis is actively triggered by *M. tuberculosis* and that this benefits the pathogen.

Interestingly, the regulation of both HIF-1α and iNOS follow a similar pattern during *M. tuberculosis* infection, with HIF-1α stabilization and transcriptional activity increasing dramatically only with the combination of *M. tuberculosis* infection and IFN-γ activation. iNOS transcription and nitric oxide production are also synergistically regulated by *M. tuberculosis* infection and IFN-γ activation, with only minimal transcriptional upregulation and nitric oxide production with infection alone, but extraordinarily high transcript levels (similar abundance to actin) with the addition of IFN-γ. A substantial portion of my thesis work has focused on the interconnections between these three prominent IFN-γ dependent processes (a shift to aerobic glycolysis, HIF-1α stabilization, and nitric oxide production) occurring in macrophages during *M. tuberculosis* infection.

The initial observations I made connecting these processes were that glycolytic inhibition with 2DG reduced nitric oxide production by ~50% and dramatically abrogated HIF-1α stabilization. Interestingly, iNOS deficient macrophages also had a large defect in HIF-1α stabilization, and a defect in upregulation of glycolytic genes and flux through glycolysis. And finally, HIF-1α deficient macrophages had a ~50% defect in nitric oxide production, a ~50% defect in upregulation of glycolytic genes, and a ~50% defect in flux through glycolysis. Thus, all three of these responses appear to be mutually reinforcing, with inhibition of any of the three causing a defect in the other two. A major challenge in understanding how these multiple and interconnected IFN-γ driven responses control *M. tuberculosis* infection are my data indicating that HIF-1α deficient macrophages, iNOS deficient macrophages, and macrophages treated with 2DG have very similar defects in killing of *M. tuberculosis*.

Although glycolytic genes are canonical transcriptional targets of HIF-1α, and my work indicates that this is the case during IFN-γ activation of *M. tuberculosis* infected macrophages, HIF-1α transcriptional activity alone is not a satisfactory mechanism for the upregulation of glycolysis during infection. While there is a clear defect in the HIF-1α knockout macrophages, it is only ~2fold. The transcription of *Pfkfb3*, an aerobic glycolysis marker, is upregulated ~30x in wildtype macrophages during *M. tuberculosis* infection of IFN-γ activated macrophages, and in contrast is upregulated ~15x in HIF-1α deficient macrophages. Thus, there is clearly IFN-γ dependent, HIF-1α independent upregulation of glycolysis during infection. Interestingly, the dependence of HIF-1α stabilization on glycolytic flux is more pronounced, with an almost complete loss of HIF-1α stabilization following 2DG treatment. So, although HIF-1α and aerobic glycolysis appear to linked by positive feedback, HIF-1α is more "downstream" of aerobic glycolysis in macrophages activated with IFN-γ and infected with *M. tuberculosis*. This leaves an understanding of how IFN-γ triggers a shift to aerobic glycolysis an open and interesting question.

Also remaining as an open question is how exactly HIF-1α is stabilized downstream of aerobic glycolysis. A variety of stimuli other than hypoxia are reported to lead to HIF-1α stabilization. These include accumulation of succinate, accumulation of lactate, as well as nitric oxide. Although I have identified nitric oxide as essential for the stabilization of HIF-1α during *M. tuberculosis* infection of IFN-γ activated macrophages, the mechanism through which this occurs is still unclear. As iNOS deficient macrophages are defective in upregulation of aerobic glycolysis, it is possible that the large defect in HIF-1α stabilization in iNOS deficient macrophages is indirect, and due to a defect in upregulation of aerobic glycolysis and subsequent accumulation of lactate.

Additionally, although my work indicates that a transition to aerobic glycolysis is required for IFN-γ dependent killing of *M. tuberculosis*, it remains unclear whether this is mediated through any process other than the stabilization of HIF-1α. One indication that HIF-1α activation is the primary pathway through which aerobic glycolysis mediates killing of *M. tuberculosis* is the observation that while 2DG treatment of wildtype macrophages prevents killing of *M. tuberculosis* to a similar extent that HIF-1α deficiency does, 2DG treatment of HIF-1α deficient macrophages does not further prevent restriction of bacterial growth. So, this raises the question of what exactly HIF-1α is doing that is required for killing of *M. tuberculosis*.

HIF-1α amplifies IFN-γ activation:

To try and understand which HIF-1α dependent responses are responsible for IFN-γ dependent killing of *M. tuberculosis* in macrophages, I performed RNAseq on wildtype, HIF-1α, and iNOS deficient macrophages. I found that ~1500 genes were significantly differentially expressed in HIF-1α deficient macrophages compared to wildtype during *M. tuberculosis* infection with IFN-γ activation. Interestingly, this set of genes encompassed nearly 50% of all genes differentially expressed between wildtype macrophages infected with *M. tuberculosis* and activated with IFN-γ compared to *M. tuberculosis* infection alone. This implies that HIF-1α is a core component of the IFN-γ activation program in macrophages, but also implies that HIF-1α stabilization is not a very proximal effector of IFN-γ dependent killing of *M. tuberculosis*. Although I found that HIF-1α regulated multiple responses thought to be important for control of *M. tuberculosis* infection (iNOS, IL-1, and PGE_2 most prominently), it remains unclear which of these effects are responsible for HIF-1α dependent bacterial killing. It is certainly possible that none of the individual IFN-γ regulated responses that are amplified by HIF-1α transcriptional activity are alone responsible for the observed phenotype that HIF-1α deficient macrophages fail to kill *M. tuberculosis*.

While I have identified HIF-1α as an important amplifier of IFN-γ mediated activation of macrophages during *M. tuberculosis* infection, this work unfortunately adds little mechanistic insight into what specific IFN-γ dependent effectors are responsible for killing *M. tuberculosis*. Although the finding that aerobic glycolysis is required for killing of *M. tuberculosis* seemed as though it might lead to mechanistic understanding, it mainly lead back to HIF-1α and a broad amplification of the IFN-γ dependent program of macrophage activation. Thus, aerobic glycolysis and HIF-1α are crucial for successful macrophage activation in the context of *M. tuberculosis* infection, but we still do not understand what the business end of this IFN-γ mediated response is.

Perhaps the most useful line of inquiry involves stepping back and performing an unbiased screen in macrophages to test which genes when absent prevent IFN-γ mediated control of infection. One approach to performing this screen is to use macrophage survival as a proxy for control of *M. tuberculosis* replication, and perform a CRISPR/Cas9 screen utilizing a pooled guide library, and see which guides drop out after carrying out an infection with IFN-γ activation. Hopefully such a screen produces the expected hits of IFN-γR, STAT1 and HIF-1α, but also more specific effectors that will suggest more direct mechanisms to explore.

IFN-γ promotes both pro and anti-inflammatory responses via HIF-1α and iNOS:

One of the major surprises in performing RNAseq on HIF-1α and iNOS deficient macrophages was the observation there was a small but important set of genes oppositely regulated in HIF-1α and iNOS knockouts. Given the positive regulation of HIF-1α by iNOS and the positive regulation of iNOS by HIF-1α, it was not surprising that the vast majority of genes regulated by both HIF-1α and iNOS were regulated in the same direction. However, ~5% of genes regulated by both HIF-1α and iNOS were oppositely regulated, and this subset of genes was heavily enriched for inflammatory cytokines and chemokines (including IL-1, IL-6, CXCL1, and CXCL3). While HIF-1α deficient macrophages were broadly deficient in inflammatory cytokine expression, iNOS deficient macrophages had highly elevated levels compared to wildtype macrophages. This

resulted in quite extreme differences in inflammatory cytokine levels in HIF-1α deficient compared to iNOS deficient macrophages. Indeed, the levels of *Il1b* and *Il1a* transcript were ~50x and ~100x elevated in iNOS deficient compared to HIF-1α deficient macrophages.

This data indicates that IFN-γ is turning on both a strong activator (HIF-1α) and repressor (iNOS) of inflammatory cytokine production simultaneously. This implies that the levels of inflammation during the adaptive response to *M. tuberculosis* must be carefully calibrated, and IFN-γ signaling plays a large role in this process via HIF-1α and iNOS. The aberrantly high levels of multiple inflammatory cytokines and chemokines in iNOS deficient macrophages is particularly interesting given the proposed role of iNOS in preventing lung immunopathology during *M. tuberculosis* infection (5). The proposed mechanism involves inactivation of the NLRP3 inflammasome by direct nitrosylation, leading to enhanced cleavage of pro-IL-1b (5). However, my data indicated that nitric oxide has a potent anti-inflammatory role upstream of this, and acts to suppress transcription of inflammatory cytokines and chemokines. The most likely candidate transcription factor to mediate this phenotype was NF-kB, and I found that NF-kB reporter activity was elevated when iNOS was inhibited, and that levels of the RelA/p65 subunit of NF-kB in the nucleus were elevated in iNOS deficient macrophages during *M. tuberculosis* infection of IFN-γ activated macrophages.

One explanation for the immunopathology in the lungs of iNOS deficient mice during infection with *M. tuberculosis* is an elevated influx of neutrophils (5). This is an appealing hypothesis, as elevated IL-1b and CXCL1 could lead to elevated attraction of neutrophils. I tested whether depletion of neutrophils from iNOS deficient mice could rescue their susceptibility to infection, and was somewhat surprised to find that antibody mediated depletion of neutrophils had no protective effect on survival of iNOS deficient mice, and made them succumb to infection slightly faster. It is unclear what to make of this result, as it is possible that the rapid clearance of neutrophils is not immunologically silent and exacerbates inflammation, the opposite of the intended effect. It may be useful to follow up on these results by trying methods of blunting neutrophil inflammatory response other than antibody depletion, such as treating mice with a MPO inhibitor, and seeing if this rescues the susceptibility of iNOS knockout mice.

Another avenue worth pursuing is testing the effects of IFN-γ directly on neutrophils during infection. A preliminary experiment that will likely be performed is to infect mice lacking the IFN-γ receptor specifically in neutrophils, and then perform RNAseq on neutrophils from the blood and lungs of infected mice. It remains unclear how exactly nitric oxide prevents tissue damage in the lungs, and what the roles of neutrophils during *M. tuberculosis* infection are. These are interesting and important open questions that will change our understanding of immune response to *M. tuberculosis*.

References:

1. MacMicking, J. D. Immune Control of Tuberculosis by IFN- -Inducible LRG-47. *Science* 302: 654–659.
2. Watson, O.W., P.S. Manzanillo, and J.S. Cox. Extracellular M. tuberculosis DNA Targets Bacteria for Autophagy by Activating the Host DNA-Sensing Pathway. *Cell* 150(4): 803-815.
3. Kimmey, J.M., J.P. Huynh, L.A. Weiss, S. Park, A. Kambal, J. Debnath, H. W. Virgin, and C.L. Stallings. Unique role for ATG5 in PMN-mediated immunopathology during M. tuberculosis infection. *Nature* 528(7583):565-569.
4. Darwin, K. H. 2003. The Proteasome of Mycobacterium tuberculosis Is Required for Resistance to Nitric Oxide. *Science* 302: 1963–1966.
5. Mishra, B. B., V. A. K. Rathinam, G. W. Martens, A. J. Martinot, H. Kornfeld, K. A. Fitzgerald, and C. M. Sassetti. 2012. Nitric oxide controls the immunopathology of tuberculosis by inhibiting NLRP3 inflammasome–dependent processing of IL-1β. *Nat. Immunol.* 14: 52–60.
6. Singh, V., S. Jamwal, R. Jain, P. Verma, R. Gokhale, and K. V. S. Rao. 2012. Mycobacterium tuberculosis-Driven Targeted Recalibration of Macrophage Lipid Homeostasis Promotes the Foamy Phenotype. *Cell Host Microbe* 12: 669–681.
7. Mehrotra, P., S. V. Jamwal, N. Saquib, N. Sinha, Z. Siddiqui, V. Manivel, S. Chatterjee, and K. V. S. Rao. 2014. Pathogenicity of Mycobacterium tuberculosis is expressed by regulating metabolic thresholds of the host macrophage. *PLOS Pathogens* 10: e1004265.
8. Tannahill, G. M., A. M. Curtis, J. Adamik, E. M. Palsson-McDermott, A. F. McGettrick, G. Goel, C. Frezza, N. J. Bernard, B. Kelly, N. H. Foley, L. Zheng, A. Gardet, Z. Tong, S. S. Jany, S. C. Corr, M. Haneklaus, B. E. Caffrey, K. Pierce, S. Walmsley, F. C. Beasley, E. Cummins, V. nizet, M. Whyte, C. T. Taylor, H. Lin, S. L. Masters, E. Gottlieb, V. P. Kelly, C. Clish, P. E. Auron, R. J. Xavier, and L. A. J. O'Neill. 2013. Succinate is an inflammatory signal that induces IL-1β through HIF-1α. *Nature* 496: 238–242.